

**Role of ROS and ROS generating enzymes
in the human ovary**

Theresa Buck



**Dissertation der Fakultät für Biologie
der Ludwig-Maximilians-Universität München**

München 2018

Diese Dissertation wurde angefertigt
unter der Leitung von Prof. Dr. Artur Mayerhofer
im Bereich der Zellbiologie, Anatomie III,
am BioMedizinischen Centrum München
der Ludwig-Maximilians-Universität

Erstgutachter: PD Dr. Lars Kunz

Zweitgutachter: Prof. Dr. Gisela Grupe

Tag der Abgabe: 12. Juni 2018

Tag der mündlichen Prüfung: 18. September 2018

Eidesstattliche Erklärung

Ich versichere hiermit an Eides statt, dass meine Dissertation selbstständig und ohne unerlaubte Hilfsmittel angefertigt worden ist.

Die vorliegende Dissertation wurde weder ganz, noch teilweise bei einer anderen Prüfungskommission vorgelegt.

Ich habe noch zu keinem früheren Zeitpunkt versucht, eine Dissertation einzureichen oder an einer Doktorprüfung teilzunehmen.

München, den 12. Juni 2018

(Theresa Buck)

Steigst du nicht auf die Berge, so siehst du auch nicht in die Ferne.

Che Guevara

:

List of contents

List of contents	V
List of figures	VIII
List of supplementary figures	IX
List of tables	X
List of abbreviations	XI
Summary	XIV
Zusammenfassung	XVI
1. Introduction	1
1.1 Ovary and follicle development	1
1.1.1 Function and structure of the ovary	1
1.1.2 Follicular phase and its hormonal regulation	1
1.1.3 Luteal phase	4
1.2 Ovarian steroidogenesis	4
1.3 In-vitro fertilization (IVF)	5
1.3.1 Granulosa cells (GCs)	7
1.3.2 Granulosa-like tumour cell line - KGN	7
1.4 FSH, FSHR and signalling	7
1.5 Reactive oxygen species (ROS)	9
1.5.1 Different types of ROS.....	9
1.5.2 Sources of ROS.....	9
1.5.3 Functional roles in the ovary.....	10
1.5.4 Oxidative stress (OS) and fertility	11
1.5.5 Hydrogen peroxide - a signalling molecule	11
1.6 Characteristics of NADPH oxidases (NOX)	13
1.6.1 Function, structure, and activation.....	13
1.6.2 Localization and distribution	15
1.6.3 NOX4	16
1.7 Aquaporins/poroxiporins	17
1.8 Antioxidant defence mechanisms	18
1.9 Aims of the study	19
2. Results	20
2.1 NOX and ROS in cultured human GCs	20
2.1.1 Identification of NOX.....	20

2.1.2	Localization of NOX4 and NOX5	20
2.1.3	Localization of NOX4 in ovarian tissue	21
2.1.4	Functional activity of NOX4	22
2.1.5	Influence of FSH and hCG	25
2.1.6	Roles of H ₂ O ₂	30
2.1.7	Role of aquaporins/porixiporins	32
2.2	NOX and ROS in the proliferating cell model KGN	33
2.2.1	NOX expression and localization.....	33
2.2.2	Roles of NOX4.....	34
3.	<i>Discussion</i>.....	37
3.1	Identification of NOX enzymes in ovarian cells.....	37
3.2	NOX-derived ROS.....	38
3.3	Regulation by FSH and hCG.....	40
3.4	H ₂ O ₂ transport	41
3.5	Physiological roles of H ₂ O ₂	42
3.5.1	Studies in cultured human GCs.....	42
3.5.2	Studies in KGN cells	44
4.	<i>Material and Methods</i>	46
4.1	Cell culture.....	46
4.1.1	Human GC isolation, culture, and treatment	46
4.1.2	Cultivation of KGN	47
4.2	Immunological analysis	47
4.2.1	Western immunoblotting	47
4.2.2	Immunocytochemistry.....	48
4.2.3	Immunohistochemistry.....	49
4.2.4	Human cytokine array.....	50
4.3	Analytical methods	50
4.3.1	Reverse transcription-PCR and quantitative RT-PCR.....	50
4.3.2	Cell viability assay	54
4.3.3	Cytotoxicity assay	55
4.3.4	Superoxide anion detection	55
4.3.5	Measurement of ROS generation.....	55
4.3.6	Measurement of H ₂ O ₂ generation.....	56
4.3.7	Measurement of H ₂ O ₂ uptake via aquaporins	56
4.4	Statistics	56
4.5	Material	57

4.5.1	Primers	57
4.5.2	Antibodies	58
4.5.3	Consumables	59
4.5.4	Chemicals	60
4.5.5	Buffers and solutions	62
4.5.6	Cell culture media and reagents	63
4.5.7	Kits and assays	63
4.5.8	Equipment	64
4.5.9	Biological material	65
5.	<i>References</i>	66
6.	<i>Acknowledgements</i>	74
7.	<i>Supplement</i>	76
8.	<i>Appendix</i>	79
8.1	Publications	79
8.2	Poster	79

List of figures

FIGURE 1 - OVARIAN FOLLICULAR DEVELOPMENT.....	2
FIGURE 2 - FEEDBACK LOOPS IN THE HYPOTHALAMIC-PITUITARY-OVARIAN AXIS.....	4
FIGURE 3 - SYNTHESIS OF STEROID HORMONES IN THE OVARY.....	5
FIGURE 4 - CONVERSION OF H ₂ O ₂ INTO ROS.....	12
FIGURE 5 - ROLE OF H ₂ O ₂ IN REDOX SIGNALLING AND IN OXIDATIVE DAMAGE.....	13
FIGURE 6 - COMPOSITION OF NOX ENZYME COMPLEXES.....	14
FIGURE 7 - SIGNALLING PATHWAYS OF NOX4.....	17
FIGURE 8 - NOX EXPRESSION IN CULTURED HUMAN GCs.....	20
FIGURE 9 - LOCALIZATION OF NOX4 IN CULTURED HUMAN GCs.....	21
FIGURE 10 - LOCALIZATION OF NOX5 IN CULTURED HUMAN GCs.....	21
FIGURE 11 - PRESENCE OF NOX4 IN OVARIAN CELLS EX VIVO.....	22
FIGURE 12 - BASAL ROS INCLUDING H ₂ O ₂ AND O ₂ ⁻ PRODUCTION OF CULTURED HUMAN GCs.....	23
FIGURE 13 - INHIBITION OF NOX4 ACTIVITY IN CULTURED HUMAN GCs.....	24
FIGURE 14 - GKT137831 DID NOT AFFECT VIABILITY AND MORPHOLOGY OF CULTURED HUMAN GCs.....	25
FIGURE 15 - EXPRESSION OF <i>LHR</i> AND <i>FSHR</i>	25
FIGURE 16 - FSH INCREASES PHOSPHORYLATION OF MAPK AND MRNA LEVELS OF <i>ADAM17</i>	26
FIGURE 17 - FSH/HCG INFLUENCES RECEPTORS.....	26
FIGURE 18 - NO ACUTE EFFECT OF FSH/HCG ON ROS PRODUCTION.....	27
FIGURE 19 - FSH/HCG INCREASED LEVELS OF DUOX.....	28
FIGURE 20 - ROS PRODUCTION WAS NOT INFLUENCED BY PRE-TREATMENT WITH FSH/HCG.....	28
FIGURE 21 - FSH/HCG INFLUENCED EXPRESSION OF ANTIOXIDATIVE ENZYMES.....	29
FIGURE 22 - REGULATION OF STEROIDOGENESIS BY FSH/HCG.....	29
FIGURE 23 - INFLUENCE OF H ₂ O ₂ ON PHOSPHORYLATION OF MAPK.....	30
FIGURE 24 - ACTION OF NOX4 AND CATALASE-BLOCKER.....	31
FIGURE 25 - H ₂ O ₂ INCREASED CYTOKINE EXPRESSION.....	32
FIGURE 26 - H ₂ O ₂ -TRANSPORTING AQUAPORINS IN CULTURED HUMAN GCs.....	33
FIGURE 27 - NOX EXPRESSION IN KGN.....	34
FIGURE 28 - INHIBITION OF NOX4 ACTIVITY IN KGN INDUCED LOWER PRODUCTION OF ROS AND H ₂ O ₂	35
FIGURE 29 - ACTIONS OF NOX4-BLOCKER IN KGN.....	36
FIGURE 30 - EXPRESSION LEVELS OF MULTIPLE REFERENCE GENES DO NOT CHANGE AFTER TREATMENT.....	54

List of supplementary figures

SUPPLEMENTARY FIGURE 1 - LOCALIZATION OF NOX4 IN CULTURED HUMAN GCs.	76
SUPPLEMENTARY FIGURE 2 - NOX4 LOCALIZATION IN THE CL.....	76
SUPPLEMENTARY FIGURE 3 - FSH INCREASED STAR PROTEIN EXPRESSION IN CULTURED HUMAN GCs.....	77
SUPPLEMENTARY FIGURE 4 - H ₂ O ₂ -TRANSPORTING PEROXIPORINS IN CULTURED HUMAN GCs.....	77
SUPPLEMENTARY FIGURE 5 - PRELIMINARY EXPERIMENTS WITH SIRNA TRANSFECTION IN KGN.	78

List of tables

TABLE 1 - CHARACTERISTICS AND EXPRESSION SITES OF NADPH OXIDASE FAMILY.....	15
TABLE 2 - STIMULANTS AND INHIBITORS.	47
TABLE 3 - COMPOSITION OF SDS-PAGE.	48
TABLE 4 - REVERSE TRANSCRIPTION.....	51
TABLE 5 - REACTION MIX FOR ONE RT-PCR SAMPLE.	52
TABLE 6 - THERMOCYCLER SETTINGS FOR RT-PCR.	52
TABLE 7 - LIGHTCYCLER SETTINGS FOR QRT-PCR.	53
TABLE 8 - INFORMATION ABOUT OLIGONUCLEOTIDE PRIMERS USED FOR PCR STUDIES.	57
TABLE 9 - LIST OF PRIMARY ANTIBODIES.....	58
TABLE 10 - LIST OF SECONDARY ANTIBODIES.....	58
TABLE 11 - BLOCKING PEPTIDE.	59
TABLE 12 - LIST OF USED CONSUMABLES.	59
TABLE 13 - LIST OF USED CHEMICALS.....	60
TABLE 14 - COMPOSITION OF USED BUFFERS AND SOLUTIONS.....	62
TABLE 15 - LIST OF CELL CULTURE MEDIA AND SUPPLEMENTS.	63
TABLE 16 - LIST OF USED KITS.	63
TABLE 17 - LIST OF USED EQUIPMENT.	64
TABLE 18 - LIST OF BIOLOGICAL MATERIAL AND CELLS.....	65

List of abbreviations

°C	Degree Celsius
3-AT	3-Amino-1,2,4-triazole
A	Androgen
ABC	Avidin-biotin complex
Ang II	Angiotensin II
AMH	Anti-Muellerian hormone
APS	Ammonium persulphate
AQP	Aquaporin
ART	Assisted reproductive technology
au	Arbitrary units
BLAST	Basic Local Alignment Search Tool
cDNA	Complementary DNA
Cat	Catalase
CL	Corpus luteum
Cq	Quantification cycle
ctrl.	Control
CYP11A1	Cytochrome P450 family 11 subfamily A member 1
d	Day
DAB	3,3'-diaminobenzidine
DAPI	4',6-Diamidin-2-phenylindol
DCF	2',7'-dichlorofluorescein
DEPC	Diethylpyrocarbonate
DFG	Deutsche Forschungsgemeinschaft
DMEM	Dulbecco's modified Eagle's medium
DMSO	Dimethyl sulfoxide
DNA	Deoxyribonucleic acid
dNTP	Deoxynucleotide triphosphates
DTT	Dithiothreitol
DUOX	Dual oxidase
E ₂	Oestradiol
EC	Extra cellular
ECL	Enhanced-Chemiluminescent-Substrate
EDTA	Ethylenediaminetetraacetic acid
EGFR	Epithelial growth factor receptor
ERK	Extracellular-signal regulated kinase
EtOH	Ethanol
FCS	Fetal calf serum
FF	Follicular fluid
Fig.	Figure
FSH	Follicle stimulating hormone
FSHR	Follicle stimulating hormone receptor
GAPDH	Glyceraldehyde 3-phosphate dehydrogenase
GC	Granulosa cell
gDNA	Genomic deoxyribonucleic acid
GPX	Glutathione peroxidase
GnRH	Gonadotropin-releasing hormone
GRO α	Growth-related oncogene alpha

GST	Glutathione S-transferase
GTP	Guanosine triphosphate
h	Hour/s
H ₂ DCFDA	2',7'-dichlorodihydrofluorescein diacetate
H ₂ O ₂	Hydrogen peroxide
hCG	Human chorionic gonadotropin
HEPES	4-(2-hydroxyethyl)-1-piperazineethanesulfonic acid
ICC	Immunocytochemistry
IGF-1	Insulin-like growth factor-1
IgG	Immunoglobulin G
IHC	Immunohistochemistry
IL-8	Interleukin 8
IU	International unit
IVF	In-vitro fertilization
kDa	Kilodalton
KGN	Granulosa-like tumour cell line
LDH	Lactate dehydrogenase
LGC	Luteinised granulosa cell
LH	Luteinised hormone
LHR	Luteinised hormone receptor
LMU	Ludwig-Maximilian-University
LTC	Luteinised theca cell
MAPK	Mitogen-activated protein kinase
MCP1	Monocyte chemoattractant protein 1
min	Minutes
MKP-1	MAPK phosphatase-1
MMP	Matrix metalloprotease
mRNA	Messenger ribonucleic acid
No.	Number
NOX	NADPH oxidase
ns	Not significant
OHSS	Ovarian hyperstimulation syndrome
OS	Oxidative stress
P	Progesterone
P/S	Penicillin/Streptomycin
PAGE	Polyacrylamide gel electrophoresis
PBS	Phosphate buffered saline
PCNA	Proliferating cell nuclear antigen
PCOS	Polycystic ovarian syndrome
PCR	Polymerase chain reaction
PRX	Peroxiredoxin
PDGF	Platelet-derived growth factor
PIPES	Piperazine-N,N'-bis(2-ethanesulfonic acid)
PKA	Protein kinase A
PM	Plasma membrane
PMA	Phorbol-12-myristate-13-acetate
pMAPK	Phosphorylated mitogen-activated protein kinase
PO1	Peroxy Orange 1
POX	Horseradish peroxidase

PPIA	Peptidylprolyl isomerase A
qRT-PCR	Quantitative real-time polymerase chain reaction
rel.	Relative
RLU	Relative light units
RNA	Ribonucleic acid
RNS	Reactive nitrogen species
ROS	Reactive oxygen species
RPL19	Ribosomal Protein L19
rpm	Rounds per minute
RT	Room temperature
-RT	Without reverse transcriptase
RT-PCR	Reverse transcription polymerase chain reaction
s	Seconds
SDS	Sodium dodecyl sulfate
SEM	Standard error of the mean
siRNA	Small interfering ribonucleic acid
SNP	Single nucleotide polymorphism
SOD	Superoxide dismutase
StAR	Steroidogenic Acute Regulator
Tab.	Table
Taq	<i>Thermophilus aquaticus</i>
TBE	Tris/Boric acid/EDTA
TBS-T	Tris-buffered saline-Tween®20
TC	Theca cell
TEMED	N, N, N', N'-Tetramethylethylenediamin
TGF- β	Transforming growth factor- β
TNF	Tumour necrosis factor
Tris	Tris(hydroxymethyl)aminomethan
UBC	Ubiquitin C
V	Volt
WB	Western blot

Summary

Reactive oxygen species (ROS) have long been regarded as destructive molecules that have harmful effects. However, research data emerging over the last decade have demonstrated that ROS can positively influence a range of cellular events in a manner similar to that seen for traditional second messenger molecules. Hydrogen peroxide (H_2O_2) appears to be the main ROS with such signalling properties, and this molecule has been shown to affect a variety of cellular functions. Its synthesis by the NADPH oxidase (NOX) family of enzymes and how these enzymes are regulated in the human ovary are poorly investigated topics. In the ovary, ROS are involved in fundamental reproductive processes, as implicated by previous studies. However, ROS can also cause oxidative stress, which is associated with impaired oocyte quality and a negative outcome of assisted reproductive techniques.

Oocytes grow and mature in ovarian follicles, formed by granulosa cells (GCs) and theca cells (TCs). NOX4, a member of the ROS-producing NOX family, was identified in cultured human in-vitro fertilization (IVF)-derived GCs as well as in corresponding GCs and TCs of growing preantral and antral follicles in human ovarian sections. It was further detected in GC- and TC-derived luteal cells of the corpus luteum. IVF-derived GCs resemble ovulatory GCs and/or the corpus luteum, but do not proliferate. Therefore, as a model for the growing follicle, the granulosa-like tumour cell line KGN was further studied. These cells also express NOX4.

Accumulation of ROS in the medium of cultured GCs and KGN could be detected and was inhibited by the specific NOX4 blocker GKT137831. This blocker reduced specifically the production of H_2O_2 by around 45 % in GCs and KGN. This indicates a major contribution of NOX4 activity to the generation of H_2O_2 . This is a rather long-lived and the only membrane-permeable ROS. H_2O_2 may diffuse to neighbouring cells, and studies implicated aquaporins in the uptake of extracellular H_2O_2 into GCs. The gonadotropins follicle stimulating hormone (FSH) and human chorionic gonadotropin (hCG) play a key role in reproduction. They induce the maturation of ovarian follicles, and the ovulation process. FSH and hCG, however, did not alter expression of *NOX4*, but elevated mRNA expression of antioxidant enzymes including catalase. This indicates a role of these hormones in ovarian ROS homeostasis.

H_2O_2 and FSH also increased MAPK-phosphorylation, suggesting convergence of the signalling pathways. Furthermore, H_2O_2 , when added to GCs, elevated several cytokines. This implicates H_2O_2 in inflammatory events, which are possibly involved in ovulation and/or regression of the corpus luteum. Inhibition of H_2O_2 production by GKT137831 did not affect cell viability of GCs but lowered expression of *CYP11A1*, a crucial enzyme for steroid synthesis. This suggests involvement in the maintenance of the steroidogenic phenotype of GCs.

In proliferating KGN cells, GKT137831 reduced cell growth. This may implicate a role of H_2O_2 in cell proliferation and possibly in follicular growth.

Taken together, the results imply important roles of H₂O₂ in the regulation of GCs. As ROS are potentially harmful molecules, the full elucidation of the two sides of the ROS-signalling system in the human ovary is important to guide future therapeutic strategies.

Zusammenfassung

Reaktive Sauerstoffspezies (englisch reactive oxygen species, ROS) wurden lange Zeit als potentiell schädliche Moleküle betrachtet, die nachteilige Effekte haben. Forschungsdaten des letzten Jahrzehnts zeigen jedoch, dass ROS eine Reihe von zellulären Ereignissen positiv beeinflussen können, ähnlich wie traditionelle Second Messenger Moleküle. Wasserstoffperoxid (H_2O_2) scheint das wichtigste ROS mit einer solchen Signaleigenschaft zu sein. Es wurde beobachtet, dass dieses Molekül eine Vielfalt von zellulären Funktionen beeinflusst. Seine Synthese durch die Enzymfamilie NADPH Oxidasen (NOX) und dessen Regulierung im menschlichen Ovar sind kaum erforschte Themen. ROS sind im Ovar in fundamentalen Reproduktionsprozessen involviert, was frühere Studien implizieren. Allerdings können ROS auch oxidativen Stress verursachen, welcher mit schlechter Oozytenqualität und negativem Ergebnis bei assistierten Reproduktionstechniken verbunden ist.

Oozyten wachsen und reifen in ovariellen Follikeln, welche aus Granulosazellen (GZs) und Thekazellen (TZs) gebildet werden. NOX4 ist ein Mitglied der ROS-produzierenden NOX Familie und wurde sowohl in kultivierten menschlichen GZs, die aus In-Vitro-Fertilisation (IVF) stammen, als auch in den korrespondierenden GZs und TZs von wachsenden Preantral- und Antralfollikeln in menschlichen Ovarschnitten identifiziert. Des Weiteren wurde es in Lutealzellen des Gelbkörpers, welche aus den GZs und TZs hervorgehen, festgestellt. IVF-abstammende GZs ähneln den ovulatorischen GZs und/oder dem Gelbkörper, aber proliferieren nicht. Deshalb wurde zusätzlich die Granulosa-ähnliche Tumorzelllinie KGN als weiteres Model für den wachsenden Follikel untersucht. Diese Zellen exprimieren auch NOX4. Die Akkumulation von ROS im Medium durch kultivierte GZs und KGN konnte ermittelt werden und wurde von einem spezifischen NOX4 Blocker GKT137831 gehemmt. Dieser Blocker reduzierte spezifisch die H_2O_2 -Produktion um 45 % in GZs und KGN, was auf einen erheblichen Beitrag der NOX4-Aktivität an der H_2O_2 -Produktion hinweist. Dies ist vielmehr ein langlebiges und das einzig membran-permeable ROS.

H_2O_2 könnte zu Nachbarzellen diffundieren und Studien weisen auf eine Aufnahme von extrazellulärem H_2O_2 in GZs hin, an welcher Aquaporine beteiligt sind.

Die Gonadotropine, follikelstimulierendes Hormon (FSH) und humanes Choriongonadotropin (hCG), spielen eine Schlüsselrolle in der Reproduktion. Sie induzieren die Reifung von ovariellen Follikeln und den Eisprung. FSH und hCG veränderten jedoch nicht die Expression von *NOX4*, aber erhöhten die Expression von antioxidativen Enzymen, einschließlich der Katalase. Dies weist auf einen Einfluss dieser Hormone auf die ovarielle ROS-Homöostase hin.

H_2O_2 und FSH erhöhten auch die MAPK-Phosphorylierung, was auf eine Konvergenz der Signalwege hinweist. Zusätzlich erhöhte H_2O_2 nach Zugabe zu den GZs einige Zytokine. Dies

bringt H_2O_2 mit inflammatorischen Ereignissen in Verbindung, welche möglicherweise beim Eisprung und/oder dem Abbau des Gelbkörpers beteiligt sind.

Die Hemmung der H_2O_2 -Produktion durch GKT137831 zeigte keinen Einfluss auf die Zellviabilität, aber senkte die Expression von *CYP11A1*, ein zentrales Enzym der Steroidsynthese. Dies deutet auf eine Beteiligung des Erhalts des steroidogenen Phänotyps der GZs hin.

In proliferierenden KGN Zellen reduzierte GKT137831 das Zellwachstum. Dies könnte eine Rolle von H_2O_2 in der Zellproliferation und möglicherweise im Follikelwachstum implizieren.

Die Ergebnisse dieser Studie deuten zusammenfassend auf eine wichtige Signalrolle von H_2O_2 in der Regulierung der GZs hin. Da ROS potenziell schädliche Moleküle sind, ist die vollständige Aufklärung der gegensätzlichen Seiten des ROS-signalisierenden Systems im menschlichen Ovar wichtig, um zukünftige therapeutische Ansätze zu entwickeln.

1. Introduction

1.1 Ovary and follicle development

1.1.1 Function and structure of the ovary

The mammalian ovary, i.e. the female gonad, is a highly organized organ composed of two regions with indistinct boundaries, namely an outer cortex and an inner medulla. The cortex is occupied by the developing follicles, while the inner medulla contains prominent blood vessels, lymphatics and nerves. The ovaries, which are paired organs lying on either side of the uterus, have two main functions: the production and release of functional female gametes (the oocytes) and a substantial endocrine function. The production of steroid hormones includes oestrogens, which are essential for the development of female genitalia, and progesterone, which is necessary for the establishment of pregnancy. The ovary presents a composite of germ cells (oocytes or eggs) and somatic cells (granulosa cells, thecal cells, and stromal cells) whose interactions edict maturation of oocytes, development of follicles, ovulation, and formation of the corpus luteum (CL). Folliculogenesis is a dynamic process involving a continuous differentiation of the three cell types. The oocyte and the surrounding granulosa cells (GCs) and theca cells (TCs) are under the control of two hormones, the follicle-stimulating hormone (FSH) and the luteinising hormone (LH). These hormones are secreted by the anterior pituitary gland under the control of pulses of gonadotropin-releasing hormone (GnRH) from the hypothalamus (Edson et al., 2009; Georges et al., 2014; Richards et al., 2010; Ross et al., 2015).

GCs, proliferating in association with the oocyte within developing follicles, play a central role in the coordination of folliculogenesis through their direct communication with the oocyte and TCs. In addition, GCs are sensitive to the pituitary hormones FSH and LH and produce oestrogens, anti-Muellerian hormone (AMH), activins etc. (Georges et al., 2014).

1.1.2 Follicular phase and its hormonal regulation

The maturation of a follicle can be classified into two phases according to its developmental stage and gonadotropin dependence, see Figure 1:

1. Preantral phase: follicular growth from primordial to primary and secondary stages (FSH/LH -independent phase).
2. Antral phase: transition from preantral to antral and preovulatory stage and to the ovulation (FSH/LH -dependent phase).

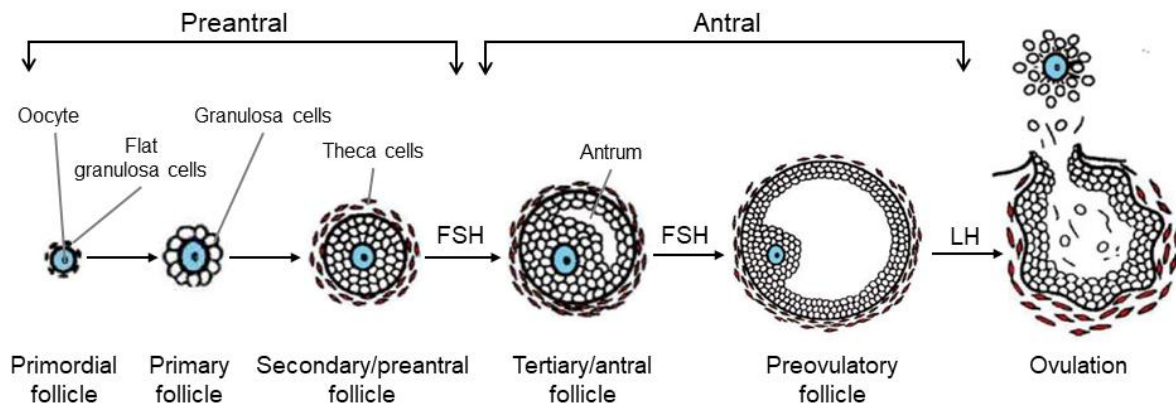


Figure 1 - Ovarian follicular development. Follicles progress through various stages of development from primordial to preovulatory/Graafian. Preantral phase: growth and formation of primordial follicles gets activated which form the primary follicles before they develop to secondary follicles. Antral phase: transition to tertiary/antral follicle consisting of an antral-filled follicular fluid cavity. Selection occurs between growing follicles, and only one continue growing to the preovulatory stage till ovulation while others undergo atresia. Whereas follicular growth to the secondary/preantral stage is independent of gonadotropins, progression beyond this stage strictly depends on FSH stimulation. A peak of FSH and LH triggers the ovulation. Modified after (Orisaka et al., 2009).

During the entire period of female reproductive life, there is a finite reservoir of germ cells, the primordial follicles, which become activated and are continuously recruited to undergo folliculogenesis. This process is very dynamic, strongly controlled and still not fully understood (Sanchez et al., 2012).

The growing follicle consists of an enlarging oocyte encapsulated by a single layer of cuboidal epithelial cells. With continued development, this lining becomes stratified epithelium composed of cuboidal GCs surrounded by an outer layer of TCs (primary follicle) followed by the formation of the so-called zona pellucida. This is an acellular layer of proteoglycans and glycoproteins that separates the developing oocyte from the surrounding GCs. A basal lamina separates the GCs from the TCs. These cells secrete androgens, which are converted into oestrogens in GCs. GCs begin to proliferate more and more and form a multilayer around the oocyte (secondary to late preantral follicles).

Ovarian follicular development and ovulation are regulated by hypothalamic (GnRH) and pituitary (LH and FSH) hormones. GnRH acts in the anterior pituitary gland to stimulate synthesis and secretion of FSH and LH. FSH and LH act on their specific receptors in the plasma membranes (PMs) of GCs and TCs of growing follicles (Luderer, 2014). Thus, the secondary follicle is the first stage of FSH receptivity, as now the follicle has acquired FSH receptors (FSHR), and preovulatory follicles have an absolute requirement for gonadotropins for survival (Kishi et al., 2018).

The ovarian steroids, oestradiol (E_2) and progesterone (P), and the peptide hormone, inhibin, are synthesized in the GCs and TCs. These hormones feed back to regulate the synthesis and secretion of GnRH, LH, and FSH, see Figure 2 (Richards et al., 2010).

By the sustained proliferation of GCs, the antrum is formed (tertiary/antral follicle) and GCs are separated into two populations with distinct characteristics and functions: mural GCs (endocrine function by producing steroid hormones) and cumulus cells (supportive function for oocyte development). The antrum is filled with follicular fluid (FF) which is in immediate proximity to the oocyte and enables the communication between the cells (Hennet et al., 2012). While many follicles undergo atresia, only one or a limited number of follicles are selected from the cohort of recruited follicles, develop to preovulatory stage (Graafian follicle) surrounded by two layers of theca (theca interna and externa), and ovulate. The follicle produces enough oestrogens resulting in a decrease in plasma FSH. This negative feedback combined with an increase of inhibin secretion by GCs causes a decrease in FSH and results in atresia (follicle degradation) of the non-dominant follicles (Ginther et al., 2001). Also, numerous peptides secreted by the GCs of the growing follicles may play an autocrine/paracrine role in the inhibition of progress of the nearby follicles (Reed et al., 2000).

Due to the rising levels of oestrogen in the preovulatory follicle, a positive feedback loop causes a rise of levels of LH. As a consequence, the so-called LH surge leads to a high concentration of LH and 24 h later to the release of the mature oocyte, i.e. the ovulation. The LH surge induces luteinisation of the GCs and TCs and forms the CL, which is required for establishing and maintaining pregnancy (Araujo et al., 2014; Georges et al., 2014; Orisaka et al., 2009; Reed et al., 2000).

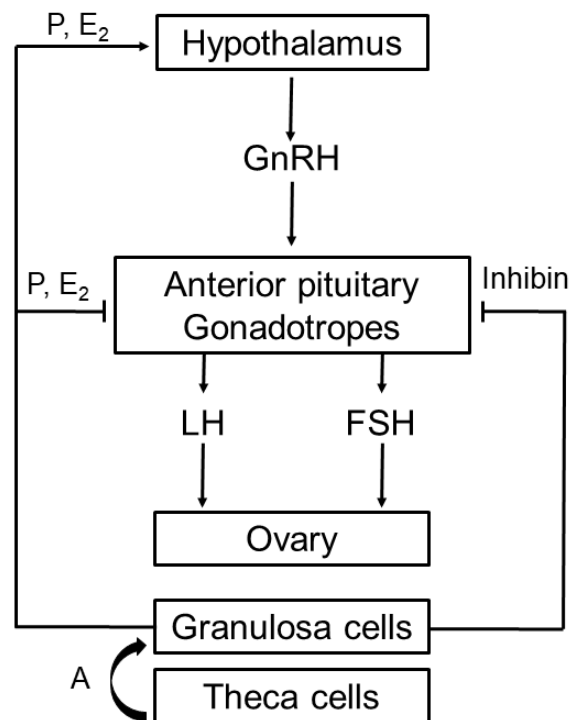


Figure 2 - Feedback loops in the hypothalamic-pituitary-ovarian axis. Synthesis and secretion of FSH and LH by the anterior pituitary is regulated by GnRH from the hypothalamus. Follicular growth and hormone synthesis is stimulated by FSH and LH acting on ovarian GCs and TCs. GCs secrete inhibin that inhibits FSH synthesis and secretion by the pituitary. The negative feedback loop triggered by E₂ and P stops secretion of GnRH, LH, and FSH. When E₂ reaches a threshold, it has a positive feedback effect on hypothalamic GnRH followed by ovulation. GnRH, gonadotropin-releasing hormone; FSH, follicle-stimulating hormone; LH, luteinising hormone; A, androgens; E₂, oestradiol; P, progesterone. Modified after (Luderer, 2014).

1.1.3 Luteal phase

This phase begins after ovulation and lasts usually 14 days. After the release of the mature oocyte, there are remaining GCs, which form together with the theca-lutein cells the CL. The CL presents an important transient endocrine organ and is the main source of steroid hormones. Its main function is to prepare the endometrium of the uterus for implantation of the fertilized oocyte by secreting progesterone and oestrogens (Devoto et al., 2009; Reed et al., 2000). The basal lamina dissolves and capillaries invade into the granulosa layer of cells. The steady LH support is essential for the life span of the CL. The expression of LH receptor (LHR) is fundamental during pregnancy. CL function declines by the end of the luteal phase unless hCG is produced due to a pregnancy.

If pregnancy does not occur, the CL degenerates under influence of oestradiol and prostaglandins, and forms a scar tissue called corpus albicans (Reed et al., 2000).

1.2 Ovarian steroidogenesis

Steroidogenesis is the biological process in which cholesterol is converted to biologically active steroid hormones regulating a wide variety of developmental and physiological processes from fetal life to adulthood (Miller et al., 2011). Different groups of steroid hormones are generally known and can be distinguished based on their physiological function: mineralocorticoids; glucocorticoids and sex hormones. The latter consists of oestrogens, which induce female secondary sexual characteristics; progestins, which are essential for reproduction; and androgens, which induce male secondary sexual characteristics (Miller, 1988). All steroid hormones are derived from cholesterol and differ only in the ring structure and the attached side chains. They are also lipid soluble and can thus permeate freely the PMs. There are different steroidogenic tissues where the synthesis primary takes place: cortisol and androgens are produced in the adrenal cortex; testosterone in the testis; oestrogens and progesterone in the ovary and progesterone in the placenta.

There are two crucial proteins priming the steroid synthesis, namely cytochrome P450 family 11 subfamily A member 1 (CYP11A1) and Steroidogenesis Acute Regulator (StAR). CYP11A1, also known as cholesterol side-chain cleavage enzyme, is the enzyme that converts cholesterol to pregnenolone. It is encoded by the *CYP11A1* gene and is associated with the

matrix side of the inner mitochondrial membrane (Miller, 2017). In the adrenals and gonads, StAR is responsible for the rapid transport of cholesterol from the outer mitochondrial to the inner mitochondrial membrane (Miller et al., 2011).

During the follicular phase, the major product generated by follicles is oestradiol, whereas during the luteal phase, the major products of the CL are the progestins. In the follicular phase, LH initiates the TCs to convert cholesterol to androstenedione (Figure 3). The next step, generation of oestradiol from androstenedione, requires aromatase which is not available in TCs. Thus, the androstenedione diffuses to the GCs where the aromatase converts the androstenedione to oestradiol. This aromatase activity has been stimulated by FSH. In the luteal phase, the vascularization of the CL makes low density lipoprotein, a source for cholesterol, available to the granulosa-lutein cells. Thus, both the theca-lutein and the granulosa-lutein cells can produce progesterone, the major product of the CL (Koeppen et al., 2009).

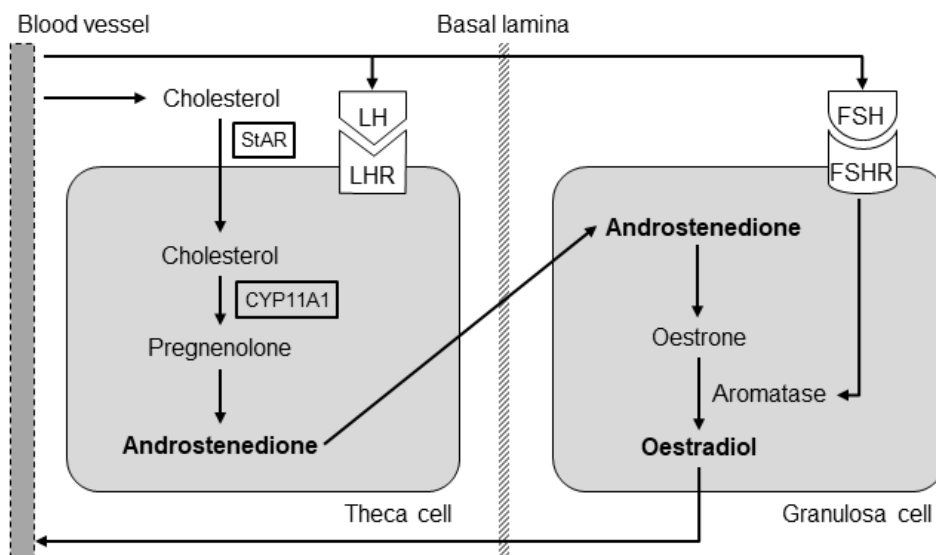


Figure 3 - Synthesis of steroid hormones in the ovary. Schematic outline of the two gonadotropin hypothesis of regulation of oestrogen synthesis in the human ovary. The transport of cholesterol from the cytoplasm into the mitochondria of TCs is triggered by StAR. Followed by the conversion of cholesterol to pregnenolone by CYP11A1. After several stages androstenedione is generated which is transported into GCs where it gets aromatized by the enzyme aromatase to form oestrogens.

1.3 In-vitro fertilization (IVF)

After the successful implementation of the IVF technology in the year 1978 (Steptoe et al., 1978), the estimation of worldwide born babies due to IVF is 7 million. Almost 20 % of couples worldwide suffer from some form of infertility problem. Today, the main reason for infertility is the increasing age in women, but also physiological causes are associated (Hamilton et al., 2006). Also, lifestyle factors such as smoking, bodyweight and stress can induce infertility.

Europe is leading in assisted reproductive techniques (ART) by reporting 50 % of all treatment cycles and 35 % mean pregnancy rate per embryo transfer (Duranthon et al., 2018).

The process of IVF involves daily injections of the gonadotropins FSH and LH/hCG to stimulate follicular development and to increase the number of oocytes available for fertilization (Macklon et al., 2006). The use of gonadotropins for ovarian stimulations is essential in the treatment of infertility. However, the use of FSH remains associated with severe disadvantages such as the risk of ovarian hyperstimulation syndrome (OHSS), a potentially life-threatening condition (Vloeberghs et al., 2009).

Clinical gonadotropin treatment for induction of ovulation in anovulatory women began in the 1960s, and for stimulating multi-follicular development in ovulatory women, began in the 1980s (Practice Committee of American Society for Reproductive Medicine, 2008). In natural cycles, GnRH stimulates the secretion of FSH and LH, which are regulating follicle development in the ovary and the selection of a dominant follicle. The inducing step for the ovulation is caused by a mid-cycle surge of LH (Alper et al., 2017).

There are various gonadotropin products available for controlled ovarian stimulation protocols. The most commonly used gonadotropins to trigger the follicular development and maturation are highly purified urinary human menopausal gonadotropin and recombinant FSH. Final oocyte maturation and ovulation is typically initiated by a bolus of either GnRH agonist or human chorionic gonadotropin (hCG), or both. hCG, a hormone that is biologically similar to LH, but has a longer half-life, can be human derived from urine of pregnant women or manufactured using recombinant technology (Practice Committee of American Society for Reproductive Medicine, 2008).

Transvaginal ultrasonography serves for monitoring the growing follicles. After a successful ovarian stimulation, mature follicles are gained by means of ultrasound-guided transvaginal aspiration of FF. Obtained oocytes get isolated from the aspirated fluid and in general fertilized in vitro by culturing together with motile sperms. The other option of fertilization is to use the intracytoplasmic sperm injection, where a single sperm is injected into the oocyte using a thin glass pipette. Originally, this method was applied to treat male infertility, but is nowadays often used for IVF. After the subsequent cultivation of multiple embryos, the selected one is transferred to the uterus. The cultivation can last three days till the fertilized oocyte reaches an eight-cell stage or the blastocyst embryo stage after five days. Are there more good-quality embryos as than needed for the transfer, they are often cryopreserved (Van Voorhis, 2007).

1.3.1 Granulosa cells (GCs)

Due to the easy access during ART and the essential roles of GCs in the development of the oocyte and maintenance of pregnancy, luteinised GCs are identified as a valuable tool for studies in reproductive biology (Greenseid et al., 2011). Somatic GCs show as special feature the remaining interaction to the germ cell during growth, differentiation, maturation and fertilization of the oocyte, and they are essential for a successful maturation (Buccione et al., 1990). Due to their significant role within the follicle, GCs are suitable for investigation of physiological and pathological processes within the human ovary. Human primary luteinised GCs can be easily obtained for *in vitro* studies to clarify multiple questions in ovarian functions. The GCs are isolated before the ovulation but were already in contact with LH. GCs and FFs present a suitable model to study mechanisms in mature follicles or CL.

1.3.2 Granulosa-like tumour cell line - KGN

As cultured human GCs do not proliferate and to study proliferation, a crucial mechanism in follicular growth, the granulosa-like tumour cell line KGN was implemented.

The KGN cell line stem from pelvic space tumour diagnosed as ovarian cancer stage III. The cultured cell line maintains most physiological activities including the expression of functional FSHR, as well as the same pattern of steroidogenesis as those observed in primary ovarian GCs (Nishi et al., 2001). Also other similarities including cAMP-inducible aromatase expression and gonadotropin responsiveness makes this cell line attractive for studying ovarian G-protein-coupled-receptor signal transduction. In addition, KGN cells were characterized to a specific mutation in a transcriptome factor involved in proliferation and differentiation in GCs (Tremblay et al., 2017). Therefore, KGN cells became more attractive to study various aspects of physiological regulations of human ovarian GCs.

A recent published transcriptome analysis in KGN revealed that protein kinase A (PKA) and C signalling pathways play an important role in various major functions of ovarian follicle development such as cell differentiation, final maturation, luteinisation, and ovulation (Tremblay et al., 2017). Another transcriptional analysis was performed with KGN cells to reflect that mutant of the transcription factor *FOXL2* is able to differentially regulate the expression of many genes, including *StAR* (Rosario et al., 2012).

1.4 FSH, FSHR and signalling

Follicle stimulating hormone (FSH) is released from the anterior pituitary and targets GCs of growing follicles in the ovary and Sertoli cells in the testis, which both express FSHR (Simoni

et al., 1997). FSH is essential for normal growth and maturation of ovarian follicles in women and for normal spermatogenesis in men (Themmen et al., 2000).

FSH, is a heterodimeric pituitary glycoprotein. It shares an α -subunit with other glycoprotein hormones, and is characterized by a specific β -subunit (Gloaguen et al., 2011). FSH binds to and activates the FSHR, which belongs to the G protein-coupled receptors (7 transmembrane domains receptor family). This leads to the activation of a battery of signalling pathways depending on the developmental and physiological context. In females, FSH mainly acts to regulate ovarian folliculogenesis and steroidogenesis (Das et al., 2018).

The human *FSHR* gene is large and contains more than 1300 single nucleotide polymorphisms (SNPs), of which only eight are located in the coding region. The correct function of FSHR is of high importance. Mutations can cause significant reproductive defects in both sexes (Laan et al., 2012). It has also been reported that FSHR isoforms differ in sensitivity to FSH stimulation, hence they have a significant effect on female serum FSH concentration and ovarian FSH response (Perez Mayorga et al., 2000).

Activation of the FSHR is linked to diverse downstream signalling pathways. In GCs, one of the downstream consequences of FSHR stimulation is the classical $G\alpha_s$ /cAMP/PKA signalling pathway. Hereby, the FSHR couples to $G\alpha_s$ subunit after FSH activation, which in turn induces activity of adenylyl cyclase. The resulting cAMP activates PKA (Gloaguen et al., 2011). As a consequence, many targets in the nucleus or the cytosol are being phosphorylated by the active catalytic subunits of PKA. The mitogen-activated protein kinase (MAPK)/extracellular-signal regulated kinase (ERK) pathway is also induced by FSH (Gloaguen et al., 2011). A further important transduction mechanism linked to FSHR leads to transactivation of the epithelial growth factor receptor (EGFR). A possible mechanism resulting in EGFR activation upon FSH stimulation involves the metalloprotease ADAM17. Once activated by phosphorylation, ADAM17 cleaves pro-EGF-like protein, releasing an EGF-like ligand, which then binds to and activates EGFR (Yamashita et al., 2009). A downstream event of EGFR includes reactive oxygen species (ROS). It has been demonstrated that for growth factors such as EGF, ligand binding stimulated a burst of ROS production. Inhibiting this increase in ROS levels (including hydrogen peroxide; H_2O_2) was shown to block normal signalling induced by EGF (Finkel, 2011). EGFR transactivation also results in activation of Ras, which in turn induces the Raf1/MEK/ERK MAPK module. Furthermore, it has been reported that in GCs, sustained FSH exposure results in a self-activation loop involving the MAPK module (Gloaguen et al., 2011).

In addition to the typical target cells in the gonads, i.e. GCs and Sertoli cells, FSHR was also reported to be expressed on the surface of the blood vessels of a wide range of tumours (Radu et al., 2010). In this context, a recent report showed that in ovarian tumour cells, FSH increased ROS levels (Yang et al., 2014; Zhang et al., 2013). The mechanisms involved are not well known and this aspect has not been described in ovarian GCs, yet.

1.5 Reactive oxygen species (ROS)

1.5.1 Different types of ROS

ROS, by-products of cellular respiration, protein folding, and end products of multiple metabolic reactions, are generated by the sequential addition of electrons to molecular oxygen, forming two different types of radicals, namely free and non-free radicals (Reczek et al., 2015). Free radicals include hydroxyl radical (OH^\bullet), superoxide anion radical ($\text{O}_2^{\bullet-}$), and nitric oxide (NO^\bullet) and among non-free radicals include H_2O_2 and peroxynitrite (ONOO^-) (Spitz et al., 2004). Whereas $\text{O}_2^{\bullet-}$ and OH^\bullet are, due to their unpaired electron, short-lived and highly reactive with cellular macromolecules, H_2O_2 is long-lived and membrane-permeable, and so the only ROS which can diffuse from its site of origin within or among cells, and may specifically act as extracellular, short-range auto-/paracrine signalling factor (Giorgio et al., 2007; Luderer, 2014). Furthermore, it is becoming clear that specifically H_2O_2 plays fundamental roles in cell proliferation, migration and metabolism, as well as cell death (Sies, 2017). H_2O_2 and other ROS play an important role in oxidation of redox-sensitive cysteine residues in proteins altering their function (Jones, 2006, 2008).

1.5.2 Sources of ROS

Several intracellular sources of ROS or modes of generation of ROS exist (Finkel, 2011; Sies, 2017), ranging from the mitochondrial respiratory chain to diverse oxidases, which produce oxidants as part of their normal enzymatic function. During mitochondrial oxidative phosphorylation, oxygen is converted to $\text{O}_2^{\bullet-}$ and H_2O_2 (Finkel, 2011; Giorgio et al., 2007). Enzymes, which produce H_2O_2 , are distributed in the cell including phagocyte NADPH oxidase (NOX) on the cell membranes, peroxisomal oxidases in the peroxisomes, sulfhydryl oxidase in the endoplasmic reticulum (ER), superoxide dismutase (SOD) 1 and cyclooxygenase in the cytoplasm, and SOD2 in the mitochondria (Giorgio et al., 2007). Also, steroidogenic cytochrome P450 enzymes occurring in the ovary (Hanukoglu, 2006) and xenobiotics (Pizzino et al., 2017) can generate ROS.

However, in the human ovary very little is known about these sources, or the mechanisms of their actions compared to animal models. It was shown that ROS levels in IVF-derived, cultured human GCs are increased upon cellular uptake and intracellular enzymatic metabolism of the catecholamines dopamine and norepinephrine in FF. The studies suggest that dopamine and the dopamine-metabolizing enzymes monoamine oxidases are players in the human ovarian follicle, which in a dopamine-independent way appear to contribute to ROS homeostasis (Blohberger et al., 2016; Saller et al., 2014; Saller et al., 2012). ROS generation in GCs was also increased upon activation of EGFR induced by FSH, as well as pigment epithelium derived growth factor (Adam et al., 2012; Kampfer et al., 2014).

The major enzymatic generator of intracellular oxidants is, however, a family of transmembrane-bound enzymes, called NADPH oxidases.

1.5.3 Functional roles in the ovary

ROS and reactive nitrogen species (RNS) are generated in the body and although historically considered as purely damaging, function as physiological regulators of hormone actions and signalling pathways, to affect e.g. processes in the female gonad (Finkel, 2011; Reczek et al., 2015).

It is still not well known what roles physiological ROS levels may play, but reports about the beneficial functions of ROS in many physiological events is increasing, as well as in the homeostasis of ovarian follicles. In fact, follicular vascularity, intrafollicular oxygen content and mitochondrial activity are factors supporting an optimal oocyte development (Finkel, 2011; Maraldi et al., 2016). Consequently, some studies found a positive correlation between FF ROS levels and maturation parameters. For example, ROS were reported to improve bovine oocyte developmental potential during *in vitro* maturation and women with a positive IVF outcome had significantly higher ROS levels in the FF than non-pregnant patients (Attaran et al., 2000; Revelli et al., 2009). Another study in mice confirmed that ROS plays an important role in oocyte maturation. They stated that NOX and its ROS products are essential to FSH-induced cumulus-oocyte complex maturation (Chen et al., 2014). Low levels of ROS may trigger oocyte maturation following the LH surge (Downs et al., 1988).

In response to the pre-ovulatory gonadotropin surges, antioxidant levels fall and ROS levels rise. Studies provide the evidence that the absence of ROS prevent ovulation as well as a whole repertoire of essential pre-ovulatory responses. ROS are indispensable ovarian molecules for ovulatory-associated cellular events like cumulus expansion or LH-induced progesterone production by pre-ovulatory follicles. Furthermore, ROS in GCs appear to act as mediators of p42/44 MAPK-signalling, which implicates an important role of redox signalling in the ovary (Sato et al., 1992; Shkolnik et al., 2011).

There are some published studies in animal models elucidating possible roles of ROS such as a work in the rat revealed roles in ovulation (Shkolnik et al., 2011). In the CL, ROS are beneficial for steroid production shown in a rat model (Carlson et al., 1993).

Nonetheless, the precise role that ROS play remains controversial and very less is known about these processes in humans (Finkel, 2011).

1.5.4 Oxidative stress (OS) and fertility

ROS are a “double-edged sword” due to the fact that a dysregulation of ROS levels may cause or accelerate pathological conditions. OS, a state characterized by an uncontrolled accumulation of ROS, has been identified to play a key role in infertility in males and females (Avila et al., 2016; Devine et al., 2012; Finkel, 2011; Jones, 2006, 2008). Multiple reasons leading to OS are e.g. environmental changes, lifestyle changes, pathological conditions or drugs treatment (Agarwal et al., 2012).

Regarding spermatogenesis, it has been reported that OS secondary leads to increased lipid peroxidation, biomembrane damage or protein and DNA damage of sperm (Avila et al., 2016). The maturation of an oocyte depends on a complex process of proliferation and differentiation of several cell types during follicle development that govern gamete quality. Systemic and local studies regarding process of follicular maturation, oocyte quality, and global fertility efficiency in combination with the level of OS resulted in direct relationship between fundamental processes and OS in the ovary. These processes include atresia of primordial and primary follicles, oxidative damage of lipids resulting in poor oocyte quality, oocyte fertilization, early embryonic development, and decreased female fertility (Luderer, 2014; Prasad et al., 2016; Rizzo et al., 2012). It has been reported that increased levels of OS markers and decreased levels of antioxidants are related to poor IVF outcome (Avila et al., 2016). The repeated ovarian stimulation by exogenous gonadotropin induces OS in the ovary and leads to ovulation of poor quality oocytes (Prasad et al., 2016). OS is known to play a pathogenic role in endometriosis (Nassif et al., 2016) and polycystic ovarian syndrome (PCOS) (Avila et al., 2016). An increase in OS in the GCs correlates with reduced expression of FSHR and may be implicated in poor response of FSH in women with aging (Avila et al., 2016).

1.5.5 Hydrogen peroxide - a signalling molecule

Hydrogen peroxide (H_2O_2) is a long-lived and the only membrane-permeable ROS (Schroder et al., 2012). H_2O_2 can be converted into OH^\bullet , see Figure 4 (Bienert et al., 2006). It acts as signalling molecule in various cellular processes as either a paracrine or an autocrine signal.

An intercellular signalling function means that the signal molecule needs to be transported across at least one membrane. The extracellular enzyme activities of NOX enzymes localized on the PM result in the generation of extracellular ROS, including H_2O_2 (Bienert et al., 2014).

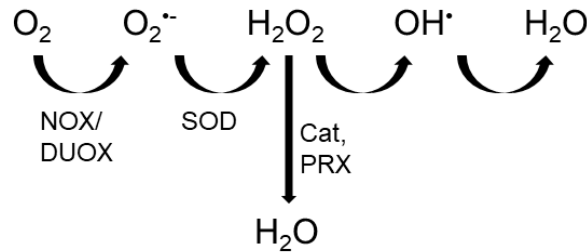


Figure 4 - Conversion of H_2O_2 into ROS. H_2O_2 can be converted into other more reactive ROS by various means including enzymes. The reduction of the hydroxyl radical to water occurs non-enzymatically. Modified after (Bienert et al., 2006)

For a long time, it has been known as a hazardous ROS with the potential to damage proteins, lipids and nucleic acids. However, recently, the picture of H_2O_2 has changed towards seeing H_2O_2 as having an indispensable role in a large variety of pathways. It plays an essential role in the redox signalling network, and hence in cell proliferation, migration and death (see Figure 5). As one of the most abundant and stable ROS molecules in the organisms, H_2O_2 regulates a large set of developmental and physiological processes as well as stress response within the cells. Either it triggers directly chemical reactions or influences responsive targets, or it acts via signalling pathways involving MAPKs (Bienert et al., 2014). It has been reported that MAPKs are activated in response to H_2O_2 (Bienert et al., 2006). However, the regulation of H_2O_2 signalling is not fully understood and might take place at multiple levels in the signalling pathway from receptor to nucleus.

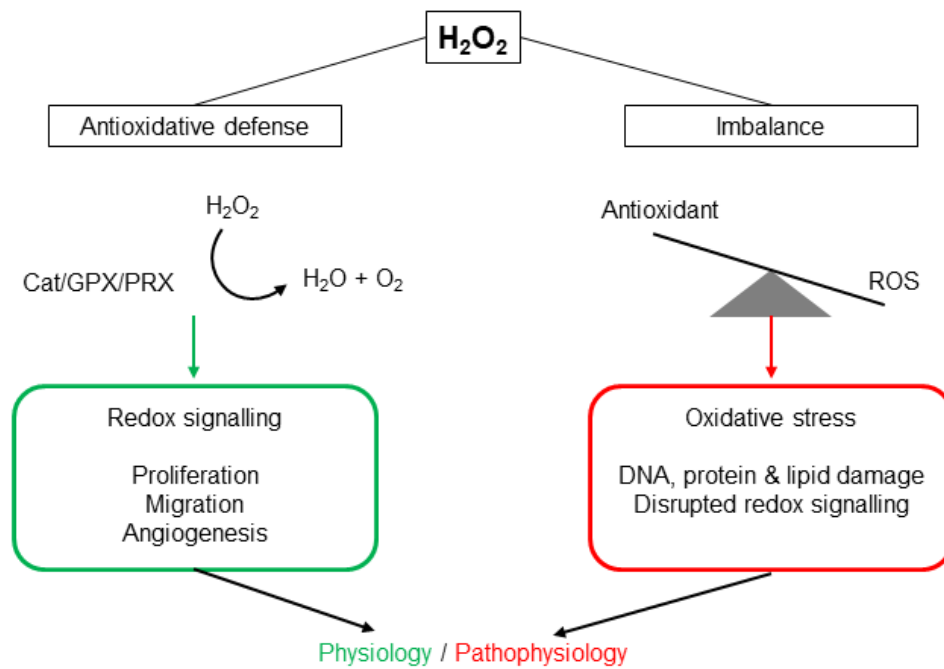


Figure 5 - Role of H_2O_2 in redox signalling and in oxidative damage. NOX enzymes are activated upon ligand-receptor interaction, and extracellular SOD converts the $O_2^{\cdot-}$, generated by NOX, to H_2O_2 , which is imported by AQPs (peroxiporins).

1.6 Characteristics of NADPH oxidases (NOX)

1.6.1 Function, structure, and activation

The phagocyte NADPH oxidases (NOX) are enzymes, which generate ROS not as by-products, but rather as the primary function of the enzyme system. They produce ROS by moving an electron across cellular membranes and transferring it to oxygen. Thereby, they generate the $O_2^{\cdot-}$, which usually is very rapidly dismutated to H_2O_2 (Bedard et al., 2007; Lambeth et al., 2014). This function is not limited to phagocytes, but the ROS-producing enzymes are described in essentially every tissue (Bedard et al., 2007; Sirokmány et al., 2016). NOX enzymes have been reported to be involved in host defence, hormone synthesis, fertilization, cell proliferation and differentiation (Bedard et al., 2007; Lambeth et al., 2014).

NOX enzymes are multicomponent, transmembrane proteins, of which seven members are known: NOX1-5 and dual oxidases (DUOX) 1 and 2; see Figure 6 and e.g. (Guo et al., 2015; Sirokmány et al., 2016; Wong et al., 2004).

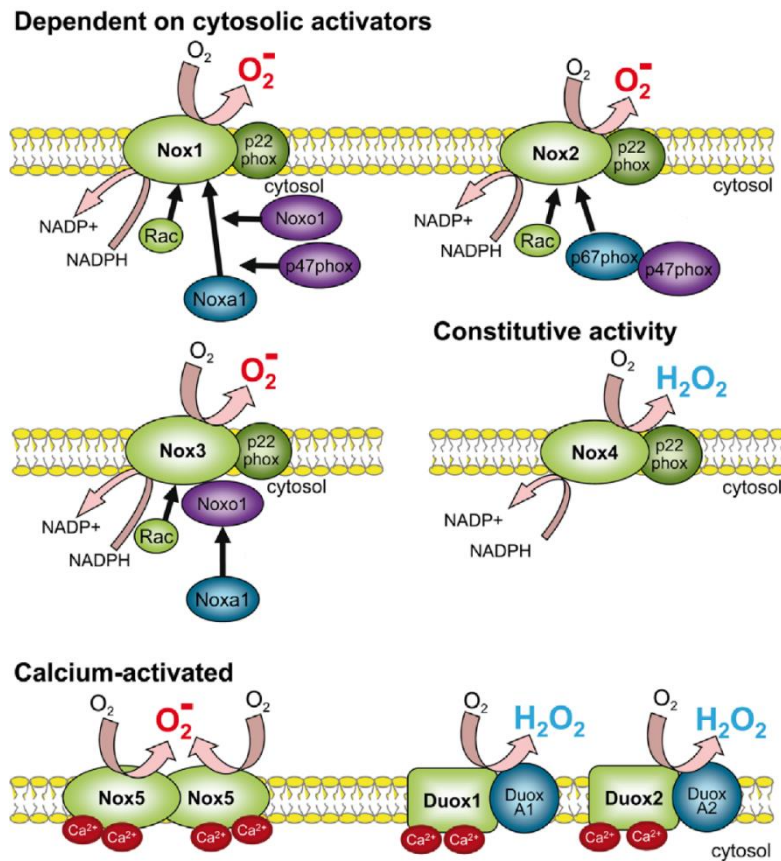


Figure 6 - Composition of NOX enzyme complexes. Seven NADPH oxidase enzymes have been described and can be classified by domain structure, regulation, and ROS product. All NOX isoforms are membrane proteins that are localized in the PM or cellular compartments' membranes. Oxidase activity occurs when NADPH binds to NOX on the cytosolic side, where it transfers electrons to oxygen on the outer membrane surface. Stabilizing or maturation factors of NOX1-4 are p22^{phox} in green and DUOXA1/2 for DUOX enzymes in blue. Modified from (Brandes et al., 2014).

The members of the NOX family differ according to the ROS that is produced (Table 1). NOX1-3 and NOX5 generate primarily O_2^- , whereas the major product of NOX4, DUOX1, and DUOX2 is H_2O_2 (Lambeth et al., 2014).

The enzyme family originates from phagocytic cells and contains a homologous catalytic subunit, NOX (Altenhofer et al., 2015; Sirokmány et al., 2016). All family members have some conserved structural properties in common: 1. a NADPH-binding site at the C-terminus, 2. a FAD-binding region, 3. six transmembrane helices, and 4. four highly conserved heme-binding histidines (Bedard et al., 2007). The name dual oxidase 1 and 2 originate from an additional transmembrane domain and an extracellular N-terminus containing a peroxidase-like domain. The transmembrane protein is dependent on interaction partners for the correct trafficking to its site of activity, its maturation and heme incorporation, as well as for maturation and stabilization (Brandes et al., 2014). There are cytoplasmic and membrane-associated proteins (Table 1), as well as stimuli like calcium, which interact with NOX members increasing the enzymatic ROS production (Altenhofer et al., 2015; Meitzler et al., 2014). All NOX homologues

except NOX5 have the same interaction partner, namely p22^{phox}, a small membrane-bound associate factor that is necessary for complex formation and stability.

NOX4 presents a constitutively active form due to the fact that no other activation requirements, aside from interaction with p22^{phox} is needed (Meitzler et al., 2014). NOX5, DUOX1 and 2 do not need additional activating subunits, but are activated by Ca²⁺ (Bedard et al., 2007). DUOX1 and 2 are required as scaffold for maturation and proper function of DUOX1 and 2 (Brandes et al., 2014).

1.6.2 Localization and distribution

While the NOX family seems to be widely distributed from the kidney, and the thyroid tissues to the brain and inner ear, cellular localization is somewhat less diverse (see Table 1).

DUOXs were found in different tissues (DUOX1 in the mammalian thyroid and in respiratory epithelia; DUOX2 in the thyroid and in gastrointestinal glandular epithelia), but not yet in the human gonads. A reproductive role in an insect was reported for DUOX-generated H₂O₂ that fuels egg chorion hardening, and thereby plays an essential role during eggshell waterproofing (Dias et al., 2013). In contrast, the NOX4 and NOX5 forms were found in the human gonads. Of those, NOX4 and 5 were described in human GCs previously by RT-PCR (Kampfer et al., 2014), NOX1-3 were not found, and DUOX1 and 2 were not studied yet.

NOX5 is also the least well understood of the NOX isoforms, since the gene is not present in mice or rats (Bedard et al., 2007). NOX5, the Ca²⁺-activated NOX isoform, is highly expressed in human testis. In ovary, expression of NOX2, in addition to NOX4, and NOX5 was reported, but it is very likely that ovarian NOX2 originates from leukocytes (Cheng et al., 2001). That leaves NOX4 and 5 specifically found in the (human) male and female gonad, but the knowledge about expression and functional roles in testis and ovary is at best rudimentary.

Table 1 - Characteristics and expression sites of NADPH oxidase family. Modified after (Bedard et al., 2007; Meitzler et al., 2014)

Enzyme	Interaction partners	Cellular localization	Major tissue distribution	ROS products
NOX1	p22 ^{phox} , NOXA1/p67 ^{phox} , NOXO1/p47 ^{phox} , Rac	PM, lipid rafts	Colon epithelium	O ₂ ⁻
NOX2	p22 ^{phox} , p67 ^{phox} , p47 ^{phox} , Rac	PM	Phagocytes	O ₂ ⁻
NOX3	p22 ^{phox} , NOXA1/p67 ^{phox} , NOXO1/p47 ^{phox} , Rac	PM	Inner ear	O ₂ ⁻
NOX4	p22 ^{phox}	PM, ER, mitochondrial and nuclear membranes	Kidney, ovary, brain	O ₂ ⁻ /H ₂ O ₂

NOX5		PM, ER, nuclear membrane	Spleen, testis, lymph nodes	$O_2^{\cdot-}$
DUOX1	DUOXA1	PM	Thyroid, lung, prostate, testis	H_2O_2
DUOX2	DUOXA2	PM, ER, vesicles	Thyroid, salivary gland, colon, pancreas	H_2O_2

1.6.3 NOX4

In the year 2001, a novel non-phagocytic NOX enzyme NOX4 was identified in the kidney (Shiose et al., 2001). Compared to the other homologues, NOX4 is highly expressed, demonstrates unique structures, and results therefore in the only isoform producing constitutively H_2O_2 (Brown et al., 2009). Another ROS released from NOX4 is $O_2^{\cdot-}$, however due to its rapid conversion to H_2O_2 by SOD, it is almost undetectable (Brown et al., 2009).

In general, NOX4 tissue distribution is ubiquitous, and NOX4 shows an especially high expression in kidney and blood vessels. The sub-cellular localization of NOX4 is cell-type specific and ranges from mitochondria, ER, focal adhesions, nucleus, and PM (Block et al., 2009).

The NOX4 gene is located on chromosome 11 and the existence of four NOX4 splice variants has been reported (Bedard et al., 2007). The other NOX genes are located on chromosome 22 (Guo et al., 2015).

As mentioned above, NOX4 only requires the membrane subunit p22^{phox} for ROS-producing activity. It has been shown that the activity of NOX4 is proportional to NOX4 protein expression alone (Brown et al., 2009). The regulation of protein expression is not clearly understood yet, but there is a series of exogenous and endogenous stimulus. A number of stimuli have been identified as transcriptional regulators: hypoxia, angiotensin II (Ang II), platelet-derived growth factor (PDGF), transforming growth factor β (TGF- β) and insulin, see Figure 7 (Brown et al., 2009; Guo et al., 2015).

NOX4-derived ROS production has multiple faces in regulating the cellular physiology and pathology. While high levels of ROS and dysregulated production cause cell damage and death, ROS at regulated levels serve as second messengers. Notably, NOX4-derived H_2O_2 promotes cell proliferation in multiple cell types. Moreover, it activates MAPK family members, which phosphorylate and activate MEF2C, a transcription factor important in cardiomyocyte differentiation (Guo et al., 2015). It also upregulates MAPK phosphatase-1 (MKP-1), which reduces activation of extracellular signal regulated kinase (ERK) 1/2. Cell migration plays essential roles in physiology including wound healing and embryogenesis and multiple evidences showed that NOX4 is involved in this process. Activation of matrix metalloprotease (MMP)-2 initiating migration is induced by insulin-like growth factor-1 (IGF-1) that is mediated

by NOX4. Previous reports showed that NOX4 is involved in cell death inducing apoptosis in many cells. Data suggested that NOX4 plays a role in TGF- β and tumour necrosis factor (TNF)- α -induced oxidative stress (OS) leading to apoptosis (Guo et al., 2015).

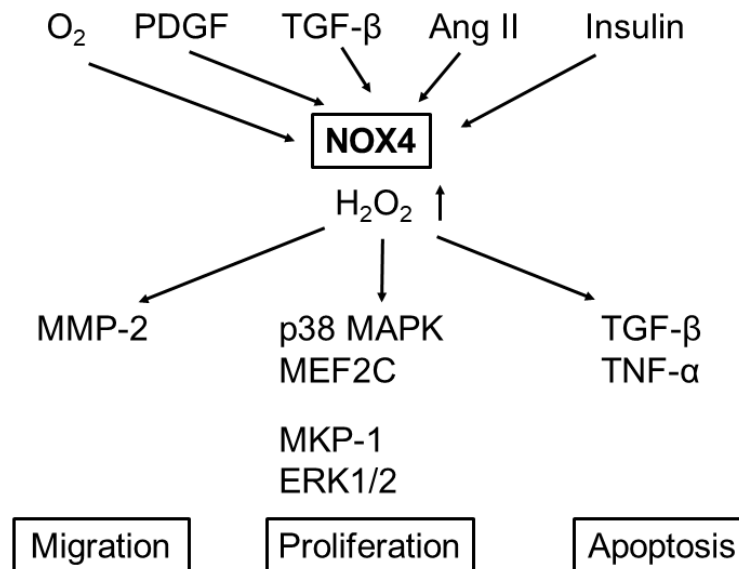


Figure 7 - Signalling pathways of NOX4. NOX4-derived H₂O₂ is thought to be elevated by multiple exogenous and endogenous stimulus followed by activation of downstream redox sensitive proteins. Downstream signalling by NOX4 activity occurs in many fundamental cellular processes like cell proliferation, migration and apoptosis. Modified after (Guo et al., 2015).

Interestingly, a recent study not only confirmed expression of NOX4 in IVF-derived GCs, but demonstrated lower NOX4 levels in GCs from women older than 40 years (Maraldi et al., 2016). This correlates with the naturally occurring decline in fertility with age. Beneficial and physiological roles of H₂O₂ and NOX4 have also been reported for the vasculature (Sies et al., 2017).

1.7 Aquaporins/porixiporins

H₂O₂, which is produced in membrane-surrounded organelles, such as mitochondria, peroxisomes, nuclei, and the ER, as well as at the PM, has been demonstrated to act as a signal molecule outside these organelles and inside the cell. This is of particular interest here, since an intracellular signal needs to be kept within a cell, while an extracellular signal implies that the signal molecule needs to be transported across at least one membrane: 1. the PM of the H₂O₂-producing cell and 2. the PM of H₂O₂ signal-perceiving cell. In neither case, unlimited diffusion of H₂O₂ across membranes would be compatible with its role as a signal molecule and both mechanisms again imply that there is a need to control transport of H₂O₂ across membranes. Experimental findings have suggested, that aquaporins (AQPs) are responsible

for the facilitated diffusion of H_2O_2 across membranes (Bienert et al., 2014; Bienert et al., 2007; Bienert et al., 2006).

AQPs are part of the major intrinsic proteins (MIPs), a large family of transmembrane channel proteins, and also known as water channels. The AQP family consists of small membrane-spanning proteins (monomer size around 30 kDa) that are present at PMs in many cell types. These proteins consist of cytoplasmic N and C termini and six membrane spanning α -helical domains (Verkman et al., 2000). MIPs build tetramers, in which a monomer presents a hydrophilic bidirectional channel pathway facilitating the transport of substrates given by their chemical gradient. Several AQPs are highly selective for the passage of water, whereas others also transport glycerol or a variety of metabolically important small uncharged solutes, like urea, carbon dioxide, nitric oxide, and H_2O_2 (Bienert et al., 2014).

Some AQPs (3, 8 and 9) facilitate the transport of H_2O_2 across biological membranes, for which they are called peroxiporins (Miller et al., 2010; Sies, 2017; Watanabe et al., 2016).

1.8 Antioxidant defence mechanisms

As mentioned above, a complex set of antioxidant molecules is needed for the maintenance of intracellular redox homeostasis (Figure 5). To ensure an equilibrated cellular homeostasis, a correct balance between the production of oxygen radicals and antioxidant agents is of crucial significance (Gupta et al., 2014). Hence, there are two cellular protective mechanisms against ROS generation: first, activation of expression of enzymes neutralizing ROS, mainly SOD, catalase (Cat), peroxiredoxin (PRX), glutathione peroxidase (GPX), and second, neutralizing ROS by several antioxidant substances like albumin, glutathione or vitamin C (Birben et al., 2012). But also AQPs play an important role by regulating the transport of H_2O_2 (Patterson et al., 2015). Cat, GPXs and PRXs e.g. convert H_2O_2 to water, while SODs convert O_2^- into H_2O_2 . However, the relative contributions of these enzymes in ROS removal depend on the site of generation and the enzymatic equipment (Sies, 2017). So, GPXs and PRXs are likely distributed in multiple cell compartments (e.g. the cytosol, mitochondria, and ER), whereas the occurrence of Cat is mostly limited to the peroxisomes (Reczek et al., 2015). Nonenzymatic antioxidants including the vitamins ascorbic acid, vitamin E, and vitamin A directly scavenge free radicals (Luderer, 2014).

An adequate balance between the production of oxygen radicals and these antioxidant agents is of utmost importance for the maintenance of cellular homeostasis allowing appropriate cellular development and function. An imbalance leads to increased damage to the main types of cellular molecules and induces OS (Avila et al., 2016).

1.9 Aims of the study

Although historically viewed as purely harmful, recent evidence suggests that reactive oxygen species (ROS) function as important physiological regulators of intracellular signalling pathways. Emerging evidence suggests that ROS regulate diverse physiological parameters ranging from the response to growth factor stimulation to the generation of the inflammatory response, and that dysregulated ROS signalling may contribute to a host of human diseases including oxidative stress (OS). OS may contribute to several diseased states affecting female reproduction. However, it became clear that hydrogen peroxide (H_2O_2), an oxygen metabolite and messenger molecule, serves fundamental regulatory functions in metabolism beyond the role as damage signal. One important generator of ROS is a family of membrane-bound enzymes that rely on NADPH for their activity. The only clear function of these NADPH-dependent oxidases (NOX) is the regulated generation of ROS.

The central question of this study was to clarify the sources and roles of ROS in the human ovary. Therefore, NOX enzymes in in-vitro fertilization (IVF)-derived, differentiated GCs were examined by focusing on NOX4 as a H_2O_2 -producing enzyme. Because primary IVF-derived GCs do not proliferate and to explore a possible involvement of NOX4-derived H_2O_2 in proliferation, the granulosa-like tumour cell line KGN was used as additional model of this study.

The first aim of the dissertation was to explore whether IVF-derived cultured human granulosa-lutein cells and KGN cells express functional NOX4, linked to the production of H_2O_2 . This was approached by the elucidation of gene and protein expression using cultured cells as well as ovarian sections. Functional, cellular studies verified the production of specific ROS species.

Follicular stimulating hormone (FSH) and human chorionic hormone (hCG) are central regulators of female reproductive function and extensively used in reproductive medicine and assisted reproductive technology. However, these gonadotropins are involved in downstream signalling pathways including ROS generation, possibly via the NOX enzymes, which could result in noxious consequences. Thus, the second aim was to explore whether the gonadotropic hormones FSH/hCG are involved in ROS production.

H_2O_2 modulates the activity of phosphatases and many other signalling molecules through oxidation of redox-sensitive cysteine residues in proteins, which led to the notion that initiation of ROS signalling is broad, and may play an essential role in signalling pathways in the human ovary. Hence, a third question of this study was: what are the functional roles of physiological H_2O_2 in ovarian cells?

2. Results

2.1 NOX and ROS in cultured human GCs

2.1.1 Identification of NOX

The presence of the NOX family *in vitro* was shown by RT-PCR and Western blotting experiments. RT-PCR followed by sequencing revealed that GCs on the day of isolation (day 0 = d0) and on culture day 3 (d3) express *NOX4*, *NOX5*, and *DUOX1* and *DUOX2* (Figure 8A). This experiment was repeated using n = 5 independent pooled GC preparations. *NOX1-3* are not expressed by GCs as described previously (Kampfer et al., 2014).

NOX4 protein was detected in three GC preparations by use of a specific anti-*NOX4* antibody and WB (Figure 8B; *NOX4*: 68 kDa). Also, *NOX5* was detectable at the expected size of 86 kDa (Figure 8C; n = 3). Experimental studies on *DUOX1/2* were limited by the lack of specific antibodies.

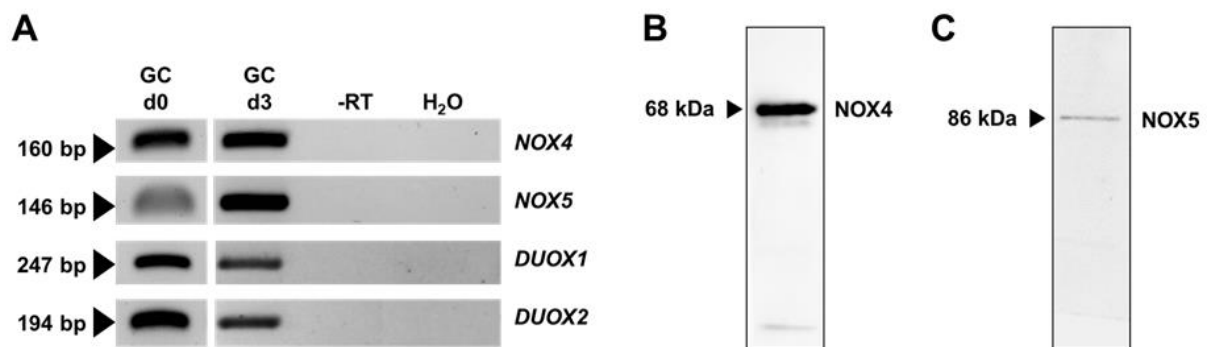


Figure 8 - NOX expression in cultured human GCs. (A) RT-PCR identified *NOX4/5* and *DUOX1/2* after isolation (d0) and on culture day 3 (pooled GCs from two to five individuals). Controls including RNA (-RT) and H₂O instead of cDNA (H₂O) were negative. (B) *NOX4* protein was detected by WB (Antibody No. 1). (C) The identification of *NOX5* was confirmed by WB.

2.1.2 Localization of *NOX4* and *NOX5*

To localize *NOX4*, immunocytochemistry was performed using the same antibody as for WB (Table 9), and *NOX4* protein was identified in the cytoplasm and the nucleus of GCs on culture day 3 (Figure 9; experiment repeated with four independent GC pools). Negative controls of all immunocytochemical experiments performed without primary antibody did not show any staining (data not shown).

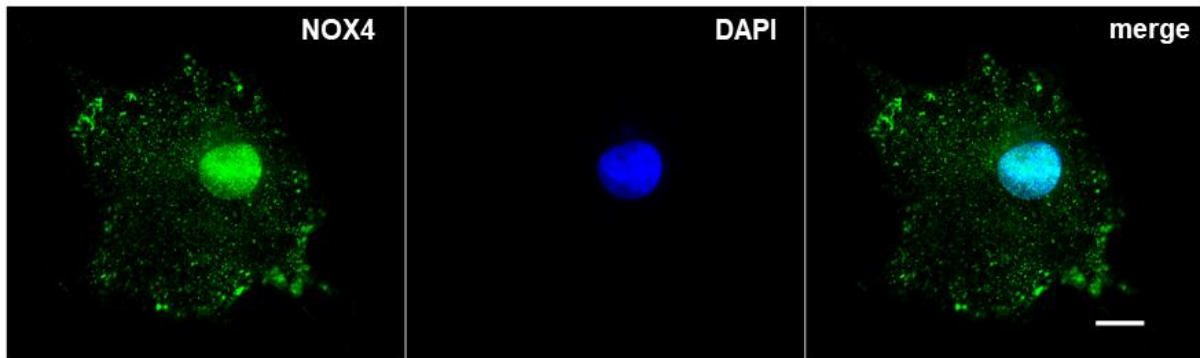


Figure 9 - Localization of NOX4 in cultured human GCs. Localization of NOX4 (green) was detected by immunocytochemistry. Staining in intracellular compartments and the nucleus (blue: DAPI counterstain) of GCs (d3; antibody No. 1). Scale bar = 10 μ m.

NOX5 localization was detected in GCs on culture day 2 mainly in intracellular compartments. Staining was also seen in organelle-like membranes, and nucleus lacked staining.

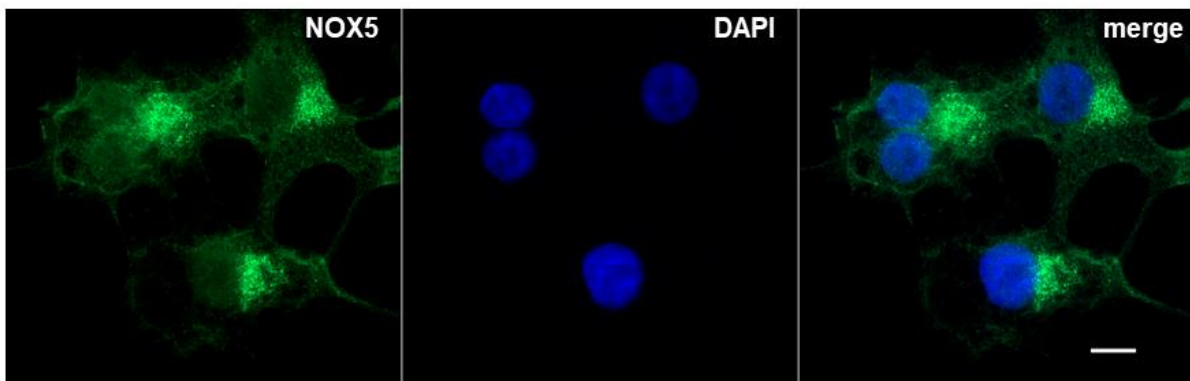


Figure 10 - Localization of NOX5 in cultured human GCs. NOX5-positive staining (green) on culture day 2 (blue: DAPI counterstain). Scale bar = 10 μ m.

2.1.3 Localization of NOX4 in ovarian tissue

Immunohistochemistry revealed NOX4 in preantral and antral follicles of different sizes and the CL of the human ovary. Follicular GCs, theca cells, and small and large luteal cells were stained in the cytoplasm (Figure 11). This staining pattern was obtained with the same antibody as used for the WB (Figure 11). Specificity of this antibody was shown by replacing the primary antibody by serum (serum control), which lacked staining (Figure 11D+F).

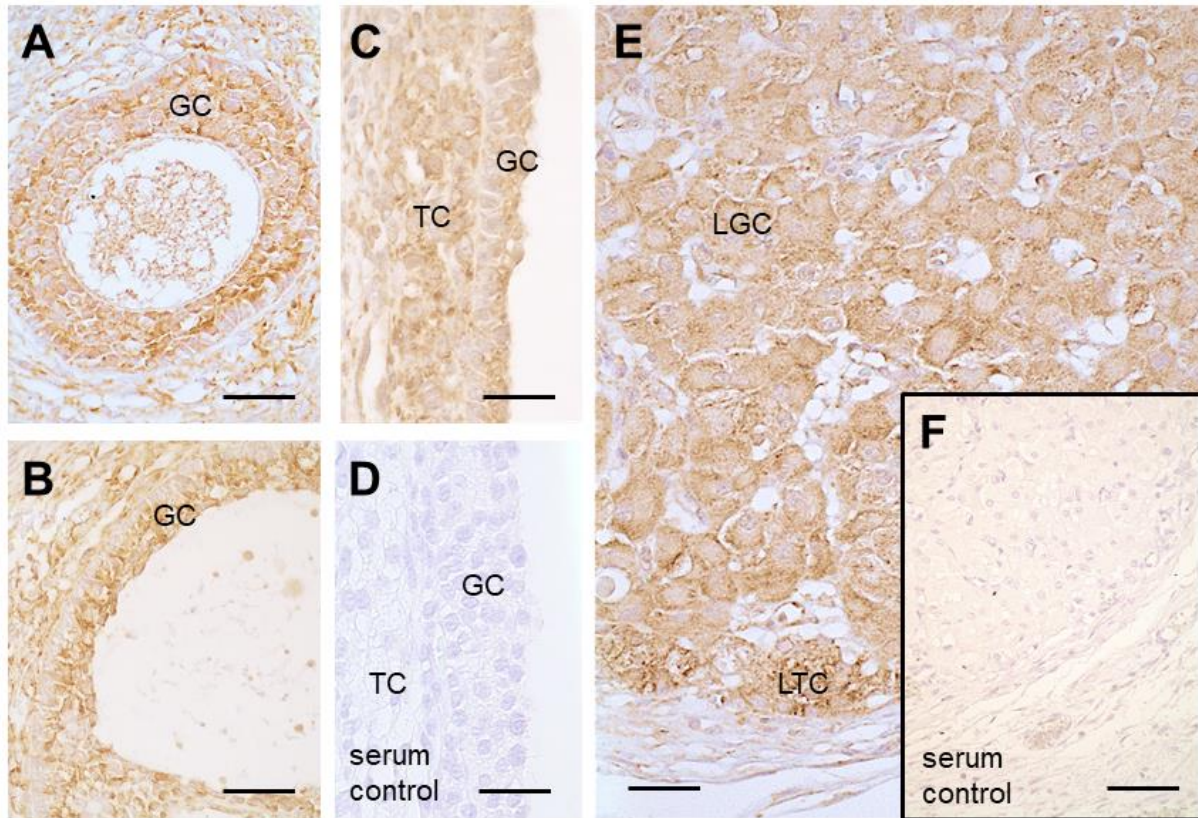


Figure 11 - Presence of NOX4 in ovarian cells *ex vivo*. Immunohistochemistry using human ovarian sections and anti-NOX4 antibody (No. 1) showed positive staining for NOX4 in granulosa (GC) and theca cells (TC) of a secondary follicle (A), of a small antral follicle (B), of a large antral follicle (C) as well as in luteinised GC (LGC) and luteinised TC (LTC) of the CL (E). Serum controls lacked primary antibody and are negative (D and F). Scale bars: A-E= 30 μ m, F = 50 μ m.

2.1.4 Functional activity of NOX4

To examine the function of NOX4, the general ROS production and specific ROS, namely H_2O_2 and $\text{O}_2^{\cdot -}$ were determined. Fluorometrical measurements of ROS employing H_2DCFDA (Figure 12A; n = 8 GC pools) and measurements of H_2O_2 by Amplex[®] Red reagent (Figure 12B; n = 4) confirmed basal generation of ROS, including H_2O_2 . $\text{O}_2^{\cdot -}$ was detected only in small amounts (Figure 12C; n = 4) by the oxidation of luminol. An increase in ROS, and specifically in H_2O_2 during the 2 h measurement-period was seen in all independent measurements. The initial values and increments differed, which is likely due to heterogeneity of primary cells taken from different patients.

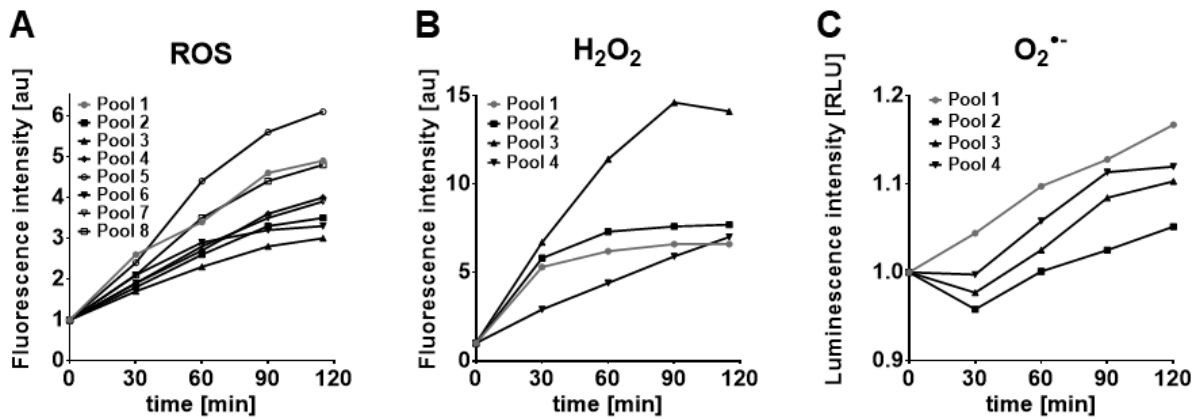


Figure 12 - Basal ROS including H₂O₂ and O₂^{•-} production of cultured human GCs. Basal production of ROS (identified by the indicator dye H₂DCFDA, n = 8), specifically of H₂O₂ (measured by Amplex[®] Red, n = 4) was measured on culture day 2 to 4 for 2 h (A+B). (C) Graph shows basal production of O₂^{•-} determined by chemiluminescence measurements over 2 h on culture day 2 to 3 (n = 4). Each line presents an independent measurement of a patient pool, and results are presented as mean only (six technical repetitions) and as fold-change relative to t₀.

To inhibit the activity of NOX4, the specific NOX4-blocker GKT137831 was added 24 h prior measurement. The blocker significantly reduced ROS generation by 55 % and H₂O₂ production by 36 %, respectively, after 2 h of measurement (Figure 13A+C). Data are depicted as percentage deviation between blocked values and control values at endpoint of 2 h. Also, the values of inhibited versus control group of a representative measurement over 2 h is shown (Figure 13B+D; n = 1). Values are shown as mean only of six technical replicates.

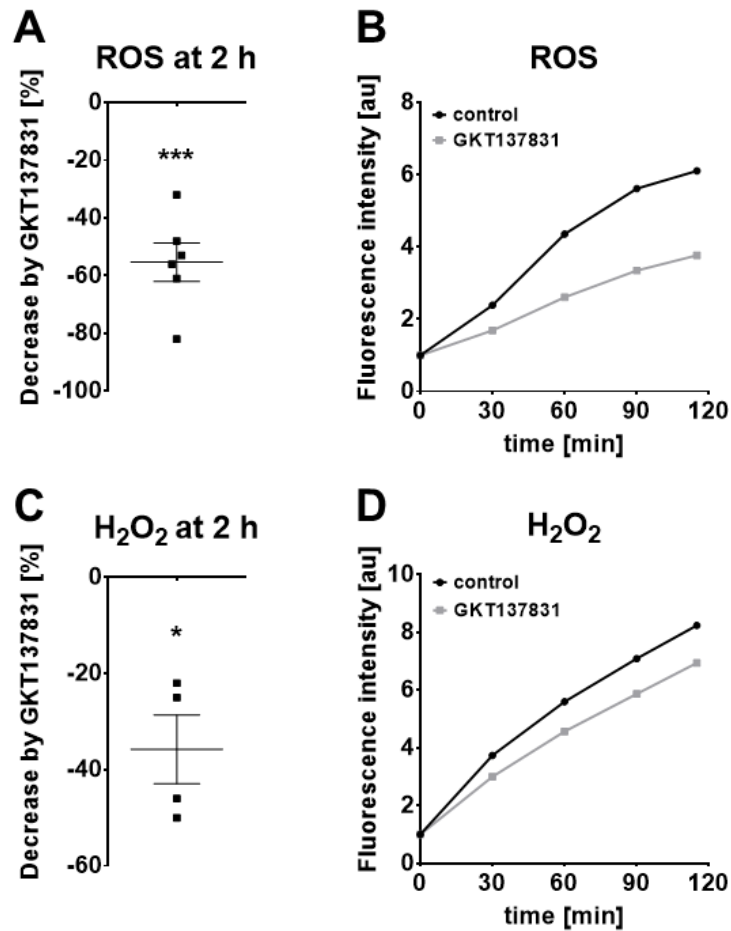


Figure 13 - Inhibition of NOX4 activity in cultured human GCs. The NOX4 blocker GKT137831 (20 μ M) reduced the ROS/H₂O₂ levels. Endpoint values at 2 h (means \pm SEM) of multiple independent measurements show significant reduction of ROS production by 55 % (A; n = 6) and of H₂O₂ generation by 36 % (C; n = 4). (B) and (D) show the measurements of one representative example (mean only) over 2 h. Statistics: one-sample *t* test, theoretical mean: 0 (* $p < 0.05$; *** $p < 0.001$).

To exclude cytotoxic effects of the blocker, the ATP content and cell morphology of treated cells were determined. The blocker did neither affect ATP content consequently cell viability nor morphology of GCs after 24 h treatment (Figure 14; n = 3).

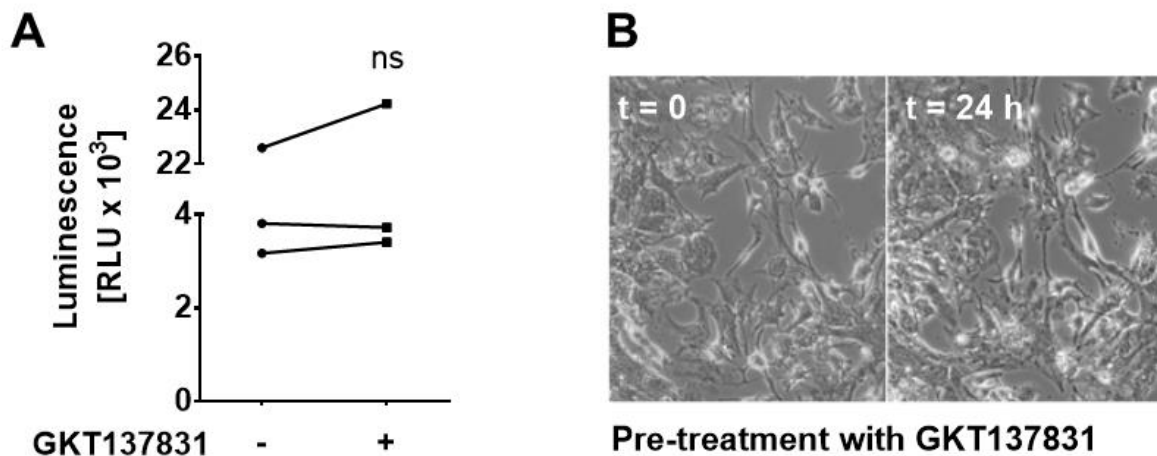


Figure 14 - GKT137831 did not affect viability and morphology of cultured human GCs. 24 h pre-treatment with 20 μ M GKT137831 did neither alter ATP content in GCs (indicator for viable cells), compared to control group (A; n = 3), nor did it change cell morphology (B). Statistics: paired *t* test with single measurements.

2.1.5 Influence of FSH and hCG

2.1.5.1 Regulation of receptors and signalling pathways

FSH and LH/hCG are considered the principal reproductive hormones. Consequently, cultured human luteinised GCs express receptors for both (Figure 15 and (Simoni et al., 1997)).

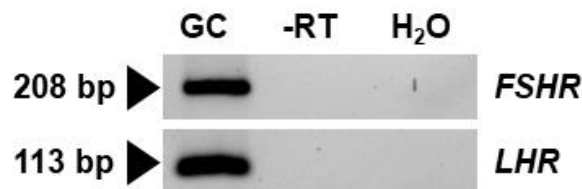


Figure 15 - Expression of *LHR* and *FSHR*. RT-PCR identified *FSHR* and *LHR* in pooled GCs on culture day 4. Controls including RNA (-RT) and H₂O instead of cDNA (H₂O) were negative.

FSH treatment (2 h) yielded an increased MAPK phosphorylation as revealed by immunoblotting (Figure 16A). Three out of four experiments resulted in elevated protein levels of pMAPK compared to MAPK of FSH treated GCs normalized to control cells (data not shown). Also, 24 h treatment of FSH/hCG influenced mRNA levels of *ADAM17*, a metalloprotease involved in activation of EGFR.

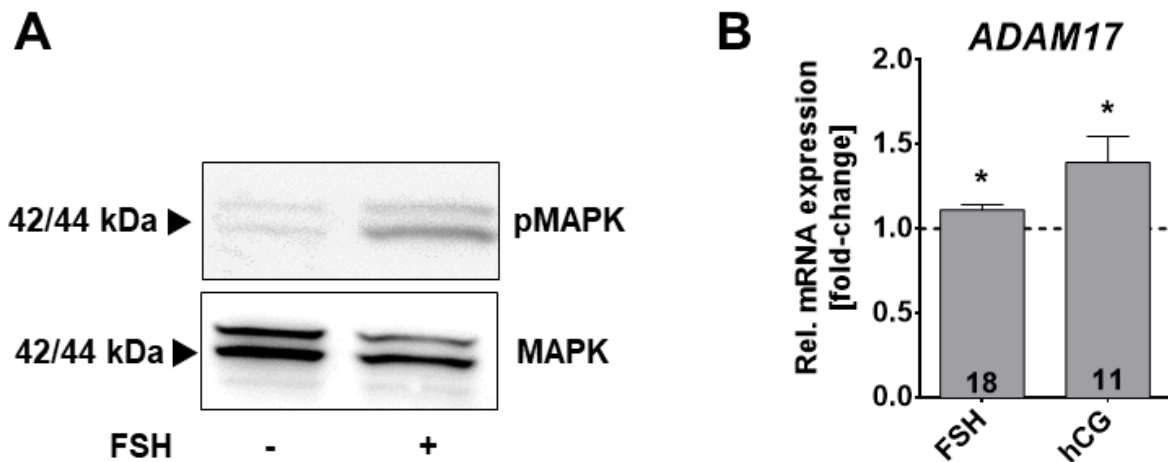


Figure 16 - FSH increases phosphorylation of MAPK and mRNA levels of *ADAM17*. (A) WB membrane of a representative example shows the increase in phosphorylated MAPK in GCs on culture day 4 after FSH treatment (2 h). (B) qRT-PCR revealed that mRNA levels of *ADAM17* were significantly elevated after hormonal stimulation (24 h). All values shown were normalized to *RPL19* (means \pm SEM). For statistics, $\Delta\Delta Cq$ values were used. Numbers of repeated experiments are shown inside the columns. Statistics: one-sample *t* test, theoretical mean: 1 (* $p < 0.05$).

FSH/hCG showed a complex influence on mRNA levels of *FSHR* and *LHR* (Figure 17). FSH increased mRNA expression level of *LHR*, while hCG elevated *LHR*, but decreased *FSHR* expression.

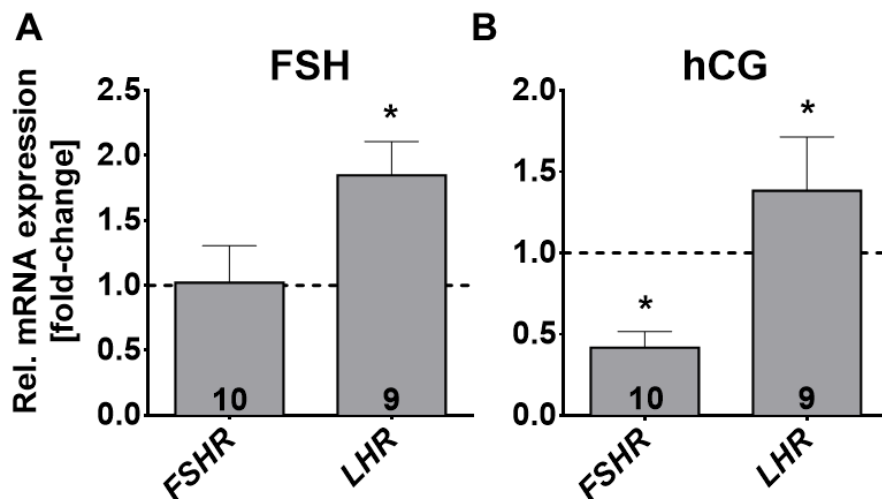


Figure 17 - FSH/hCG influences receptors. FSH significantly increased expression of *LHR* and hCG of *FSHR*, respectively, as seen by qRT-PCR. All values shown were normalized to *RPL19* (means \pm SEM). For statistics, $\Delta\Delta Cq$ values were used. Numbers of repeated experiments are shown inside the columns. Statistics: one-sample *t* test, theoretical mean: 1 (* $p < 0.05$).

2.1.5.2 FSH/hCG and ROS production in cultured human GCs

The hormonal treatment with FSH/hCG did not influence the basal ROS production of cultured GCs. Neither the acute stimulation nor the hormonal pre-treatment had any consequences on ROS production. Overall ROS generation after 2 h of stimulation with 1 IU/ml FSH or 10 IU/ml hCG was measured over 2 h (Figure 18). All values are depicted as mean \pm SEM from four independent experiments and normalized to the starting point (relative to t_0). The end-point values at 2 h relative to control made clear that there was no difference between control and stimulated group (Figure 18C).

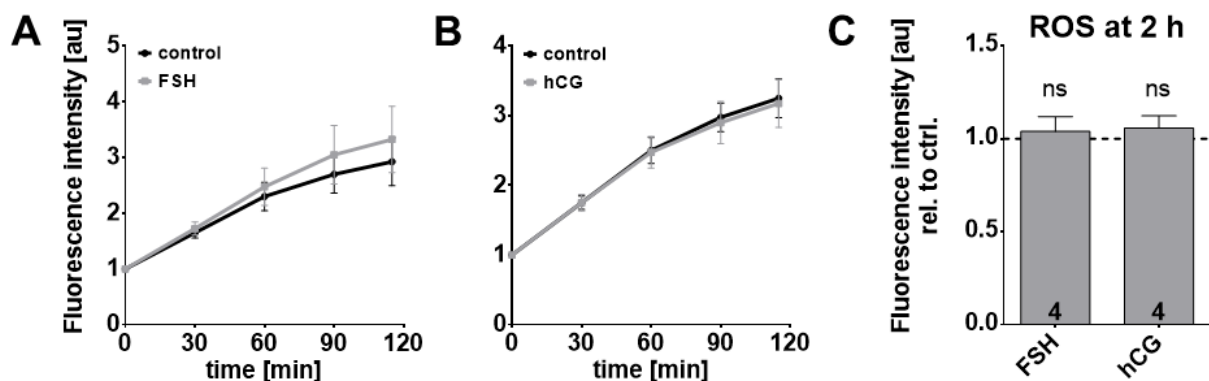


Figure 18 - No acute effect of FSH/hCG on ROS production. (A) Measurements of ROS using H₂DCFDA did not show a difference in ROS production after acute addition of FSH/hCG (n = 4). (A) and (B) depict process of ROS-production over 2 h (n = 4). Values (means \pm SEM) are shown as fold-change to t_0 . (C) End-point values at 2 h are shown relative to control. Statistics: one-sample *t* test, theoretical mean: 1.

Addition of either hormone for 24 h did not affect levels of the main source of ROS, namely *NOX4* mRNA, but elevated those of *DUOX 1* and 2. FSH significantly elevated mRNA of *DUOX2*, whereas hCG significantly increased mRNA levels of *DUOX1/2* (Figure 19).

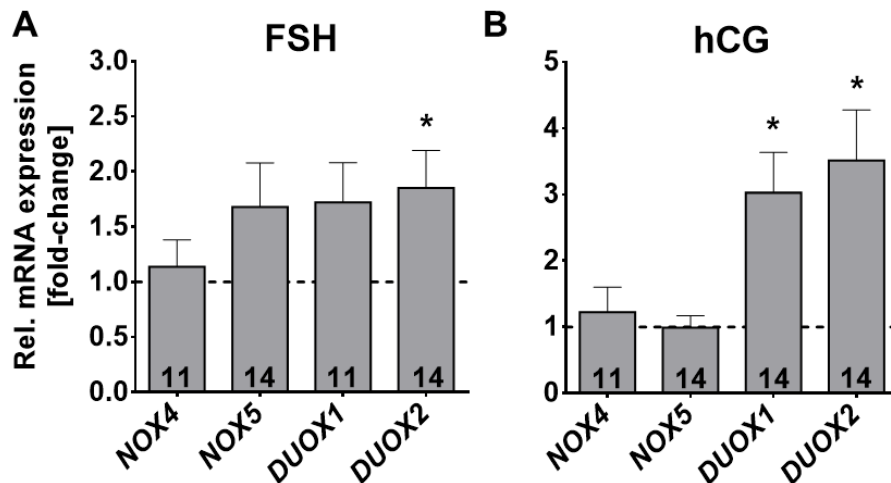


Figure 19 - FSH/hCG increased levels of DUOX. qRT-PCR showed that mRNA expression levels of *NOX/DUOX* were changed after hormonal stimulation for 24 h of GCs. Results (means \pm SEM) shown were normalized to *RPL19*. For statistics, $\Delta\Delta Cq$ values were used. Numbers of repeated experiments are shown inside the columns. Statistics: one-sample *t* test, theoretical mean: 1 (* $p < 0.05$).

Also, a hormonal pre-treatment did not change the overall ROS production of cultured human GCs. No difference in ROS levels were detected after 24 h of stimulation with 1 IU/ml FSH or 10 IU/ml hCG (Figure 20).

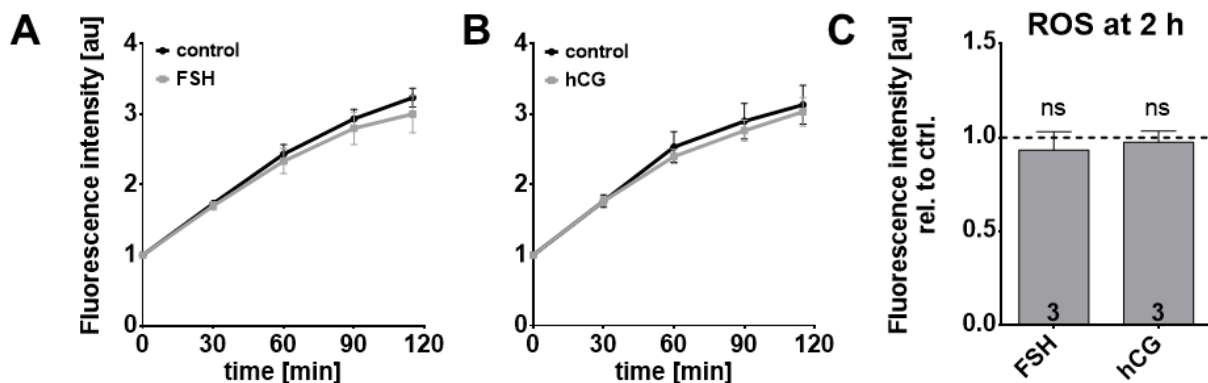


Figure 20 - ROS production was not influenced by pre-treatment with FSH/hCG. (A) and (B) ROS formation (using H_2DCFDA) over 2 h did not show a difference between stimulated and control cells after hormonal pre-treatment for 24 h. Values (means \pm SEM) are presented relative to t_0 . (C) End-point values at 2 h of measurement relative to control are depicted. Statistics: one-sample *t* test, theoretical mean: 1.

A hormonal pre-treatment led to an increase of mRNA levels of the antioxidative system. FSH significantly up-regulated *SOD 1*, *Cat*, *DJ-1* and *GST*, whereas hCG significantly elevated mRNA levels of *SOD1*, *Cat* and *GST* (Figure 21).

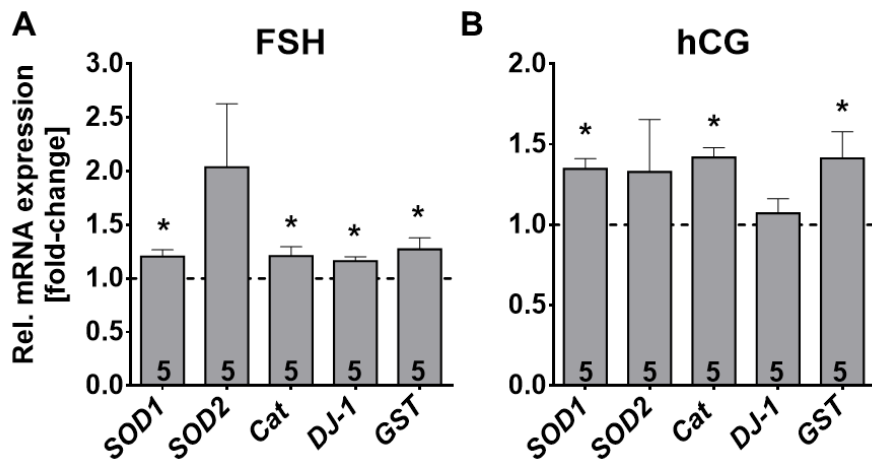


Figure 21 - FSH/hCG influenced expression of antioxidative enzymes. qRT-PCR showed that mRNA expression levels of *SOD1/2*, *Cat*, *DJ-1*, and *GST* were elevated after hormonal stimulation for 24 h of GCs. Results (means \pm SEM) shown were normalized to *RPL19*. For statistics, $\Delta\Delta Cq$ values were used. Numbers of repeated experiments are shown inside the columns. Statistics: one-sample *t* test, theoretical mean: 1 (* $p < 0.05$).

In addition, FSH and hCG are involved in regulation of steroid biosynthesis by up-regulating mRNA levels of two crucial enzymes of the biosynthesis, namely *StAR* and *CYP11A1* (Figure 22). The expression of those was significantly increased after hormonal treatment (24 h). Also, the protein expression of *StAR* was elevated after FSH treatment as seen by immunoblotting (Supplementary Figure 3).

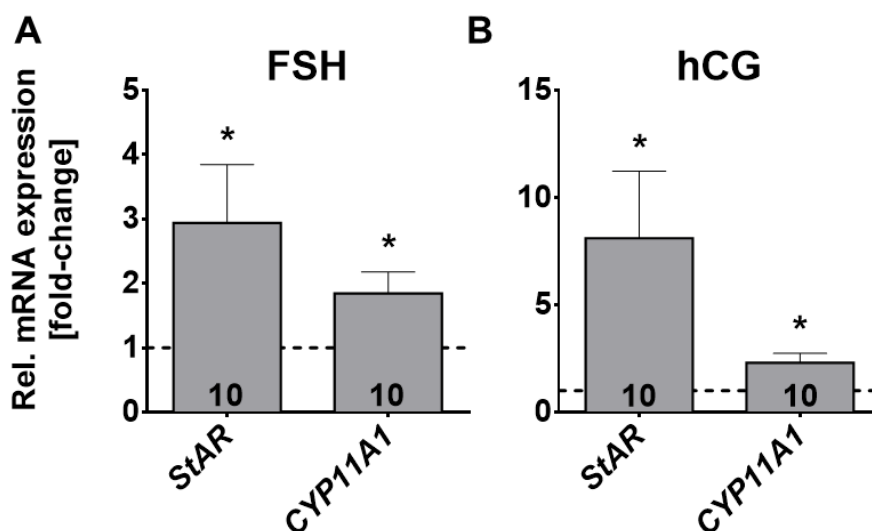


Figure 22 - Regulation of steroidogenesis by FSH/hCG. Gene-expression analysis elucidated that FSH and hCG treatment led to significant increase in *StAR* and *CYP11A1* mRNA levels ($n = 10$). All values shown were normalized to *RPL19* (means \pm SEM). For statistics, $\Delta\Delta Cq$ values were used. Statistics: one-sample *t* test, theoretical mean: 1 (* $p < 0.05$).

2.1.6 Roles of H₂O₂

To explore specific roles of NOX4-derived H₂O₂ in GCs three strategies were employed.

Consequences of direct addition of H₂O₂ were studied, as well as consequences of the NOX4 blocker GKT137831, thereby lowering production of H₂O₂, and consequences of the irreversible Cat blocker 3-AT, hereby inhibiting breakdown of H₂O₂ (Margoliash et al., 1960; Ruiz-Ojeda et al., 2016).

H₂O₂ treatment (2 h) resulted in an increased MAPK phosphorylation expression (representative examples shown in Figure 23). Two out of three experiments resulted in elevated protein levels of pMAPK compared to MAPK of H₂O₂ treated GCs normalized to control cells (data not shown).

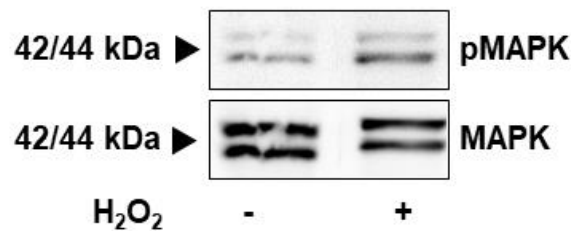


Figure 23 - Influence of H₂O₂ on phosphorylation of MAPK. WB membrane shows the expression of MAPK and pMAPK of treated and untreated GCs on culture day 1 (arrows show expected size at 42 and 44 kDa).

GKT137831 did not affect cell viability (Figure 14), but lowered expression levels of *CYP11A1* (Figure 24B; n = 8) as seen by qRT-PCR. 3-AT reduced cell viability (Figure 24C; n = 3), detected by ATP-assay, but did not affect *CYP11A1* levels (Figure 24A; n = 4).

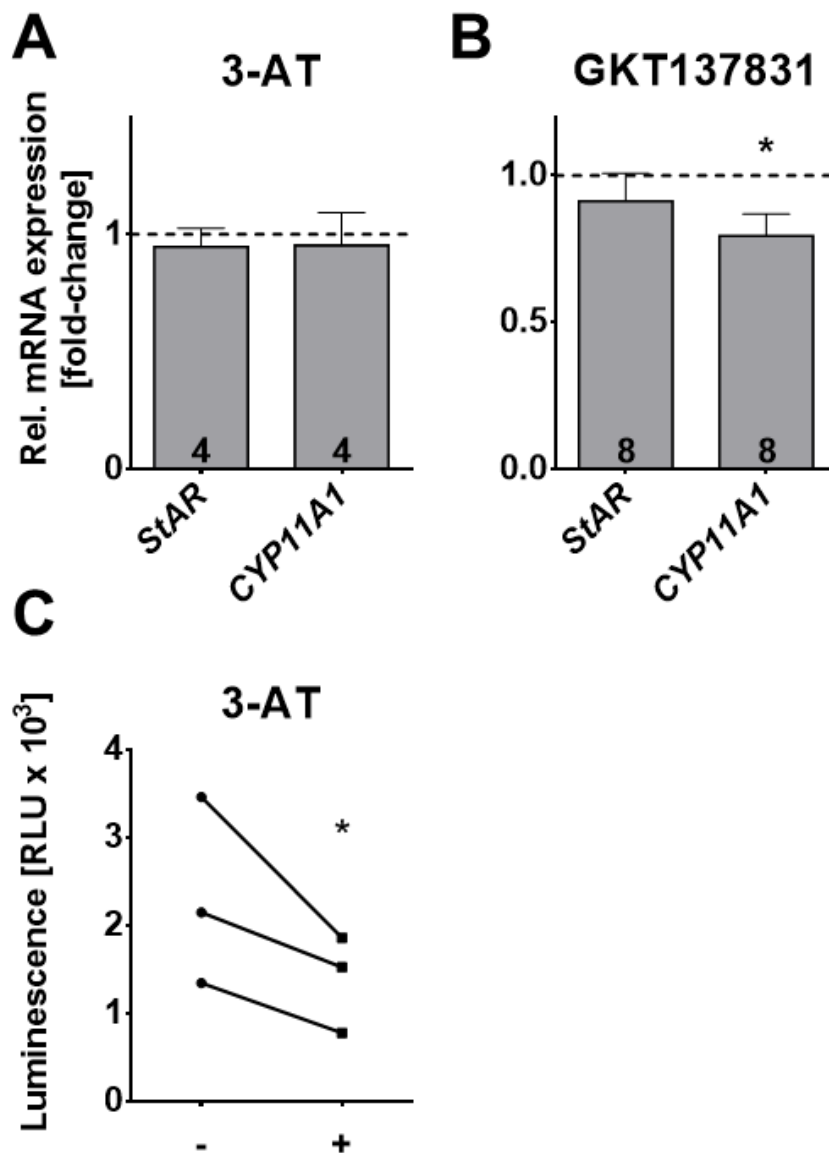


Figure 24 - Action of NOX4 and catalase-blocker. GCs (pools of two to five preparations) were cultured for up to 4 days, stimulated with 10 mM 3-AT or 20 μ M GKT137831 for 24 h on culture day 2 to 4, respectively, and mRNA expression levels of *StAR* and *CYP11A1* were determined by qRT-PCR (A + B). Relative mRNA expression levels are presented as fold-change relative to the expression levels of according controls. *RPL19* was used as control gene. For statistics, $\Delta\Delta Cq$ values were used. Statistics: one-sample *t* test, theoretical mean: 1 (* $p < 0.05$). (C) 24 h incubation with 10 mM 3-AT significantly reduced ATP content and hence viability of GCs. All values are shown as means \pm SEM. Statistics: paired *t* test with single measurements (* $p < 0.05$).

In addition, it has been shown that the treatment of H_2O_2 (50 μ M) for 24 h increased the protein expression of multiple cytokines measured in supernatant of GCs. Shown are the one which are at least increased by 1.5-fold compared to untreated control (Figure 25).

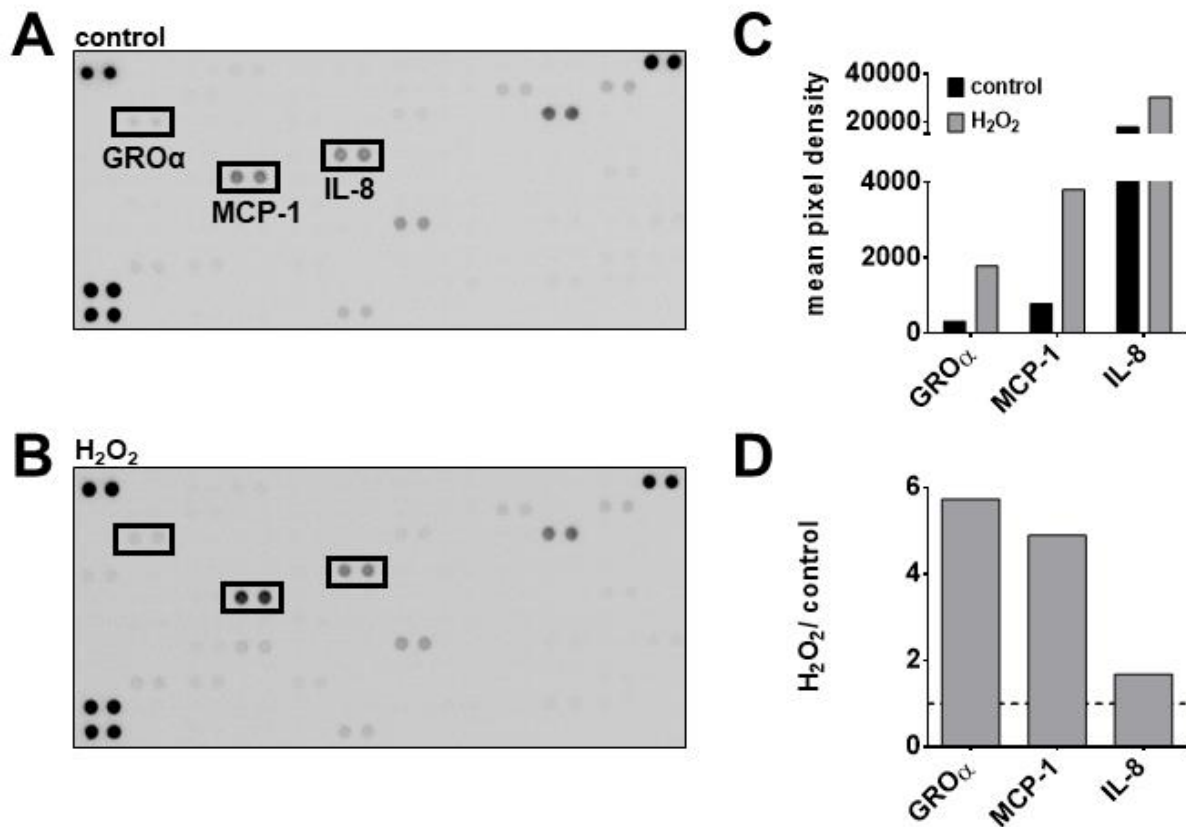


Figure 25 - H₂O₂ increased cytokine expression. Detection of relative expression levels of cytokines and chemokines of H₂O₂ treated GCs vs. control group (culture day 3-4, 24 h stimulation). Nitrocellulose membrane treated with cell culture supernatant of control GCs (A) showed spots which had higher intensity after treatment with 50 μ M H₂O₂ (B) representing GRO α , MCP-1 and IL-8. Graph (C) shows mean pixel density of control vs. treated group and (D) presents the normalized values relative to control.

2.1.7 Role of aquaporins/porixiporins

Recently, our group showed the expression of AQP3, 8, and 9 by RT-PCR (Supplementary Figure 4A; performed by Theo Hack). Treatment of GCs with the AQP inhibitor AgNO₃ did not influence cell viability (ATP assay, Figure 26C; n = 3). Quantitative fluorometric evaluations showed that the increase in intracellular fluorescence intensity upon extracellular application of H₂O₂ was significantly reduced in the presence of AgNO₃ (Figure 26D+E; data were generated in cooperation with Theo Hack).

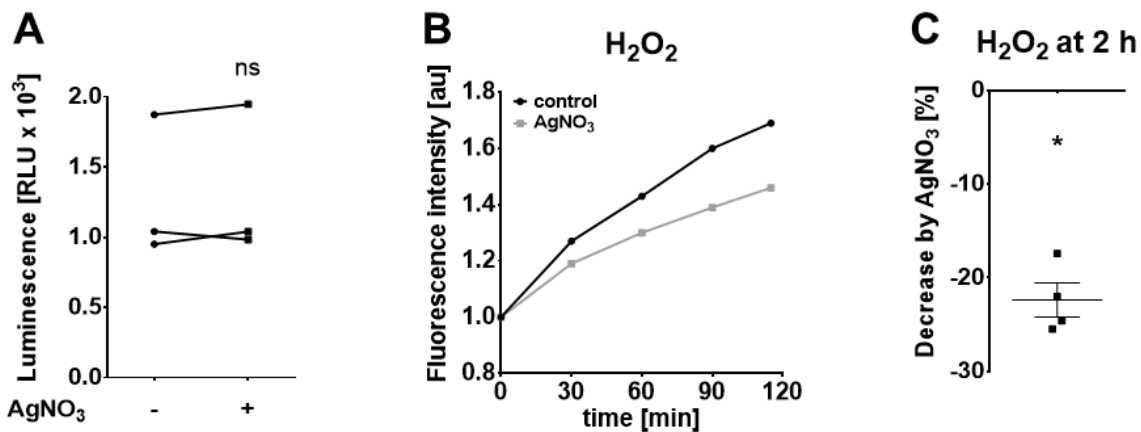


Figure 26 - H₂O₂-transporting aquaporins in cultured human GCs. (A) Shown are ATP values from GCs treated with aquaporine blocker AgNO₃ (500 nM) and PO1 compared with control cells treated with PO1 only. Statistics: paired *t* test with single measurements. (B) H₂O₂ generation of GCs treated with AgNO₃ (500 nM) compared to control group is shown. Fluorescence values are depicted as mean of six technical repetitions of a representative example over 2 h (relative to t₀; n = 1). (C) Percentage decreases of four H₂O₂ measurements compared to control. AgNO₃ (500 nM) significantly decreased H₂O₂ production by 22 %. Statistics: one-sample *t* test, theoretical mean: 0 (* *p*<0.05).

2.2 NOX and ROS in the proliferating cell model KGN

2.2.1 NOX expression and localization

To also study the role of NOX and ROS in GC proliferation, the human granulosa tumour cell line KGN as a proliferating GC model was used. qRT-PCR followed by sequencing revealed that KGN cells express *NOX4*, *NOX5*, and *DUOX2*, but not *DUOX1* (Figure 27A). This experiment was repeated using three different KGN passages. Figure 27B shows a Western blot membrane positive for NOX4 protein using anti-NOX4 antibody No. 1 (three repetitions). NOX4 protein was identified in intracellular compartments and the nucleus of KGN using immunocytochemistry (Figure 27C; experiment repeated with three KGN passages).

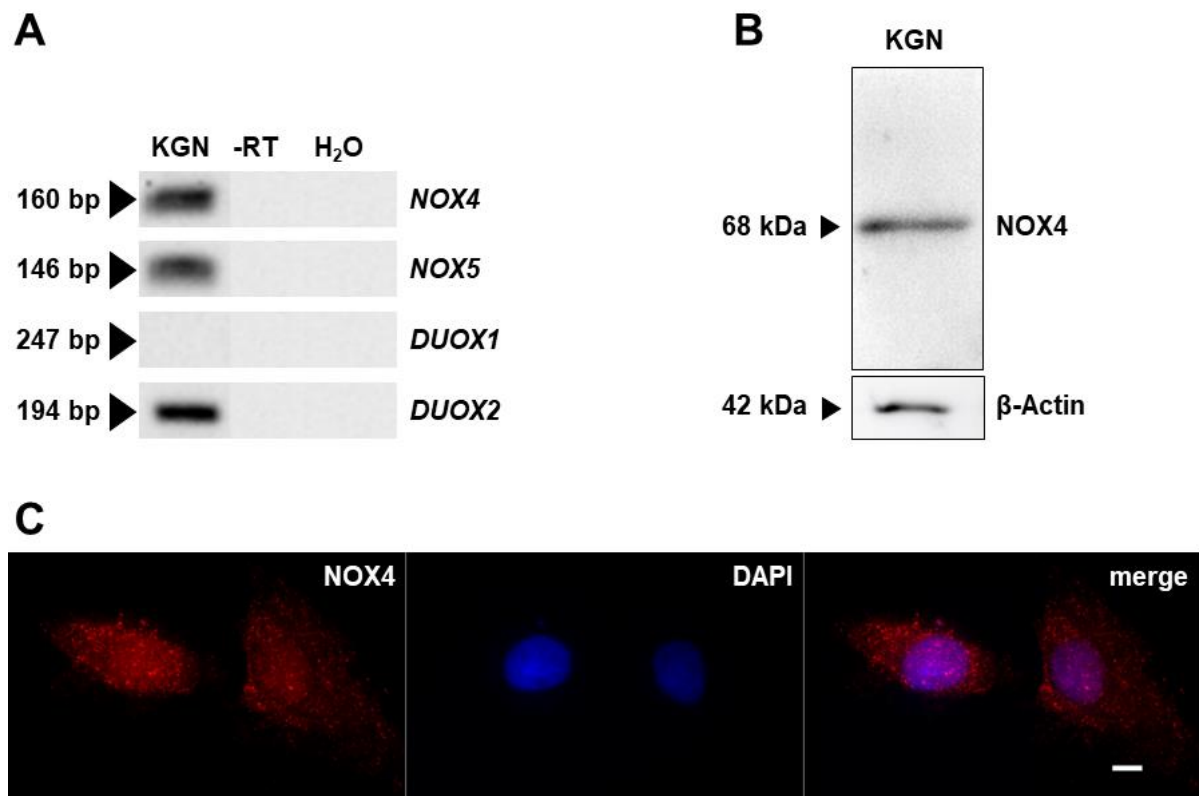


Figure 27 - NOX expression in KGN. RT-PCR identified *NOX4/5* and *DUOX2* in cultured KGN. Controls including RNA (-RT) and H₂O instead of cDNA (H₂O) were negative (A). *NOX4* protein was detected in KGN by immunoblotting (B). The arrow shows the expected size (68 kDa). (C) Localization of *NOX4* (red) was detected by immunocytochemistry. Staining in intracellular compartments and the nucleus (blue: DAPI counterstain) of KGN (antibody No. 1). Scale bar = 10 μ m. Controls without primary antibody were negative (not shown).

2.2.2 Roles of NOX4

ROS and H₂O₂ production could be identified and blocked in KGN. The ROS generation was measured fluorometrically by H₂DCFDA (Figure 28A) and H₂O₂ production by Amplex[®] Red (Figure 28B) over 2 h, and values of control versus treated cells are shown. Figure 28C shows the percentage decrease of ROS production of three independent measurements (significant decrease by 45 %).

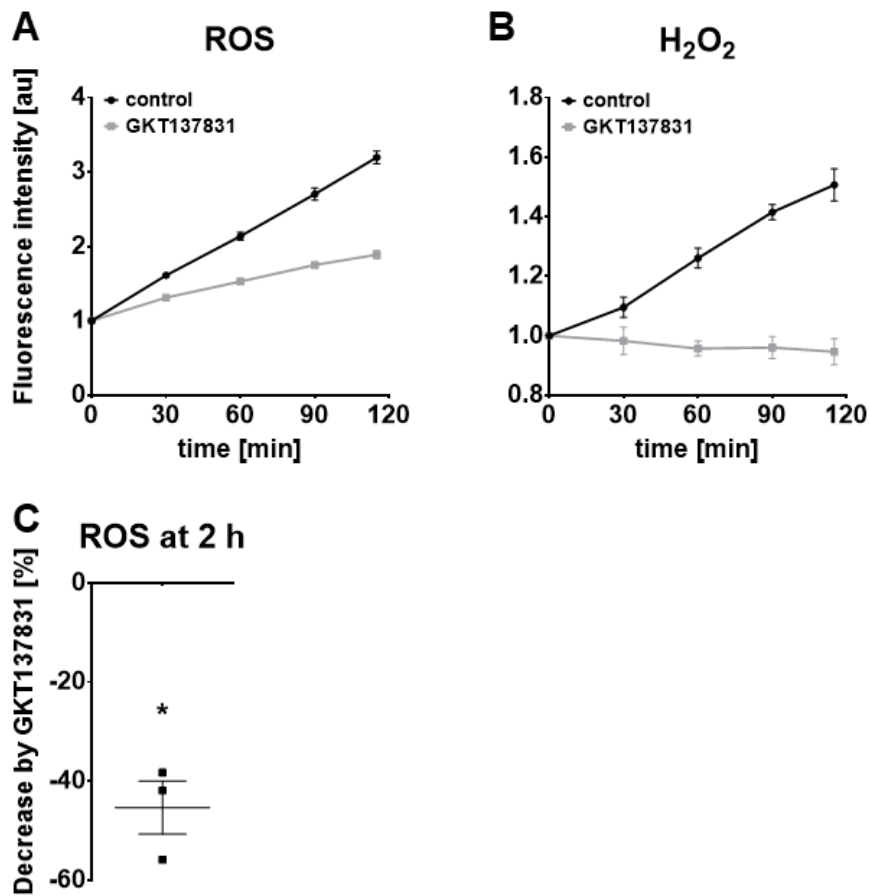


Figure 28 - Inhibition of NOX4 activity in KGN induced lower production of ROS and H₂O₂. The NOX4 blocker GKT137831 (20 μ M) reduced the ROS/H₂O₂ levels produced by KGN. Fluorescent measurements over 2 h (means \pm SEM of six technical replicates) show reduction of ROS production (A) determined by H₂DCFDA and of H₂O₂ generation (B) identified by Amplex[®] Red. Endpoint values at 2 h (means \pm SEM) of three multiple independent measurements show significant reduction of ROS production by 45 % (C; n = 3). Statistics: one-sample *t* test, theoretical mean: 0 (* *p*<0.05).

Treatment with the NOX4-blocker GKT137831 did not affect cell viability (Figure 29D; LDH assay, n = 5), but significantly reduced the cell number (Figure 29A; n = 6) and confluence of KGN cells (Figure 29B; n = 4). The treatment also reduced proliferating cell nuclear antigen (PCNA), a proliferation marker (Figure 29C; n = 4).

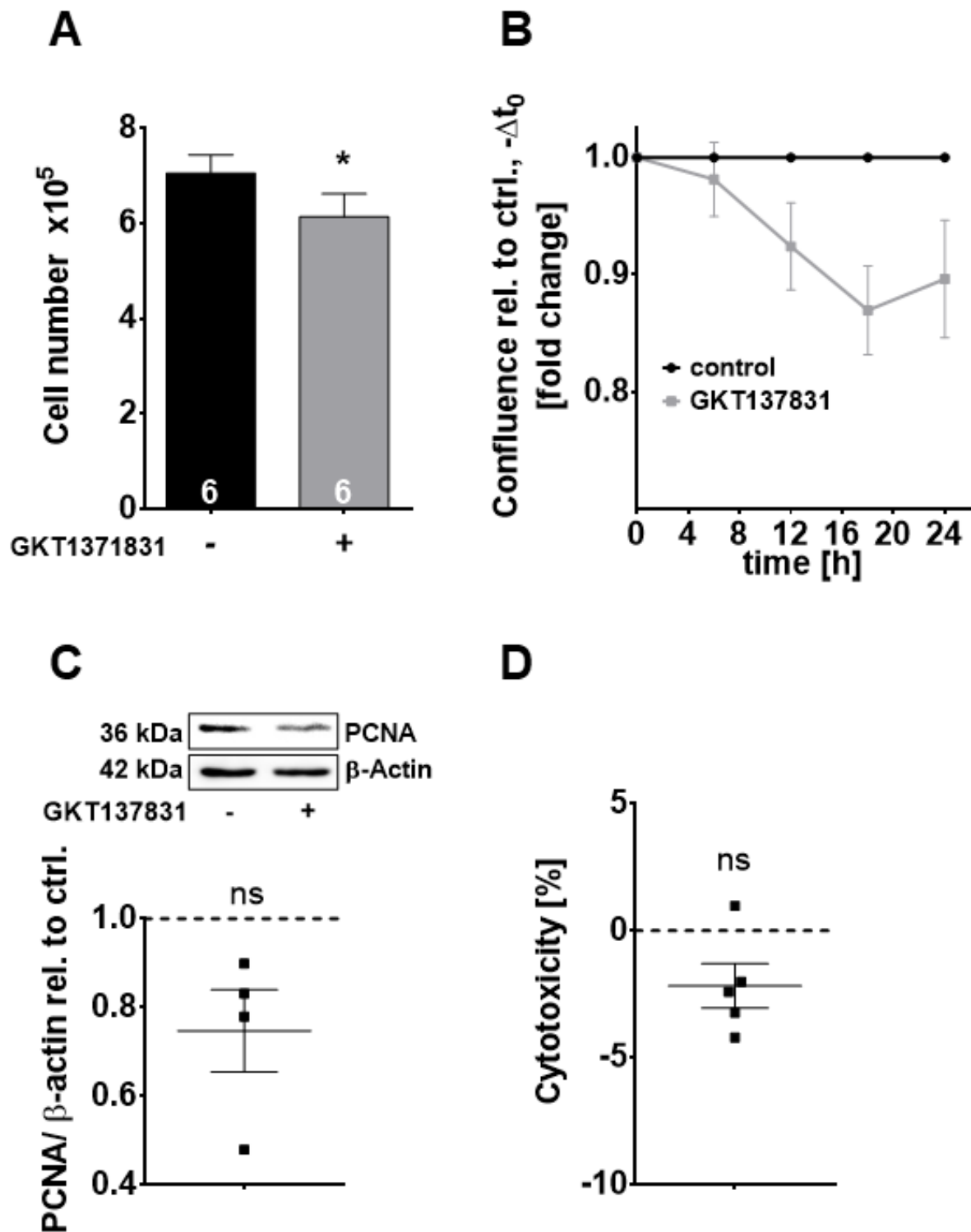


Figure 29 - Actions of NOX4-blocker in KGN. KGN treatment with GKT137831 showed a significant reduction in cell number (A; $n = 6$) and a (not significant) decrease confluence (B; $n = 4$), as well as reduced PCNA content. (C) PCNA in KGN compared to control (blotted membrane of one representative example is shown). Diagram shows PCNA levels normalized to β -actin ($n = 3$). (D) Treatment with GKT137831 had no effect on cytotoxicity in KGN compared to control (LDH cytotoxicity assay; $n = 5$). Statistics: (A+B) paired t tests (two-tailed; * $p < 0.05$); (C+D) one-sample t test, theoretical mean: 1/0.

3. Discussion

This study demonstrates that human primary luteinised GCs and proliferating KGN cells express the H₂O₂-generating NOX4. Intra- and extracellular detection of H₂O₂ imply that H₂O₂ may serve as a diffusible signalling molecule. Its cellular uptake into GCs is facilitated by AQPs. H₂O₂ is involved in the regulation of cell functions, including proliferation, steroid biosynthesis and signalling.

3.1 Identification of NOX enzymes in ovarian cells

The central question of this study was to elucidate whether the human ovary expresses NOX enzymes and whether it produces ROS. This was studied in two models: the luteinised GCs and the proliferating KGN cell line.

There are few studies examining NOX enzymes, their specific ROS products, and their roles in the ovary (Altenhofer et al., 2015; Bedard et al., 2007; Brandes et al., 2014; Sirokmany et al., 2016). *NOX1-3* genes were not found in GCs, but previous studies showed expression of *NOX4* and *NOX5* in human GCs (Bedard et al., 2007; Kampfer et al., 2014; Maraldi et al., 2016). This was confirmed by our study (Figure 8). In ovary, expression of NOX2, beside NOX4 and 5 was reported, but it is very likely that ovarian NOX2 originates from leukocytes (Cheng et al., 2001). That leaves NOX4 and 5 specifically found in the male and female gonad, but the knowledge about expression and functional roles in the human ovary is at best rudimentary. In this study, NOX4 protein was further detected by immunohistochemistry in the human ovary, in granulosa, theca and luteal cells. As previously reported, the sub-cellular localization of NOX4 is cell-type specific and ranges from mitochondria to endoplasmic reticulum, focal adhesion and nucleus (Block et al., 2009; Guo et al., 2015; Meitzler et al., 2014). In this study, immunohistochemistry elucidated NOX4-positive staining not only in the cytosolic regions (Figure 8) but also in the nucleus of luteinised cells (Supplementary Figure 2). The immunocytochemical staining in cultured human GCs revealed the presence in the PM and nucleus (Figure 9) as well as in cell organelles, probably such as mitochondria or ER (Supplementary Figure 1). Exact intracellular localization in GC requires however further examination. These results are in line with previous reports (Graham et al., 2010; Koziel et al., 2013; Kuroda et al., 2005), and could be found also *in situ*. In addition, NOX4 protein expression was confirmed in human proliferating KGN cells by immunoblotting and -staining (Figure 27). In KGN, NOX4 protein also seemed to be located in organelles. Immunocytochemical experiments in KGN cells elucidated similar staining patterns as seen in GCs.

Besides *NOX4*, gene analysis also revealed expression of *NOX5*, *DUOX1* and *2* in GCs (Figure 8). Thus, this is the first study reporting expression of *DUOX1* and *DUOX2* by cultured human GCs. *NOX5*, the Ca^{2+} -activated and human specific NOX isoform, demonstrates the least well understood of the NOX family members, because the gene is not present in mice or rats (Bedard et al., 2012). Experimental studies on *NOX5*, as well as *DUOX1/2* are limited by the lack of specific antibodies and pharmacological tools (Altenhofer et al., 2015). Nevertheless, *NOX5* protein expression in human cultured GCs could be confirmed by immunoblotting, and cellular staining also proved presence of *NOX5* in cytoplasmic compartments (Figure 8 and Figure 10). Gene expression analysis revealed mRNA expression of *NOX4*, *NOX5* and *DUOX2*, but not for *DUOX1* in the KGN cell line. Taken together, the here used cell models, GCs and KGN cell line, express both mRNA and protein of *NOX4*.

3.2 NOX-derived ROS

NOX5 generates $\text{O}_2^{\cdot-}$, while *DUOX1/2*, as well as *NOX4* generate mainly H_2O_2 (Altenhofer et al., 2015). Using a functional assay, where $\text{O}_2^{\cdot-}$ oxidases luminol resulting in the formation of chemiluminescence light, only traces of $\text{O}_2^{\cdot-}$ could be detected. Measurements of extracellular H_2O_2 by Amplex[®] Red reagent result in abundant detectable H_2O_2 amounts expressed by cultured human GCs (Figure 12). These findings are in line with the published insights that $\text{O}_2^{\cdot-}$, once generated by NOX, is very rapidly dismutated to H_2O_2 by SOD (Bedard et al., 2007; Lambeth et al., 2014). H_2O_2 may be the result of *NOX4*, as well as *DUOX1* and *DUOX2* activities. Consequently, amount of general ROS in cultured human GCs and KGN by the indicator dye H_2DCFDA was detected. In the presence of intracellular ROS, H_2DCFDA is converted to the highly fluorescent compound DCF, which was measured in both cell models, GCs (Figure 12) as well as KGN (Figure 28).

NOX4 is considered a constitutive enzyme and contributes approximately one-third of cellular H_2O_2 formation in the vascular endothelium (Altenhofer et al., 2015; Sies et al., 2017). A study in mice suggests that *NOX4* is crucial for the survival of kidney tubular cells (Nlandu Khodo et al., 2012). *NOX4*-deficient mice exhibited more interstitial fibrosis and tubular apoptosis as well as reduced expression of hypoxia-inducible factor and vascular EGF. Notably, another study shows that *NOX4*-derived ROS are involved in signalling of growth factors, e.g. via the EGFR, playing a crucial role in the ovulatory signalling cascade linked to the induction of ovulatory genes in rodents (Maraldi et al., 2016). Thus, ROS appear indispensable for ovulation, at least in rodents.

To study *NOX4*-derived H_2O_2 in ovarian cells, a purely extracellular H_2O_2 detection method by

means of the Amplex[®] Red reagent and a cell permeable boronate compound (PO1) specifically activated by intracellular H₂O₂ were applied. The fluorometrical measurements confirmed the presence of intra- and extracellular H₂O₂ in GCs (Figure 12, Figure 26, and Figure 28). The results indicate that GCs, as well as KGN, produce H₂O₂ on a basal level, which apparently can leave its intracellular sites of generation. The transport from the cell organelles through the PM may be facilitated by AQPs as discussed further in 3.4. An extracellular localization is in line with a report on the presence of H₂O₂ in human FF (Hennet et al., 2013).

To further address the NOX4-mediated ROS and especially H₂O₂ contribution in ovarian cells, GCs and KGN were tested with NOX1/4 inhibitor GKT137831. GKT137831, a novel, pharmacological compound, demonstrates a preferential inhibition of NOX1 and 4. Genetic deletion of NOX1 and 4, has revealed no significant spontaneous pathologies and a pathogenic relevance of both NOX1 and 4 across multiple organs in a wide range of diseases. This has stimulated interest in NOX inhibitors for therapeutic application. This small molecule blocker belongs to a structural class of pyrazolopyridinedione derivate, and has been reported to slow or prevent disease progression in a range of models of chronic inflammatory and fibrotic diseases by modulating common signal transduction pathways (Aoyama et al., 2012; Gaggini et al., 2011; Guo et al., 2015; Teixeira et al., 2016). A study elucidates the potential benefits of GKT137831 for attenuating proliferative pathways in pulmonary hypertension and see it as a highly promising orally bioavailable drug for the treatment of pulmonary hypertension (Green et al., 2012). In contrast to gene deletion, this inhibitor does not completely suppress ROS production, maintaining some basal level of ROS. However, it is well tolerated and effective (Teixeira et al., 2016).

As both of the used cell types do not express NOX1, GKT137831 presents a specific NOX4 blocker. To test whether GKT137831 is harmful to cultured GCs, the cell viability was measured (using an ATP assay), and the morphology of the cells was observed. Neither the viability nor the morphology was changed after GKT137831 treatment (Figure 14). In KGN, cytotoxicity of GKT137831 treatment was determined by LDH amount, which is released into the media from damaged cells indicating cellular cytotoxicity and cytolysis. GKT137831 treatment did not show any cytotoxic effect on KGN (Figure 29).

The administration of GKT137831 elucidated significant contribution of NOX4 to overall ROS generation in GCs and KGN over 2 h of measurement (Figure 13 and Figure 28). Inhibition experiments revealed a decrease of ROS production by 55 % in GCs and by 45 % in KGN at the endpoint 2 h. Regarding the H₂O₂ generation, a percentage change by -36 % in GCs and -44 % in KGN could be achieved after 2 h.

These findings elucidated a tremendous contribution of NOX4 to the general ROS and especially H₂O₂ generation in cultured GCs and KGN cells.

3.3 Regulation by FSH and hCG

The human ovarian samples available for immunohistochemistry showed expression in growing follicles. FSH is required for growth and maturation of ovarian follicles and the LH stimulation induces the ovulation process, including follicular wall rupture, GC luteinisation, cumulus cell expansion and meiotic maturation of the oocyte (Landomiel et al., 2014). Hormonal effects of hCG very closely resemble those of pituitary LH (Pierce et al., 1981). FSH and LH/hCG and its receptors play a key role in reproduction (Abel et al., 2003; Simoni et al., 1997). IVF-derived cultured GCs express both, FSHR and LHR (Figure 15).

FSHR exists as four alternatively spliced isoforms of which each one has diverse biological functions. This may help explain multiple actions of FSH including cellular growth, proliferation, differentiation, and steroidogenesis (Bhartiya et al., 2015).

Recent reports showed that GCs express EGF-like factors that activate the EGF receptor (EGFR)-mitogen-activated protein kinase (MAPK) (also known as extracellular signal-regulated kinase (ERK)) pathway. The metalloprotease ADAM17 (also called TACE), which is known to be a proteolytic enzyme of EGF-like factors in many types of tissue, was found to be expressed in FSH/LH-stimulated GCs together with activation of the EGFR-MAPK pathway (Chen et al., 2014; Yamashita et al., 2012). This is in line with the findings of the present study. Both, FSH and hCG stimulated significantly *ADAM17* mRNA expression in GCs. Further, the FSH treatment triggered the phosphorylation of MAPK seen by immunoblotting (Figure 16).

Consequently, it could be shown that human IVF-derived cultured GCs express functional active FSHR and LHR. It has been reported that LHR expression in GCs was induced by FSH. However, FSHR expression is regulated through a mechanism other than FSH and LH/hCG stimulation. Also, LH/hCG is needed for induction of LHR expression (Kishi et al., 2018). This was confirmed by the current study (Figure 17).

While FSH/hCG stimulation had no influence on mRNA expression levels of *NOX4* and *5*, FSH significantly increased *DUOX2*, and hCG elevated *DUOX1* and *2* (Figure 19). The increase was however without measurable consequences with regard to overall ROS or specifically H₂O₂ production. Neither an acute hormonal stimulation (Figure 18) nor a pre-treatment (Figure 20) of FSH/hCG resulted in an increase of ROS generation in GCs. A possible explanation is either that the consistent expression of the main contributor, NOX4, does not lead to a rise of ROS or the counteraction of the antioxidative system. The hormonal stimulation significantly

increased levels of antioxidant enzymes. Treatment with FSH significantly increased mRNA expression levels of *SOD1*, *Cat*, *DJ-1*, and *GST*, and hCG significantly up-regulated mRNA amounts of *SOD1*, *Cat*, and *GST* (Figure 21). These findings indicate roles of gonadotropins in the control of the ROS environment in GCs and, since GCs are apt models presumably in the follicle and the CL, as well.

A further effect of gonadotropins in GCs was elucidated in combination with the steroid biosynthesis. As FSH and hCG stimuli induced mRNA expression levels of the two main regulators of steroidogenesis *StAR* and *CYP11A1*, it became clear that these gonadotropins also play a crucial role in steroid synthesis (Figure 22). To underline this finding, it was shown that FSH stimulation also increased *StAR* protein expression seen by immunoblotting (Supplementary Figure 3).

3.4 H₂O₂ transport

Transcellular water movement can occur by two mechanisms. The first is by simple diffusion through the hydrophobic interior of the membrane, which is a slow and unregulated process. The second mechanism is through water channels, AQPs, which are able to support a large volume of water flow (McConnell et al., 2002). As a diffusible signalling factor, H₂O₂ may act on neighbouring cells or oocytes, this also requires a controlled transport. It is known that specific AQP isoforms facilitate the passive diffusion of H₂O₂ across biological membranes and control H₂O₂ membrane permeability and signalling in living organisms (Bienert et al., 2014). In a related study (mainly performed by Theo Hack) we examined whether H₂O₂ may be able to enter GCs. Fluorescence imaging using PO1 confirmed the intracellular uptake of extracellular H₂O₂ (not shown). AQP3, 8 and 9 facilitate transport of H₂O₂ and are referred to as peroxiporins (Miller et al., 2010; Watanabe et al., 2016). In line with previous and present studies, AQP3, 8 and 9 were identified in GCs (Supplementary Figure 4) and (Lee et al., 2016). As a new finding in GCs, it could be shown that AQPs are functionally active and contribute to the H₂O₂ transport. Blocking AQPs with AgNO₃ (Niemietz et al., 2002) in the presence of extracellular H₂O₂ showed a significant contribution of these channels in the uptake of H₂O₂ (Figure 26). The remaining H₂O₂ content may diffuse passively through the PM. Whether they are also involved in the release of this ROS remains to be studied. The results may indicate that AQPs/peroxiporins, their abundance, and possibly the subtypes expressed are involved in the uptake and thus, presumably in the subsequent intracellular actions of H₂O₂ in GCs.

3.5 Physiological roles of H₂O₂

3.5.1 Studies in cultured human GCs

Another central question of this study was whether NOX4-derived H₂O₂ plays a physiological functional role in cultured human GCs. Because of its relatively low reactivity (as a mild oxidant), H₂O₂ has a comparatively long intracellular half-life and a high diffusion rate, all of which makes H₂O₂ an efficient signalling molecule (Walker et al., 2018).

The NOX family is known to be the predominant contributor of ROS in many cellular systems (Bedard et al., 2007). NOX-derived ROS are involved in signalling of growth factors, e.g. via the EGFR, playing an indispensable role in the ovulatory signalling cascade linked to the induction of ovulatory genes (Chen et al., 2014; Maraldi et al., 2016; Shkolnik et al., 2011).

The widespread expression of NOX4 in the human ovary may imply a physiological role of NOX4-derived H₂O₂. A look to the vascular system is instructive. As determined for GCs, NOX4 activity accounts for about one-third of cellular H₂O₂ formation in vascular endothelium (Schroder et al., 2012).

To explore specific roles of NOX4-derived H₂O₂ in GCs three strategies were employed.

First, direct addition of extracellular H₂O₂; second, lowering production of H₂O₂ by applying the NOX4 blocker GKT137831, and third, inhibiting breakdown of H₂O₂ by catalase blocker 3-AT.

One functional role of H₂O₂ revealed after direct addition of H₂O₂ followed by protein expression analysis of MAPK and phosphorylated MAPK. Immunoblotting showed that addition of H₂O₂ induced phosphorylation of 42/44 MAPK (Figure 23). Thus, H₂O₂ plays an important role as signalling molecule in downstream pathways. This is in line with a recently published paper demonstrating the necessity of NOX-derived ROS for the EGF/MAPK signalling pathway in uterine leiomyomas (Mesquita et al., 2010). A further study reported that ROS is involved in activation of the EGFR which initiates a subsequent signalling cascade inducing 42/44 MAPK phosphorylation. Other signalling pathways take part in the activation of 42/44 MAPK as well. ROS may also be involved in activation of the PKA signalling and the MEK signalling cascade (Shkolnik et al., 2011).

H₂O₂ demonstrates important roles in immune system. Although, GCs are no immune cell, they are able to produce cytokines. Inflammation plays a role in ovulation and regression of CL, therefore inflammatory markers were examined. Expression analysis of cytokines and chemokines elucidated that three of them are increased considerably after H₂O₂ treatment,

namely GRO α , MCP-1 and IL-8 (Figure 25). These revealed candidates play important roles in inflammation, but unfortunately, very little is known about them in GCs. In general, growth-related oncogene alpha (GRO α) protein, also known as CXCL1, exerts its effects on endothelial cells in an autocrine fashion. Monocyte chemoattractant protein 1 (MCP1) augments monocyte anti-tumour activity. Interleukin 8 (IL-8) is a chemotactic factor that attracts neutrophils, basophils, and T-cells.

It has to be reflected that the here used human GCs have been isolated before ovulation and differentiate into luteal cells. The CL consisting of luteal cells is a unique, transient endocrine structure with the main function to produce progesterone, which is necessary for the establishment and maintenance of pregnancy (Shirasuna et al., 2017). The development of the CL following ovulation is a physiological injury involving an inflammatory response. Consequently, a high number of immune cells (neutrophils and macrophages) and considerable levels of IL-8 have been found (Best et al., 1996; Jiemtaweeboon et al., 2011). Another study reported that the early CL induces neutrophil migration *in vitro* by secreting IL-8 (Goto et al., 2002). It is also known, that macrophages are important to maintain vascular integrity in the CL (Turner et al., 2011). Thus, immune cells such as neutrophils and macrophages play a crucial role in the development of the CL and in ensuring pregnancy success (Shirasuna et al., 2017). Very little is known about the regression of the CL, however studies of many animal models have postulated that macrophage-derived secretions (e.g., TNF) participate in both the development and regression of CL (Ye et al., 2016).

This experiment was performed with one GC pool only, and therefore repetitions are required.

These findings are in line with a previous report claiming that the MAPK pathway and the expression of genes related to inflammation including interleukins and chemokines also affected by H₂O₂. Because of the multi-mechanistic nature of this molecule, they suggest novel therapeutic approaches on the use of H₂O₂ (Vilema-Enriquez et al., 2016).

GKT137831 did not affect cell viability but lowered expression levels of *CYP11A1*, as seen by qRT-PCR (Figure 14 and Figure 24). This links H₂O₂ to a positive regulation of *CYP11A1*, the crucial enzyme in steroid biosynthesis. In contrast, the catalase blocker 3-AT reduced viability of cells as determined by ATP measurements, but did not affect *CYP11A1* mRNA levels (Figure 24). The results imply a noxious action of H₂O₂ as it reduced cell viability. However, less vital cells still expressed comparable levels of *CYP11A1*. Hence, the result also links H₂O₂ to the positive regulation of the steroidogenic phenotype of GCs.

NOX4 was only recently identified to be lower in GCs of women of higher age compared with those of younger age (≥ 40 years versus ≤ 37 years) at time of IVF (Maraldi et al., 2016). Thus, age-associated factors, possibly epigenetic ones, may regulate NOX and ROS levels. As female fertility declines with age, it is possible that NOX4-generated physiological H_2O_2 may play a crucial role, and that sufficient levels are required for ovarian homeostasis.

3.5.2 Studies in KGN cells

These cells, derived from a human granulosa cell tumour (Nishi et al., 2001) proliferate, in contrast to primary GCs.

The NOX4 blocker not only reduced H_2O_2 production, but also cell number and confluence of KGN cells. The findings that no cytotoxicity was observed and PCNA (linked to proliferation) was reduced elucidated a strong evidence that physiological NOX4-generated H_2O_2 is involved in cell proliferation (Figure 29). The precise mechanisms of action and possible other roles remain to be studied. However, earlier reports confirmed these findings as H_2O_2 was shown to stimulate cell proliferation at low concentrations (Burdon et al., 1989). Also, it has been found that certain ROS, especially H_2O_2 , may also have an important physiological role in the stimulation of cell proliferation in response to peptide growth factors (Karin et al., 2001). It is now accepted that, at low levels, H_2O_2 participates in cellular differentiation, migration, and proliferation, and can dramatically alter gene expression profiles, hence the recent prominence of H_2O_2 as an important cell signalling molecule (Walker et al., 2018)

To substantiate the results of the loss of function experiments, a more specific approach like a gene knockdown by small interfering RNAs (siRNAs) would be desirable. As the transfection efficiency of primary GCs is very low, only preliminary siRNA transfection experiments in KGN cells have been performed to address this point (Supplementary Figure 5). These experiments showed both, a decrease in cell number (Supplementary Figure 5A) as well as a reduced cell confluence (Supplementary Figure 5B) of NOX4 siRNA transfected KGN compared to non-target control by more than 20 % after 48 h live cell imaging. All the NOX4 knockdown experiments are in line with the revealed data in this study, suggesting NOX4 action is involved in cell proliferation. Its precise involvement has to be further examined.

Taken together, differentiated GCs and proliferating KGN cells express NOX4, which represents a major producer of H_2O_2 in human GCs *in vitro*. While *NOX4* mRNA levels are not under the control of FSH or LH/hCG in GCs, these hormones are involved in ROS homeostasis, in downstream signalling as well as steroid synthesis. H_2O_2 may serve as a diffusible signal to neighbouring cells and peroxiporins (AQPs 3,8, and 9) facilitate H_2O_2 cellular

uptake. H_2O_2 presents a stable and abundant ROS, and acts as an important signalling molecule involved in the regulation of cell functions, like cell proliferation and steroid synthesis as well as in pathways like MAPK signalling. The consequences of H_2O_2 signalling remain to be fully explored, yet expression of NOX4 *ex vivo*, in growing follicles, and results in KGN may indicate a role in proliferation of ovarian cells.

Even though, this work reflects functional studies in isolated cells which are not equivalent with the physiological ovarian environment, there is no doubt that NOX is expressed and functionally active based on cellular studies. If applicable to the situation in the ovary, the full elucidation of the ROS-generation and signalling system in the human ovary is important to guide future therapeutic strategies to address questions in female infertility.

4. Material and Methods

4.1 Cell culture

4.1.1 Human GC isolation, culture, and treatment

Follicular fluid (FF) containing GCs was derived from patients (age range between 28 and 40 years) undergoing IVF due to poor quality of sperm or restricted tubal patency (Table 18). The stimulation of the patients and the acquisition of the aspirates were performed using standard protocols, i.e. the “long” protocol (Bulling et al., 2000; Mayerhofer et al., 1992; Mayerhofer et al., 2006; Mayerhofer et al., 1993; Saller et al., 2014; Saller et al., 2012) by A.R.T. Berg (Bogenhausen, Munich). The ethics committee of the Ludwig-Maximilian-University (LMU) of Munich approved the use of follicular aspirates and GCs for scientific experiments. The study was carried out according to the guidelines of the 1975 Declaration of Helsinki. A written consent of the patients was obtained, samples and clinical information were anonymized. Studies were performed in the course of a DFG project MA1080/26-1.

FF aspirates from two to five patients were pooled for GC preparation, following a method previously described (Ferrero et al., 2012), which utilizes a cell strainer (40 µm) for filtration. GCs, remaining in the cell strainer, were retrieved by washing with Dulbecco’s modified Eagle’s medium (DMEM)/Ham’s F12 medium. The filtrate with remaining cell aggregates was suspended mechanically by using a 0.9-mm hypodermic needle, transferred into a Falcon tube (15 ml) and centrifuged at 700 x g for 3 min. The cell pellet was resuspended in DMEM/Ham’s F12 medium supplemented with penicillin (100 U/ml), streptomycin (100 µg/ml) (P/S) and 10% FCS (Bulling et al., 2000; Mayerhofer et al., 1992) and seeded into petri dishes. The day of isolation corresponds to cultivation day 0. Cells were cultured for up to 4 days at 37 °C and with 5 % CO₂ and 95 % humidity. They were rinsed on day 1 of culture with fresh medium to remove non-adherent and dead cells. For all experimental treatments, DMEM/Ham’s F12 medium without FCS was used. For the treatment with stimulants like FSH and hCG or NOX4 and catalase inhibitors, the cells were serum starved by incubation in DMEM/Ham’s F12 containing 1% P/S for 2 h, then exposed to reagents and according control for 24 h (see Table 2), respectively, before performing the experiments. For cell-based assays performed in 96-well microtiter plates, GCs growing on one petri dish 60 x 15 mm were trypsinated, separated equally, and seeded on 6 x 6 wells (100 µl cell suspension/well) one day prior to the experiment.

Table 2 - Stimulants and inhibitors.

Treatment	Control
1 IU/ml FSH	PBS
10 IU/ml hCG	0.01 M sodium phosphate + 2.5 mg/ml D-Mannitol
10 mM 3-AT	DMEM/Ham's F12
20 μ M GKT137831	DMSO

4.1.2 Cultivation of KGN

The KGN cell line presents a steroidogenic human ovarian granulosa-like tumour cell line originating from a patient with invasive ovarian granulosa cell carcinoma. KGN was obtained from RIKEN BioResource Center, and cultured as described (Nishi et al., 2001). Briefly, KGN had a population doubling time of about 46.4 h and was cultured like GCs using culture medium consisting of DMEM/Ham's F12 medium with 1% P/S and 10% FCS at 37 °C, 5 % CO₂ and 95 % humidity. As adherent cells, they grew in culture flasks in 10 ml of culture medium. For sub-cultivation the cells were seeded at a cell density of 5.0 x 10⁵ cells/ml into fresh media every week. To count the cells, the LUNA-II automated cell counter was used, which is based on liquid lens technology (Logos Biosystems). For cell-based assays performed in 96-well microtiter plates, 1.5 x 10⁴ KGN/well were seeded (100 μ l cell suspension/well) one day prior to the experiment.

4.2 Immunological analysis

4.2.1 Western immunoblotting

1.1.1.1 Protein isolation

To isolate the whole protein lysate, the cells were removed from the surface of the cell culture vessel by cold NPE-buffer and a cell scraper. The suspension was centrifuged at 10,000 rpm at 4 °C for 3 min, and the pellet was washed with cold 10 mM PBS. After repeating this washing step, the pellet was resuspended in 100 μ l inhibitor cocktail, and the cells broken up by ultrasound. The protein concentration was measured by using the DCTM protein assay and transparent 96-well microtiter plates. The reaction is similar to the Lowry assay. The absorbance was measured at 690 nm, and the protein content was determined using a standard curve. Isolated protein was stored at -20 °C until use.

Proteins of human GCs (pooled from two to five aspirates) and KGN were then denatured using a heating cycle at 95 °C for 5 min at the presence of 10 % β -mercaptoethanol and 10 % bromophenol blue.

4.2.1.1 SDS-PAGE and Western blot

In the Western blot, cellular proteins were separated via SDS-Polyacrylamide-Gel-Electrophoresis (SDS-PAGE) by (Laemmli, 1970). Proteins were first concentrated in a running front using a low concentrated stacking gel and then separated via molecular weight using a 12 % SDS-gel (Table 3). Therefore the stacking gel was layered above the separating gel. The gel was loaded with about 10 µg protein and electrophoresed at 120 V for 1 h.

Table 3 - Composition of SDS-PAGE.

	Separating gel	Stacking gel
30 % acrylamide	5.2 ml	0.9 ml
4x separating gel buffer	3.25 ml	-
4x stacking gel buffer	-	1.5 ml
H ₂ O	4.55 ml	3.55 ml
TEMED	26 µl	15 µl
10 % APS	52 µl	25 µl

For the immunologic analysis, the proteins were transferred to a nitrocellulose membrane using a Mini Trans-Blot® cell. By a specific primary antibody and a secondary antibody conjugated with horseradish peroxidase (POX), the detection of the antigen of interest was performed (Burnette, 1981).

The transfer of the proteins onto the nitrocellulose membrane performed in transfer buffer (see Table 14) at 100 V for 75 min was verified by Ponceau-staining. To block the free binding sides, the membrane was put into powdered milk for 30 min, followed by incubation with primary antibody (Table 9) overnight at 4 °C. Blocking buffer was composed of 5 % powdered milk diluted in 1x Tris-buffered saline-Tween®20 (TBS-T), and antibodies were diluted in 0.5 % powdered milk/1x TBS-T.

Afterwards, membranes were washed intensively with 1x TBS-T (4 times for 10 min) and incubated with the corresponding secondary antibody conjugated with POX (1:10,000) (see Table 10) for 1 h at RT. After further washing steps (4 x 4 min), protein-antibody complexes were imaged on an image acquisition system (Chemi-Smart 5000) using a super sensitive Enhanced-Chemiluminescent-Substrate (ECL) (SuperSignal West Femto Maximum Sensitivity Substrate) according vendor's protocol. The intensity of the detected bands was analysed by ImageJ and compared to housekeeping proteins.

4.2.2 Immunocytochemistry

The cellular localization of NOX4/NOX5 proteins in cultured GCs and KGN was determined by immunocytochemistry. Therefore, GCs on culture day 2 or 3 or KGNs were seeded on cover

glasses placed in a 24-well plate 24 h prior use. After removing culture media by washing with 10 mM PBS (pH 7.4), the cells were fixed with ice-cold 3.7 % formaldehyde for 10 min followed by further washing steps with ice-cold PBS. To also detect intracellular target proteins, the cells were permeabilized with ice-cold 0.2 % Triton X-100/PBS on ice for 10 min. The cover glasses were then transferred into a humidified chamber where the rest of the process took place. The cells were blocked with 0.1% Triton X-100/PBS and 5% normal serum (blocking buffer) for 30 min, followed by the incubation with primary antibody diluted in 5 % normal serum/PBS (Table 9) for 2 h at RT. For control purposes, the primary antibody was replaced with normal serum. To remove unbound residuals of primary antibody, cells were washed with 0.1 % Triton X-100/PBS (3 times for 5 min). Incubation with secondary antibody conjugated with Alexa Fluor 488 or FITC (Table 10) diluted in blocking buffer was carried out for 1 h at RT. After further washing steps (3 x 5min) the cell nuclei were counterstained with 1 µg/ml DAPI for 5 min at RT. Cover glasses were then rinsed with PBS followed by mounting with a drop of glycerol-based liquid mountant onto microscope slides. After sealing of the cover glasses with nail polish and curing overnight at RT, they were stored in dark at 4 °C. Slides were examined with a fluorescence microscope (Zeiss).

4.2.3 Immunohistochemistry

Sections of human ovaries embedded in paraffin were used for immunological staining (Table 18). For the purpose of deparaffining and rehydrating of the sections, they were treated with xylol and a decreasing alcohol row (2 times xylol for 3 min; 2 times 100 % isopropyl alcohol for 3 min; once 96 %, 80 % and 70 % isopropyl alcohol for 3 min each; once PBS for 10 min). To unmask the antigens, the sections were boiled in 10 mM citrate buffer (pH 6.0) for 25 min. After a washing step with PBS (3 times for 5 min), the tissues were bordered with a PAP-pen. All further reagents were dropped on the sections very carefully. To block endogenous peroxidase, the sections were incubated with 9 % methanol and 3 % H₂O₂ in PBS for 30 min at RT in a humidified chamber. After further washing steps with PBS (3 times for 5 min), the protein-binding sides were blocked with 5 % goat normal serum for 30 min at RT in a humidified chamber. Afterwards, the incubation with the primary antibody (Table 9) diluted in 5 % goat normal serum in PBS over night at 4 °C in a humidified chamber took place. For primary antibodies made in goat, a donkey normal serum was used. For control purposes, the primary antibody was replaced by normal serum. To confirm the specificity of the primary antibody, it was pre-adsorbed with the corresponding blocking-peptide (Table 11). Therefore, a mix of the antibody and peptide was incubated at 4 °C for 2 h followed by a centrifugation step at 13,000 rpm at 4 °C. The supernatant was treated and used as the primary antibody. After the

incubation, the sections were washed with PBS (3 times for 5 min), and incubated with the corresponding secondary antibodies conjugated with biotin (Table 10) diluted in 5 % normal serum in PBS for 2 h at RT in a humidified chamber. For amplifying the target antigen signal, the sections were incubated with an Avidin–Biotin Complex (ABC) reagent for 2 h at RT in a humidified chamber according to the vendor's protocol. After further washing steps (2 times for 5 min and once with Tris/HCl for 10 min) the final staining step by the chromogen 3,3'-diaminobenzidine (DAB) took place. DAB is oxidized in the presence of peroxidase and H₂O₂ resulting in the deposition of a brown precipitate. When the satisfied intensity of staining is reached, the reaction with DAB can be stopped by ddH₂O (max. 10 min). Optional a nuclear staining with haematoxylin-eosin could be performed. Therefore, the sections were put into haematoxylin-eosin for 10 sec, stained by running tap water for 5 min, and finally dehydrated by an increasing alcohol row (96 %, 80 % and 70 % isopropyl alcohol for 3 min each; 2 times 100 % isopropyl alcohol for 3 min; 3 times xylol for 5 min). At the end, the slides were dried, embedded in mounting media Entellan®, and cured overnight at RT. Images were taken with an axiovert microscope (Zeiss).

4.2.4 Human cytokine array

GCs were treated with 50 µM H₂O₂ on culture day 3-4 and tested for cytokines using the Proteome Profiler Array by following the protocol. Briefly, after 24 h of incubation, the cell culture supernatant was centrifuged (at 8000 rpm for 3 min) and mixed with a cocktail of biotinylated detection antibodies. After incubation of sample/antibody mixture on the nitrocellulose membrane coated with selected capture antibodies, Straptavidin-HRP and chemiluminescent detection reagents were added. Successful cytokine/detection antibody complexes were detected by an image acquisition system (Chemi-Smart 5000). Analysis of spot intensities was done by using ImageJ software. For comparison of the control and treated group, means of spot densities were normalized to protein content followed by normalization of treated values to control values.

4.3 Analytical methods

4.3.1 Reverse transcription-PCR and quantitative RT-PCR

4.3.1.1 RNA isolation

Total RNA was isolated using the RNeasy Plus Micro Kit from Qiagen according to the vendor's protocol. In brief, cells were washed with PBS, lysed in RLT-buffer plus 1 % β-mercaptoethanol and homogenized by vortexing. After removing genomic DNA (gDNA) by means of a

centrifugation step (10,000 rpm, 30 sec) via a gDNA Eliminator spin column, the flow-through was mixed with 70 % ethanol (one sample volume), and total RNA was bound onto RNeasy MinElute spin column by centrifugation (10,000 rpm, 15 sec). The column was then washed with RW1 and RPE buffer (10,000 rpm, 15 sec), 80 % ethanol (10,000 rpm, 2 min), and finally dried via centrifugation (15,000 rpm, 5 min). Total RNA was then eluted with 20 µl RNase-free water and centrifuged (15,000 rpm, 1 min).

RNA concentration and purity was determined by UV-spectrometry at 260 and 280 nm using a NanoDrop® spectrophotometer. If the 260/280 ratio was about 2.0, the RNA was accepted as “pure” and could be used for experiments (storage at -80 °C).

4.3.1.2 cDNA synthesis

Complementary DNA (cDNA) was synthesized via reverse transcription by mixing 200 – 400 ng of total RNA with 1.6 µg random 15-mer primers and filling up to 11.5 µl with diethylpyrocarbonate (DEPC) water. The incubation steps and procedure are listed in Table 4, while the nucleotide mix consists of 4 µl 5x first strand buffer, 2 µl 0.1 M DTT, 1 µl 10 mM dNTPs and 0,5 µl RNasin. For control purposes, one mixture per sample without the reverse transcriptase (-RT) were also synthesized. The synthesized cDNA was stored at -20 °C.

Table 4 - Reverse transcription.

Time [min]	Temperature [°C]
10	70
5	25
Add nucleotide mix	
10	25
2	42
Add 1 µl Superscript II Reverse Transcriptase	
50	42
15	70
10	4

4.3.1.3 RT-PCR

Gene amplification was arranged with different oligomer primers synthesized by metabion international AG listed in Table 8 and a GoTaq DNA Polymerase Kit from Promega in a 25 µl reaction approach. Primers were designed using following software Primer3 and PrimerBLAST (<http://primer3.ut.ee/>; <https://www.ncbi.nlm.nih.gov/tools/primer-blast/>; 2018/03/27). The content and composition of one reaction mixture is described in Table 5 and the settings for the thermocycler is listed in Table 6. To exclude impurities, negative controls with H₂O instead of cDNA (H₂O) were performed.

Table 5 - Reaction mix for one RT-PCR sample.

Reagent	Volume [μl]
5x GoTaq-Buffer	5
dNTPs [2 mM]	2.5
Primer forward [100 μ M]	0.5
Primer reverse [100 μ M]	0.5
Nuclease free H ₂ O	15.37
cDNA Template	1
GoTaq-Polymerase	0.13

Table 6 - Thermocycler settings for RT-PCR.

Stage	Cycles	Temperature	Time
Denaturation	1	95 °C	2.5 min
Denaturation	35	95 °C	45 min
Annealing	35	60 °C	30 sec
Elongation	35	72 °C	45 sec
Final elongation	1	72 °C	5 min
Hold	-	4 °C	For ever

To visualize the PCR products, they were separated by size via gel electrophoresis. Therefore, a 2 % agarose gel was produced and mixed with Midori Green (0.005 %). The samples and a DNA ladder with known sizes (50 and 100 bp) were loaded onto the cured gel. The gel electrophoresis was performed in TBE-buffer at 90 V for 40 min and images were taken with a gel documentation system from BioRad.

Identity of all products were confirmed by sequencing by the company GATC biotech AG (Konstanz, Germany) and analysed by use of BLAST software (<https://blast.ncbi.nlm.nih.gov/Blast.cgi>; 2018/03/27).

4.3.1.4 qRT-PCR

Quantitative real-time polymerase chain reaction (qRT-PCR) was performed for relative quantification of gene expression by using the QuantiFast SYBR Green PCR Kit from Qiagen and a LightCycler® 96 System from Roche. Therefore, a master mix consisting of 1.125 μ l of forward primer (10 μ M), 1.125 μ l of reverse primer (10 μ M) and 6.25 μ l of 2x QuantiFast SYBR Green Mix was prepared, and 8.5 μ L of master mix was transferred to a Roche LightCycler®96 well plate (for primer information see Table 8). Finally, 4 μ L of pre-diluted cDNA (1:20 in RNase-free H₂O) was added to the respective wells and the plate was sealed with Roche LightCycler®480 sealing foils. A minus-reverse transcriptase control (-RT), where RNA instead of cDNA was added, and a non-target control (H₂O), H₂O instead of cDNA, served as negative

controls. For qRT-PCR analysis, technical duplicates were performed and the following cycler programme was used:

Table 7 - LightCycler settings for qRT-PCR.

Stages	Temperature [°C]	Time [sec]
Heat activation	95	300
Denaturation (40 cycles)	95	10
Annealing	60	30
Melting Curve	95	10
	65	60
	97	1
Cool Down	37	120

Relative gene expression differences were calculated by applying the comparative $\Delta\Delta Cq$ method with a static efficiency of 2 (Pfaffl, 2001) as follows:

$$\Delta Cq = Cq_{\text{target}} - Cq_{\text{reference gene}}$$

$$\Delta\Delta Cq = \Delta Cq_{\text{treatment}} - \Delta Cq_{\text{control}}$$

$$\text{Ratio} = 2^{-\Delta\Delta Cq}$$

Whereas Cq = quantification cycle describes the cycle at which the fluorescence of a sample first crosses the vertical threshold line. The arithmetic formula $2^{-\Delta\Delta Cq}$ defines the relative expression difference of a sample between treatments and control normalized to a reference gene and referred to a standard sample. As reference gene *RPL19* was used and as standard the according control (Table 2). To ensure that mRNA levels of housekeeping genes stay stable after the treatments, three further genes were tested beside *RPL19*. The mRNA levels of *RPL19*, *UBC*, *PPIA*, and *GAPDH* are not changed by the addition of FSH, hCG or GKT137831 (Figure 30).

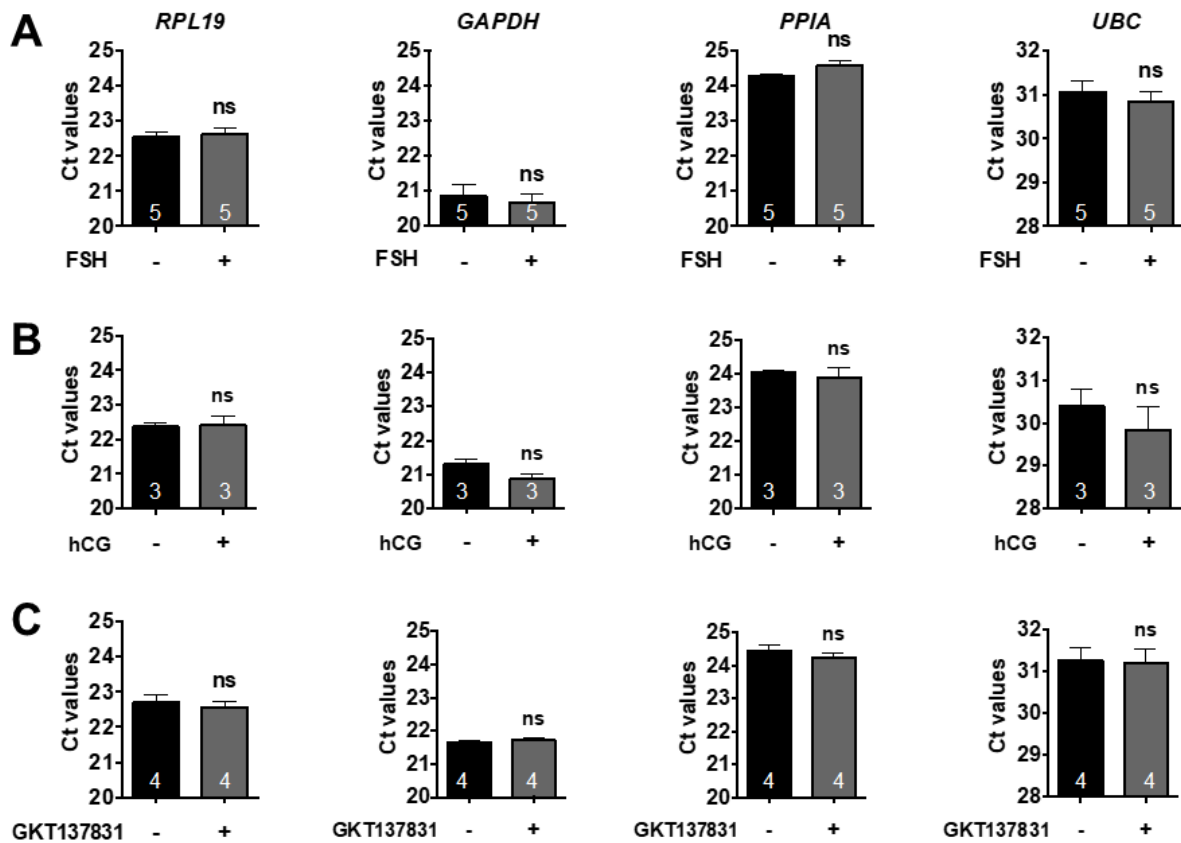


Figure 30 - Expression levels of multiple reference genes do not change after treatment. Cq values of *RPL19*, *UBC*, *PPIA*, and *GAPDH* are depicted as mean \pm SEM of GCs treated with FSH (A; n = 5), hCG (B; n = 3), and GKT137831 (C; n = 4), and do not show a difference compared to control. Statistics: paired *t* tests (two-tailed).

4.3.2 Cell viability assay

Cell viability was estimated by measuring ATP content using the CellTiter-Glo® Luminescent Cell Viability Assay. ATP serves as indicator for metabolically active cells. For the ATP assay, cells were seeded on white 96-well microtiter plates, cultured for 24 h, serum starved for 2 h, and then exposed to 20 μ M GKT137831 or 10 mM 3-AT, respectively in serum-free culture medium (100 μ l/well). After 24 h incubation, wells were washed with PBS and 100 μ l of a 1:1 mix of CellTiter-Glo® reagent, and DMEM/F12 without phenolred were added to each well containing control or stimulated cells, avoiding direct light. The contents were mixed for 2 min at 500 rpm on a plate shaker followed by incubation for 10 min at RT. The luminescence of the samples was measured by a luminometer (FLUOstar Omega) using a lens as emission filter. In addition, the cell morphology was examined and documented by a Leica microscope.

4.3.3 Cytotoxicity assay

Cytotoxicity was measured in KGN seeded in transparent 96-well microtiter plates employing the LDH Cytotoxicity Assay Kit. The assay measures lactate dehydrogenase (LDH) released into the media from damaged cells which indicates cellular cytotoxicity and cytolysis. The used diaphorase reduces a tetrazolium salt by NADPH, a product of LDH catalysis, to a red formazan product that can be measured at 490 nm. The absorbance was determined in quadruplicates after 24 h treatment with 20 μ M GKT137831 and background (690 nm) was subtracted.

4.3.4 Superoxide anion detection

Superoxide anion levels in cultured GCs were quantified in white 96-well microtiter plates using a Superoxide Anion Detection Kit according to the vendor's protocol. Superoxide anions oxidase luminol resulting in the formation of chemiluminescence light. Briefly, chemiluminescence of GCs without any stimulation was determined using a plate-reading luminometer (FLUOstar Omega) after addition of Superoxide Anion Assay Medium-Reagent Mixture containing 200 μ M luminol, 250 μ M enhancer and 200 ng/ml phorbol-12-myristate-13-acetate (PMA). As positive control 1 μ M carbachol was added, and samples without enhancer and PMA served as negative controls according to vendor's protocol. For demonstration the measured relative light units (RLU) were plotted as mean of six technical replicates each normalized to the starting value over 2 h.

4.3.5 Measurement of ROS generation

To determine ROS generation of cultured human GCs and KGN, a method based on the dye 2',7'-dichlorodihydrofluorescein diacetate (H₂DCFDA) was performed. In the presence of intracellular ROS, including H₂O₂, H₂DCFDA is converted to the highly fluorescent compound 2',7'-dichlorofluorescein (DCF). For the measurement of basal ROS level, GCs of independent preparations of cells pooled from two to five patients were seeded into black 96-well microtiter plates, cultured under standard conditions, and measured at the next day. In case of treatment with the NOX4 inhibitor and hormonal stimulation, 20 μ M GKT137831 and 1 IU/ml human recombinant FSH or 10 IU/ml hCG were added to the cells and incubated for 24 h. For each treatment, six technical replicates were prepared. Prior measurement, media was replaced by serum-free DMEM/Ham's F12 medium without phenol red, and loaded with H₂DCFDA (10 μ M) for 30 min at 37 °C. After replacing the dye with fresh media, fluorescence levels due to ROS generation were measured at 485 nm excitation/520 nm emission in a fluorimeter (FLUOstar

Omega) for 2 h at 37 °C. Fluorescence intensities are shown as means of six technical replicates, each normalized to the starting value over 2 h.

4.3.6 Measurement of H₂O₂ generation

The generation of H₂O₂ was measured using an Amplex[®] Red Kit. Briefly, cells were seeded and treated like for the ROS measurement. Amplex[®] Red reagent (10-acetyl-3,7-dihydroxyphenoxazine) was used in a final concentration of 2.5 μM and fluorescence levels were measured at 544 nm excitation/590 nm emission in a fluorimeter (FLUOstar Omega) for 2h at 37 °C. The mean values were normalized to the starting point value.

4.3.7 Measurement of H₂O₂ uptake via aquaporins

Intracellular H₂O₂ levels in culture of human GCs were quantified in black 96-well microtiter plates using a cell permeable boronate-based fluorescent probe Peroxy Orange 1 (PO1) by exogenous preloading as described by Dickinson et al. (Dickinson et al., 2010). Briefly, for the preparations and during the measurement culture medium was replaced with extra cellular (EC) fluid buffer (140 mM NaCl, 3 mM KCl, 1mM MgCl₂, 1 mM CaCl₂, 10 mM HEPES and 10 mM glucose; pH 7.4). Cells were preloaded with 1 μM PO1 and 500 nM AgNO₃, untreated control group with PO1 only, and incubated for 20 min. After replacing the dye and the blocker by fresh EC buffer, fluorescence was determined using a fluorimeter (FLUOstar Omega) after addition of 100 μM H₂O₂ in EC buffer (544 nm excitation/590 nm emission).

In addition, intracellular H₂O₂ production by PO1 was examined using a Leica confocal microscope. GCs were cultured on a μ-Dish^{35mm, high}, ibiTreat for 2 days. Prior to microscopy, culture medium was replaced by 1 μM PO1 diluted in EC buffer, the dish was placed into a heating unit at 37 °C belonging to the microscope, and after 20 min H₂O₂ (end concentration: 333 μM) was added. Fluorescence imaging was performed at t = 0 and t = 20 min (552 nm excitation/562-650 nm emission via HyD detector).

4.4 Statistics

Statistical analyses were performed using Prism 6 (GraphPad Software, San Diego, CA, USA). Data are expressed as means ± SEM unless indicated otherwise in the text and graphs. Paired *t* test, two-tailed was employed for ATP results, and one-sample *t* tests with a theoretical mean of 1 or 0 were used to verify statistic relevance of percentage decrease of ROS and H₂O₂

measurements, qRT-PCR, WB LDH, cell number, and confluence results. Statistical significance was accepted for $p < 0.05$.

4.5 Material

4.5.1 Primers

Table 8 - Information about oligonucleotide primers used for PCR studies.

Gene	Reference	Primer sequence (5'-3')	Product size [bp]
RPL19	NM_000981.3	F: agg cac atg ggc ata ggt aa R: cca tga gaa tcc gct tgt tt	199
UBC	AB_362574.1	F: gcc tta gaa ccc cag tat cag R: aag aaa acc agt gcc cta gag	74
GAPDH	NM_002046.6	F: gtc ttc act acc atg gag aag g R: tca tgg atg acc ttg gcc ag	197
PPIA	KJ_905864.1	F: aga caa ggt ccc aaa gac R: acc acc ctg aca cat aaa	118
NOX4	NM_001143837.1	F: ccg aac act ctt ggc tta cc R: gtt gag ggc att cac cag at	160
NOX5	NM_024505.3	F: gct gtc gag gag tgt gac aa R: gct cag agg caa aga tcc tg	146
DUOX1	NM_175940.2	F: cct ctg agc agt tcc tgt cc R: aaa tcc cgc aca tct tca ac	247
DUOX2	NM_014080.4	F: ggc aaa ttc tcc cgt aca ga R: agc tgg gat agg tcc tgg tt	194
SOD1	NM_000454.4	F: gaa ggt ggg gaa gca tta R: acc ttt gcc caa gtc atc tg	300
SOD2	BC_016934.1	F: ggg gtc aaa gtt cac aag ga R: cca aaa ggc aca gac tca aa	189
Catalase	NM_001752.3	F: gcc tgg gac cca att atc tt R: gaa tct ccg cac ttc tcc ag	203
DJ-1	NM_001123377.1	F: tga gtc tgc tgc tgt gaa gg R: ccg tct ttt tcc aca cga tt	201
GST	NM_146421.2	F: atg ccc atg ata ctg ggg ta R: gtg agc ccc atc aat caa gt	204
AQP3	NM_001318144.1	F: ttt ggc ttt gct gtc act ct	199

		R: gcc aga ttg cat cat aat aca gc	
AQP8	NM_001169.2	F: gtc tgg agg ctg cat gaa tc R: cca atg aag cac cta atg agc a	138
AQP9	NM_020980.4	F: cgg tgt ctc tgg tgg tca R: cca caa agg ctc cca aga ac	119
CYP11A1	NM_000781	F: agt cca cct tca cca tgt cc R: aga gaa ggg cca cat ctt ca	113
StAR	NM_000349	F: cct gag cag aag ggt gtc at R: cga tgc tga gta gcc acg ta	109
FSHR	NM_000145.2	F: ctg ctc ctg gtc tct ttg ct R: ggt ccc caa atc ctg aaa at	208
LHR	NM_000233.3	F: tgg aaa tgg att tga aga agt aca R: cac gga agg ctc cat tgt	113

4.5.2 Antibodies

Table 9 - List of primary antibodies.

Antigen	Host	Method and dilution	Reference # and manufacturer
NOX4 No. 1	rabbit	WB (1:1000) IHC (1:500) ICC (1:200)	7927; ProSci; Fort Collins, CO, USA
NOX4 No. 2	goat	IHC (1:1000)	NB110-58849; Novus Biologicals, Littleton; CO; USA
NOX4 No. 3	goat	ICC (1:50)	sc-21860; Santa Cruz, Dallas, Texas, USA
NOX5	rabbit	WB (1:2000) ICC (1:100)	ab191010; Abcam, Cambridge, UK
MAPK	rabbit	WB (1:2000)	4695; Cell Signaling, Danvers, MA, USA
pMAPK	mouse	WB (1:1000)	9106; Cell Signaling, Danvers, MA, USA
StAR	rabbit	WB (1:500)	Texas Tech University
PCNA	mouse	WB (1:2500)	610664; BD, Franklin Lakes, NJ, USA
β-Actin	mouse	WB (1:5000)	A5441; Sigma-Aldrich, St Louis, MO, USA

Table 10 - List of secondary antibodies.

Antibody	Host	Conjugate	Method and dilution	Reference #
Anti-rabbit IgG	goat	POX	WB (1:10000)	111-035-144 +
Anti-mouse IgG	donkey	POX	WB (1:10000)	715-036-150 +
Anti-rabbit IgG	goat	Alexa Fluor 488	ICC (1:1000)	R37116 **
Anti-rabbit IgG	goat	Cy3	ICC (1:800)	111-165-144 +
Anti-goat IgG	donkey	FITC	ICC (1:100)	705-096-147 +

Anti-rabbit IgG	goat	Biotin	IHC (1:500)	111-065-144 +
Anti-goat IgG	donkey	Biotin	IHC (1:500)	705-066-147 +

+ Jackson, Bar Harbor, Maine, USA

++ Thermo Fisher Scientific, Waltham, Massachusetts, USA

Table 11 - Blocking peptide.

Gene	Method and dilution	Reference # and manufacturer
NOX4	IHC (1:3)	NB110-58849PEP; Novus Biologicals, Littleton; CO; USA

4.5.3 Consumables

Table 12 - List of used consumables.

Material	Manufacturer
μ -Dish ^{35mm, high} , ibiTreat	ibidi GmbH, Martinsried, Germany
0.9-mm hypodermic needle	Braun, Melsungen, Hessen, Germany
Cell scraper	Kisker, Steinfurt, Germany
Cell strainer (40 μ m)	BD, Franklin Lakes, NJ, USA
Cover glasses (thickness no 1.5)	Paul Marienfeld, Lauda-Koenigshofen, Germany
Falcon tubes (15/50 ml)	Sarstedt, Nuernbrecht, Germany
Injekt one-way syringe (10 ml)	B. Braun, Melsungen, Germany
LUNA™ Cell Counting Slides	Logos Biosystems, Dongan-gu, South Korea
Micro tubes (0.25/0.5/1.0/2.0 ml)	Sarstedt, Nuernbrecht, Germany
Microscope slides	VWR, Darmstadt, Germany
Nitrocellulose membrane	Machery-Nagel, Dueren, Germany
Nunc EasYFlask 75cm ²	Thermo Fisher Scientific, Waltham, Massachusetts, USA
Nunc™ 96-well microtiter plates (transparent/black/white)	Thermo Fisher Scientific, Waltham, Massachusetts, USA
PAP-Pen	Science Services, Munich, Germany
Petri dish (35/60 x 15 mm)	Sarstedt, Nuernbrecht, Germany
Pipette tips (10/20/100/200/1000 μ l)	Rainin, Greifensee, Switzerland
Reagent reservoir (25 ml)	VWR, Darmstadt, Germany
Roche LightCycler®480 sealing foils	Roche, Basel, Switzerland
Roche LightCycler®96 well plate	Roche, Basel, Switzerland
TC-plate 24 well	Sarstedt, Nuernbrecht, Germany
Urine beaker	Sarstedt, Nuernbrecht, Germany

Feather Disposable Scalpel	Feather, Osaka, Japan
Serological pipettes (5/10/25/50 ml)	Sarstedt, Nuernbrecht, Germany

4.5.4 Chemicals

Table 13 - List of used chemicals.

Chemicals	Manufacturer
3.7 % formaldehyde	Sigma-Aldrich, St Louis, MO, USA
3-Amino-1,2,4-triazole (3-AT)	Sigma-Aldrich, St. Louis, Missouri, USA
4',6-Diamidin-2-phenylindol (DAPI)	Thermo Fisher Scientific, Waltham, Massachusetts, USA
5x First Strand Buffer	Invitrogen - Life Technologies, Carlsbad, CA, USA
5x Go Taq-Buffer	Promega, Madison, WI, USA
Acrylamid	AppliChem, Darmstadt, Germany
Agarose	Biozym, Hessisch Oldendorf, Germany
AgNO ₃	Honeywell, Seelze, Germany
Albumin Standard	Pierce - Thermo Fischer Scientific, Waltham, MA, USA
Ammoniumpersulfat (APS)	Merck, Darmstadt, Germany
Boric acid	Roth, Karlsruhe, Germany
Bromophenol blue	Serva, Heidelberg, Germany
CaCl x2 H ₂ O	Sigma-Aldrich, St Louis, MO, USA
Carbachol	Sigma-Aldrich, St Louis, MO, USA
Citric acid	Roth, Karlsruhe, Germany
DCFDA-H ₂	Molecular Probes, Eugene, OR, USA
Diethylpyrocarbonate (DEPC) water	Ambion - Life Technologies, Carlsbad, CA, USA
Dimethyl sulfoxide (DMSO)	Sigma-Aldrich, St. Louis, Missouri, USA
Dithiothreitol (DTT)	Invitrogen - Life Technologies, Carlsbad, CA, USA
D-Mannitol	Sigma-Aldrich, St Louis, MO, USA
dNTPs (dATP/dCTP/dGTP/dTTP)	Qiagen, Hilden, Germany
EDTA	Roth, Karlsruhe, Germany
Entellan [®]	Merck Millipore, Billerica, MA, USA
Ethanol	Roth, Karlsruhe, Germany
Follicle stimulating hormone (FSH)	Cedarlane, Burlington, NC, USA
GeneRuler 50/100 bp DNA Ladder	Thermo Fischer Scientific, Waltham, MA, USA
GKT137831	Selleckchem, Houston, TX, USA
Glucose	Sigma-Aldrich, St Louis, MO, USA
Glycerine	Merck, Darmstadt, Germany
Glycine	AppliChem, Darmstadt, Deutschland
GoTaq DNA Polymerase	Promega, Madison, WI, USA
H ₂ DCFDA	Invitrogen - Life Technologies, Carlsbad, CA, USA
H ₂ O ₂ (30 %)	Sigma-Aldrich, St Louis, MO, USA
Haematoxylin-eosin	Roth, Karlsruhe, Germany
HCl	Roth, Karlsruhe, Germany

HEPES	Sigma-Aldrich, St Louis, MO, USA
Human chorionic gonadotropin (hCG)	Sigma-Aldrich, St. Louis, Missouri, USA
Isopropyl alcohol	Roth, Karlsruhe, Germany
K ₂ HPO ₄ x 3 H ₂ O	Merck, Darmstadt, Germany
KCl	Merck, Darmstadt, Germany
Methanol	Roth, Karlsruhe, Germany
MgCl x6 H ₂ O	Sigma-Aldrich, St Louis, MO, USA
Midori Green	Nippon Genetics Europe GmbH, Dueren, Germany
N, N, N', N'-Tetramethylethyldiamin (TEMED)	Bio-Rad, Hercules, CA, USA
Na ₂ HPO ₄ x 2 H ₂ O	Merck, Darmstadt, Germany
NaCl	Roth, Karlsruhe, Germany
NaH ₂ PO ₄ x H ₂ O	Honeywell, Seelze, Germany
Normal goat serum	Sigma-Aldrich, St Louis, MO, USA
Normal rabbit serum	Chemikon, Billerica, MA, USA
PageRuler Plus Prestained Protein Ladder	Pierce - Thermo Fischer Scientific, Waltham, MA, USA
PBS	Thermo Fisher Scientific, Waltham, Massachusetts, USA
PBS-Dulbecco	Biochrom GmbH, Berlin, Germany
Peroxy Orange 1 (PO1)	Tocris, Bristol, UK
pH calibration standard pH 4/7/10	Roth, Karlsruhe, Germany
Pierce Protease and Phosphatase Inhibitor Mini Tablets	Thermo Fisher Scientific, Waltham, Massachusetts, USA
PIPES	Roth, Karlsruhe, Germany
Ponceau S	Sigma-Aldrich, St Louis, MO, USA
Powdered milk	Vitalia, Bruckmühl, Germany
ProLong™ Diamond Antifade Mountant	Thermo Fisher Scientific, Waltham, Massachusetts, USA
Random 15-mer primers	metabion international AG, Munich, Germany
Rnasin Plus	Promega, Madison, WI, USA
Saccharose	Merck, Darmstadt, Germany
Sodium Dodecyl Sulfate (SDS)	Roth, Karlsruhe, Germany
Superscript II	Invitrogen - Life Technologies, Carlsbad, CA, USA
Tris	Roth, Karlsruhe, Germany
Tri-Sodium Citrate Dihydrate	Roth, Karlsruhe, Germany
Triton X-100	Sigma-Aldrich, St Louis, MO, USA
Trypsin	PAA, Pasching, Austria
Tween 20	Roth, Karlsruhe, Germany
Xylol	Roth, Karlsruhe, Germany
β-Mercaptoethanol	Sigma-Aldrich, St Louis, MO, USA

4.5.5 Buffers and solutions

Table 14 - Composition of used buffers and solutions.

Buffer	Composition
10x Laemmli sample buffer	30.3 g Tris 144.1 g Glycine 10 g SDS Fill up to 1 l ddH ₂ O
10x PBS	4.4 g NaCl 93.3 mg KCl 400.47 mg Na ₂ HPO ₄ x2 H ₂ O 171.2 mg K ₂ HPO ₄ x3 H ₂ O Fill up to 0.5 l with ddH ₂ O; pH 7.5
10x TBE buffer	108 g Tris 55 g boric acid 40 ml 0.5 M EDTA Fill up to 1 l with ddH ₂ O; pH 8.0
10x Transfer buffer	30.3 g Tris 144.1 g Glycine Fill up to 1 l with ddH ₂ O; pH 8.3 100 ml 10x transfer buffer 100 ml Methanol Fill up to 1 l with ddH ₂ O
20x TBS-T	116.8 g NaCl 12.1 g Tris 10 ml Tween 20 Fill up to 1 l with ddH ₂ O; pH 7.5
4x Separating gel buffer	45.43 g Tris 0.75 g EDTA 1 g SDS Fill up to 0.25 l with ddH ₂ O; pH: 8.8
4x Stacking gel buffer	15.15 g Tris (0.5M) 0.75 g EDTA 1 g SDS Fill up to 0.25 l with ddH ₂ O; pH: 6.8
APS (10 %)	1 g APS 10 ml ddH ₂ O
Bromophenol blue	0.1 M Tris 2.4 ml Glycerine 50 mg SDS 1 spatte point bromophenol blue Fill up to 10 ml with ddH ₂ O; pH: 6.8
Citric acid solution	21.01 g citric acid Fill up to 1 l with ddH ₂ O
Disodium phosphate (0.1 M)	17.78 g Na ₂ HPO ₄ x 2 H ₂ O Fill up to 1 l with ddH ₂ O
EC solution	8.18 g NaCl 0.22 g KCl 0.2 g MgCl x6 H ₂ O 0.15 g CaCl x2 H ₂ O 2.38 g HEPES 1.98 g Glucose Fill up to 1 l with ddH ₂ O; pH 7.4

Inhibitor cocktail	1 inhibitor tablet in 10 ml sample buffer
Monosodium phosphate (0.1 M)	13.8 g NaH ₂ PO ₄ x H ₂ O Fill up to 1 l with ddH ₂ O
NPE-Buffer	4.4 g NaCl 1.5 g PIPES 50.15 g EDTA Fill up to 0.5 l with ddH ₂ O; pH 7.2
PBS (10 mM)	9.55 PBS Solve in 1 l ddH ₂ O
Sample buffer	1.9 g Tris 5 g SDS 25 g Saccharose Fill up to 0.25 l with ddH ₂ O; pH 6.8
Sodium citrate solution	29.41 g Tri-Sodium Citrate Dihydrate Fill up to 1 l with ddH ₂ O
Sodium phosphate (0.01 M)	Titrate 0.01 M Na ₂ HPO ₄ x 2 H ₂ O with 0.01 M NaH ₂ PO ₄ x H ₂ O till pH 7.4
Tris/HCl (50 mM)	6.06 g Tris 38.9 ml HCl Fill up to 1 l with ddH ₂ O; pH 7.6

4.5.6 Cell culture media and reagents

Table 15 - List of cell culture media and supplements.

Cell culture media and supplements	Manufacturer
DMEM/F-12	Thermo Fisher Scientific, Waltham, Massachusetts, USA
DMEM/F-12, no phenol red	Thermo Fisher Scientific, Waltham, Massachusetts, USA
Fetal calf serum (FCS)	PAA, Pasching, Austria
Penicillin/Streptomycin	PAA, Pasching, Austria

4.5.7 Kits and assays

Table 16 - List of used kits.

Kits	Manufacturer
Amplex [®] Red Kit	Invitrogen - Life Technologies, Carlsbad, CA, USA
CellTiter-Glo [®] Luminescent Cell Viability Assay	Promega, Mannheim, Germany
DC [™] Protein Assay	Bio-Rad, Hercules, CA, USA
GoTaq DNA Polymerase Kit	Promega, Mannheim, Germany

LDH Cytotoxicity Assay Kit	Pierce - Thermo Fischer Scientific, Waltham, MA, USA
MinElute Gel Extraction Kit	Qiagen, Hilden, Germany
Proteome Profiler Array - Human Cytokine	R&D Systems, Inc., Minneapolis, MN, USA
QuantiFast SYBR Green PCR Kit	Qiagen, Hilden, Germany
RNeasy Plus Micro Kit	Qiagen, Hilden, Germany
SIGMAFAST™ 3,3'-Diaminobenzidine tablets	Sigma-Aldrich, St Louis, MO, USA
Superoxide Anion Detection Kit	Calbiochem, San Diego, CA, USA
SuperSignal West Femto Maximum Sensitivity Substrate	Thermo Fisher Scientific, Waltham, Massachusetts, USA
Vectastain ABC Kit	Vector Laboratories, Burlingame, CA, USA

4.5.8 Equipment

Table 17 - List of used equipment.

Equipment	Manufacturer
Cell culture centrifuge 5810 R	Eppendorf, Hamburg, Germany
Chemi-Smart 5000	Peqlab/VWR, Erlangen, Germany
Clean bench B-[MaxPro] ² -160	Berner, Elmshorn, Germany
CO ₂ incubator - Galaxy® 170 S	Eppendorf, Hamburg, Germany
Cooling centrifuge Biofuge Fresco	Haraeus, Hanau, Germany
FLUOstar Omega	BMG Labtech, Ortenberg, Germany
Freezer -80 °C	Liebherr, Ochsenhausen, Germany
Freezer and fridges	Liebherr, Ochsenhausen, Germany
Gel Doc™ XR+ Gel Documentation System	Bio-Rad; Hercules, CA, USA
ibidi Gas Incubation System	ibidi, Planegg, Germany
ibidi Heating System	ibidi, Planegg, Germany
Leica TCS SP8 confocal microscope	Leica, Wetzlar, Germany
LightCycler® 96 System	Roche Diagnostics, Penzberg, Germany
LUNA-II™ Automated Cell Counter	Logos Biosystems, Dongan-gu, South Korea
Microliter centrifuge 5418	Eppendorf, Hamburg, Germany
Microscope Axio Observer	Zeiss, Oberkochen, Germany
Microscope Axiovert 135	Zeiss, Oberkochen, Germany

Microscope Axiovert 200 M	Zeiss, Oberkochen, Germany
Microscope DMIL LED	Leica, Wetzlar, Germany
Microwave M690	Miele, Guetersloh, Germany
Microscope confocal TCS SP8	Leica, Wetzlar, Germany
Mini Trans-Blot® cell	Bio-Rad, Hercules, CA, USA
Multichannel pipette 20-200 µl	Rainin, Greifensee, Switzerland
Multipipette® M4	Eppendorf, Hamburg, Germany
NanoDrop® spectrophotometer	Thermo Fisher Scientific, Waltham, Massachusetts, USA
Orbital shaker Duomax 1030/2030	Heidolph, Schwabach, Germany
ph-Meter FE20/EL20	Mettler-Toledo, Greifensee, Switzerland
Pipettes Research® plus 2/10/20/100/200/1000/5000 µl	Eppendorf, Hamburg, Germany
Pipetus	Hirschmann, Heilbronn, Germany
Precision balance BP 310 S	Sartorius, Goettingen, Germany
Sub Cell GT Agarose Gel System	Bio-Rad, Hercules, CA, USA
Thermomixer R	Eppendorf, Hamburg, Germany
Ultraturax T25	IKA-Werk, Staufen, Germany
Vortex Genie 2	Scientific Industries, Bohemia, NY, USA
Water bath	Memmert, Schwabach, Germany
XS-analytical balance	Mettler-Toledo, Greifensee, Switzerland

4.5.9 Biological material

Table 18 - List of biological material and cells.

Material	Origin
Ovarian sections (Homo sapiens)	Institute for cell biology (Anatomy III), LMU Munich, Germany
Follicular fluid (Homo sapiens)	A.R.T. Bogenhausen, Munich, Germany
KGN cell line	RIKEN BioResource Center

5. References

- Abel, M. H., Huhtaniemi, I., Pakarinen, P., Kumar, T. R., & Charlton, H. M. (2003). Age-related uterine and ovarian hypertrophy in FSH receptor knockout and FSHbeta subunit knockout mice. *Reproduction*, *125*(2), 165-173.
- Adam, M., Saller, S., Strobl, S., Hennebold, J. D., Dissen, G. A., Ojeda, S. R., Stouffer, R. L., Berg, D., Berg, U., & Mayerhofer, A. (2012). Decorin is a part of the ovarian extracellular matrix in primates and may act as a signaling molecule. *Hum Reprod*, *27*(11), 3249-3258. doi:10.1093/humrep/des297
- Agarwal, A., Aponte-Mellado, A., Premkumar, B. J., Shaman, A., & Gupta, S. (2012). The effects of oxidative stress on female reproduction: a review. *Reprod Biol Endocrinol*, *10*, 49. doi:10.1186/1477-7827-10-49
- Alper, M. M., & Fauser, B. C. (2017). Ovarian stimulation protocols for IVF: is more better than less? *Reprod Biomed Online*, *34*(4), 345-353. doi:10.1016/j.rbmo.2017.01.010
- Altenhofer, S., Radermacher, K. A., Kleikers, P. W., Wingler, K., & Schmidt, H. H. (2015). Evolution of NADPH Oxidase Inhibitors: Selectivity and Mechanisms for Target Engagement. *Antioxid Redox Signal*, *23*(5), 406-427. doi:10.1089/ars.2013.5814
- Aoyama, T., Paik, Y. H., Watanabe, S., Laleu, B., Gaggini, F., Fioraso-Cartier, L., Molango, S., Heitz, F., Merlot, C., Szyndralewicz, C., Page, P., & Brenner, D. A. (2012). Nicotinamide adenine dinucleotide phosphate oxidase in experimental liver fibrosis: GKT137831 as a novel potential therapeutic agent. *Hepatology*, *56*(6), 2316-2327. doi:10.1002/hep.25938
- Araujo, V. R., Gastal, M. O., Figueiredo, J. R., & Gastal, E. L. (2014). In vitro culture of bovine preantral follicles: a review. *Reprod Biol Endocrinol*, *12*, 78. doi:10.1186/1477-7827-12-78
- Attaran, M., Pasqualotto, E., Falcone, T., Goldberg, J. M., Miller, K. F., Agarwal, A., & Sharma, R. K. (2000). The effect of follicular fluid reactive oxygen species on the outcome of in vitro fertilization. *Int J Fertil Womens Med*, *45*(5), 314-320.
- Avila, J., Gonzalez-Fernandez, R., Rotoli, D., Hernandez, J., & Palumbo, A. (2016). Oxidative Stress in Granulosa-Lutein Cells From In Vitro Fertilization Patients. *Reprod Sci*, *23*(12), 1656-1661. doi:10.1177/1933719116674077
- Bedard, K., Jaquet, V., & Krause, K. H. (2012). NOX5: from basic biology to signaling and disease. *Free Radic Biol Med*, *52*(4), 725-734. doi:10.1016/j.freeradbiomed.2011.11.023
- Bedard, K., & Krause, K. H. (2007). The NOX family of ROS-generating NADPH oxidases: physiology and pathophysiology. *Physiol Rev*, *87*(1), 245-313. doi:10.1152/physrev.00044.2005
- Best, C. L., Pudney, J., Welch, W. R., Burger, N., & Hill, J. A. (1996). Localization and characterization of white blood cell populations within the human ovary throughout the menstrual cycle and menopause. *Hum Reprod*, *11*(4), 790-797.
- Bhartiya, D., & Singh, J. (2015). FSH-FSHR3-stem cells in ovary surface epithelium: basis for adult ovarian biology, failure, aging, and cancer. *Reproduction*, *149*(1), R35-48. doi:10.1530/REP-14-0220
- Bienert, G. P., & Chaumont, F. (2014). Aquaporin-facilitated transmembrane diffusion of hydrogen peroxide. *Biochim Biophys Acta*, *1840*(5), 1596-1604. doi:10.1016/j.bbagen.2013.09.017
- Bienert, G. P., Moller, A. L., Kristiansen, K. A., Schulz, A., Moller, I. M., Schjoerring, J. K., & Jahn, T. P. (2007). Specific aquaporins facilitate the diffusion of hydrogen peroxide across membranes. *J Biol Chem*, *282*(2), 1183-1192. doi:10.1074/jbc.M603761200
- Bienert, G. P., Schjoerring, J. K., & Jahn, T. P. (2006). Membrane transport of hydrogen peroxide. *Biochimica et Biophysica Acta (BBA) - Biomembranes*, *1758*(8), 994-1003. doi:https://doi.org/10.1016/j.bbamem.2006.02.015

- Birben, E., Sahiner, U. M., Sackesen, C., Erzurum, S., & Kalayci, O. (2012). Oxidative stress and antioxidant defense. *World Allergy Organ J*, 5(1), 9-19. doi:10.1097/WOX.0b013e3182439613
- Block, K., Gorin, Y., & Abboud, H. E. (2009). Subcellular localization of Nox4 and regulation in diabetes. *Proc Natl Acad Sci U S A*, 106(34), 14385-14390. doi:10.1073/pnas.0906805106
- Blohberger, J., Buck, T., Berg, D., Berg, U., Kunz, L., & Mayerhofer, A. (2016). L-DOPA in the human ovarian follicular fluid acts as an antioxidant factor on granulosa cells. *J Ovarian Res*, 9(1), 62. doi:10.1186/s13048-016-0269-0
- Brandes, R. P., Weissmann, N., & Schroder, K. (2014). Nox family NADPH oxidases: Molecular mechanisms of activation. *Free Radic Biol Med*, 76, 208-226. doi:10.1016/j.freeradbiomed.2014.07.046
- Brown, D. I., & Griending, K. K. (2009). Nox proteins in signal transduction. *Free Radic Biol Med*, 47(9), 1239-1253. doi:10.1016/j.freeradbiomed.2009.07.023
- Buccione, R., Schroeder, A. C., & Eppig, J. J. (1990). Interactions between somatic cells and germ cells throughout mammalian oogenesis. *Biol Reprod*, 43(4), 543-547.
- Bulling, A., Berg, F. D., Berg, U., Duffy, D. M., Stouffer, R. L., Ojeda, S. R., Gratzl, M., & Mayerhofer, A. (2000). Identification of an ovarian voltage-activated Na⁺-channel type: hints to involvement in luteolysis. *Mol Endocrinol*, 14(7), 1064-1074. doi:10.1210/mend.14.7.0481
- Burdon, R. H., & Rice-Evans, C. (1989). Free radicals and the regulation of mammalian cell proliferation. *Free Radic Res Commun*, 6(6), 345-358.
- Burnette, W. N. (1981). "Western Blotting": Electrophoretic transfer of proteins from sodium dodecyl sulfate-polyacrylamide gels to unmodified nitrocellulose and radiographic detection with antibody and radioiodinated protein A. *Analytical Biochemistry*, 112(2), 195-203. doi:https://doi.org/10.1016/0003-2697(81)90281-5
- Carlson, J. C., Wu, X. M., & Sawada, M. (1993). Oxygen radicals and the control of ovarian corpus luteum function. *Free Radic Biol Med*, 14(1), 79-84.
- Chen, Q., Zhang, W., Ran, H., Feng, L., Yan, H., Mu, X., Han, Y., Liu, W., Xia, G., & Wang, C. (2014). PKCdelta and theta possibly mediate FSH-induced mouse oocyte maturation via NOX-ROS-TACE cascade signaling pathway. *PLoS One*, 9(10), e111423. doi:10.1371/journal.pone.0111423
- Cheng, G., Cao, Z., Xu, X., van Meir, E. G., & Lambeth, J. D. (2001). Homologs of gp91phox: cloning and tissue expression of Nox3, Nox4, and Nox5. *Gene*, 269(1-2), 131-140.
- Das, N., & Kumar, T. R. (2018). Molecular regulation of follicle-stimulating hormone synthesis, secretion and action. *J Mol Endocrinol*, 60(3), R131-r155. doi:10.1530/jme-17-0308
- Devine, P. J., Perreault, S. D., & Luderer, U. (2012). Roles of reactive oxygen species and antioxidants in ovarian toxicity. *Biol Reprod*, 86(2), 27. doi:10.1095/biolreprod.111.095224
- Devoto, L., Fuentes, A., Kohen, P., Cespedes, P., Palomino, A., Pommer, R., Munoz, A., & Strauss, J. F., 3rd. (2009). The human corpus luteum: life cycle and function in natural cycles. *Fertil Steril*, 92(3), 1067-1079. doi:10.1016/j.fertnstert.2008.07.1745
- Dias, F. A., Gandara, A. C., Queiroz-Barros, F. G., Oliveira, R. L., Sorgine, M. H., Braz, G. R., & Oliveira, P. L. (2013). Ovarian dual oxidase (Duox) activity is essential for insect eggshell hardening and waterproofing. *J Biol Chem*, 288(49), 35058-35067. doi:10.1074/jbc.M113.522201
- Dickinson, B. C., Huynh, C., & Chang, C. J. (2010). A palette of fluorescent probes with varying emission colors for imaging hydrogen peroxide signaling in living cells. *J Am Chem Soc*, 132(16), 5906-5915. doi:10.1021/ja1014103
- Downs, S. M., Daniel, S. A., & Eppig, J. J. (1988). Induction of maturation in cumulus cell-enclosed mouse oocytes by follicle-stimulating hormone and epidermal growth factor: evidence for a positive stimulus of somatic cell origin. *J Exp Zool*, 245(1), 86-96. doi:10.1002/jez.1402450113

- Duranthon, V., & Chavatte-Palmer, P. (2018). Long term effects of ART: What do animals tell us? *Mol Reprod Dev*, *85*(4), 348-368. doi:10.1002/mrd.22970
- Edson, M. A., Nagaraja, A. K., & Matzuk, M. M. (2009). The Mammalian Ovary from Genesis to Revelation. *Endocrine Reviews*, *30*(6), 624-712. doi:10.1210/er.2009-0012
- Ferrero, H., Delgado-Rosas, F., Garcia-Pascual, C. M., Monterde, M., Zimmermann, R. C., Simon, C., Pellicer, A., & Gomez, R. (2012). Efficiency and purity provided by the existing methods for the isolation of luteinized granulosa cells: a comparative study. *Hum Reprod*, *27*(6), 1781-1789. doi:10.1093/humrep/des096
- Finkel, T. (2011). Signal transduction by reactive oxygen species. *J Cell Biol*, *194*(1), 7-15. doi:10.1083/jcb.201102095
- Gaggini, F., Laleu, B., Orchard, M., Fioraso-Cartier, L., Cagnon, L., HOUNGNINOU-MOLANGO, S., Gradia, A., Duboux, G., Merlot, C., Heitz, F., Szyndralewicz, C., & Page, P. (2011). Design, synthesis and biological activity of original pyrazolo-pyrido-diazepine, -pyrazine and -oxazine dione derivatives as novel dual Nox4/Nox1 inhibitors. *Bioorg Med Chem*, *19*(23), 6989-6999. doi:10.1016/j.bmc.2011.10.016
- Georges, A., Auguste, A., Bessiere, L., Vanet, A., Todeschini, A. L., & Veitia, R. A. (2014). FOXL2: a central transcription factor of the ovary. *J Mol Endocrinol*, *52*(1), R17-33. doi:10.1530/jme-13-0159
- Ginther, O. J., Beg, M. A., Bergfelt, D. R., Donadeu, F. X., & Kot, K. (2001). Follicle selection in monovular species. *Biol Reprod*, *65*(3), 638-647.
- Giorgio, M., Trinei, M., Migliaccio, E., & Pelicci, P. G. (2007). Hydrogen peroxide: a metabolic by-product or a common mediator of ageing signals? *Nat Rev Mol Cell Biol*, *8*(9), 722-728. doi:10.1038/nrm2240
- Gloaguen, P., Crepieux, P., Heitzler, D., Poupon, A., & Reiter, E. (2011). Mapping the follicle-stimulating hormone-induced signaling networks. *Front Endocrinol (Lausanne)*, *2*, 45. doi:10.3389/fendo.2011.00045
- Goto, J., Suganuma, N., Takata, K., Kitamura, K., Asahina, T., Kobayashi, H., Muranaka, Y., Furuhashi, M., & Kanayama, N. (2002). Morphological analyses of interleukin-8 effects on rat ovarian follicles at ovulation and luteinization in vivo. *Cytokine*, *20*(4), 168-173.
- Graham, K. A., Kulawiec, M., Owens, K. M., Li, X., Desouki, M. M., Chandra, D., & Singh, K. K. (2010). NADPH oxidase 4 is an oncoprotein localized to mitochondria. *Cancer Biol Ther*, *10*(3), 223-231.
- Green, D. E., Murphy, T. C., Kang, B. Y., Kleinhenz, J. M., Szyndralewicz, C., Page, P., Sutliff, R. L., & Hart, C. M. (2012). The Nox4 inhibitor GKT137831 attenuates hypoxia-induced pulmonary vascular cell proliferation. *Am J Respir Cell Mol Biol*, *47*(5), 718-726. doi:10.1165/rcmb.2011-0418OC
- Greenseid, K., Jindal, S., Hurwitz, J., Santoro, N., & Pal, L. (2011). Differential granulosa cell gene expression in young women with diminished ovarian reserve. *Reprod Sci*, *18*(9), 892-899. doi:10.1177/1933719111398502
- Guo, S., & Chen, X. (2015). The human Nox4: gene, structure, physiological function and pathological significance. *J Drug Target*, *23*(10), 888-896. doi:10.3109/1061186x.2015.1036276
- Gupta, R. K., Patel, A. K., Shah, N., Chaudhary, A. K., Jha, U. K., Yadav, U. C., Gupta, P. K., & Pakuwal, U. (2014). Oxidative stress and antioxidants in disease and cancer: a review. *Asian Pac J Cancer Prev*, *15*(11), 4405-4409.
- Hamilton, B. E., & Ventura, S. J. (2006). Fertility and abortion rates in the United States, 1960-2002. *Int J Androl*, *29*(1), 34-45. doi:10.1111/j.1365-2605.2005.00638.x
- Hanukoglu, I. (2006). Antioxidant protective mechanisms against reactive oxygen species (ROS) generated by mitochondrial P450 systems in steroidogenic cells. *Drug Metab Rev*, *38*(1-2), 171-196. doi:10.1080/03602530600570040
- Hennet, M. L., & Combelles, C. M. (2012). The antral follicle: a microenvironment for oocyte differentiation. *Int J Dev Biol*, *56*(10-12), 819-831. doi:10.1387/ijdb.120133cc

- Hennet, M. L., Yu, H. Y., & Combelles, C. M. (2013). Follicular fluid hydrogen peroxide and lipid hydroperoxide in bovine antral follicles of various size, atresia, and dominance status. *J Assist Reprod Genet*, *30*(3), 333-340. doi:10.1007/s10815-012-9925-5
- Jemtaweeboon, S., Shirasuna, K., Nitta, A., Kobayashi, A., Schuberth, H. J., Shimizu, T., & Miyamoto, A. (2011). Evidence that polymorphonuclear neutrophils infiltrate into the developing corpus luteum and promote angiogenesis with interleukin-8 in the cow. *Reprod Biol Endocrinol*, *9*, 79. doi:10.1186/1477-7827-9-79
- Jones, D. P. (2006). Redefining oxidative stress. *Antioxid Redox Signal*, *8*(9-10), 1865-1879. doi:10.1089/ars.2006.8.1865
- Jones, D. P. (2008). Radical-free biology of oxidative stress. *Am J Physiol Cell Physiol*, *295*(4), C849-868. doi:10.1152/ajpcell.00283.2008
- Kampfner, C., Saller, S., Windschuttl, S., Berg, D., Berg, U., & Mayerhofer, A. (2014). Pigment-Epithelium Derived Factor (PEDF) and the human ovary: a role in the generation of ROS in granulosa cells. *Life Sci*, *97*(2), 129-136. doi:10.1016/j.lfs.2013.12.007
- Karin, M., & Shaulian, E. (2001). AP-1: linking hydrogen peroxide and oxidative stress to the control of cell proliferation and death. *IUBMB Life*, *52*(1-2), 17-24. doi:10.1080/15216540252774711
- Kishi, H., Kitahara, Y., Imai, F., Nakao, K., & Suwa, H. (2018). Expression of the gonadotropin receptors during follicular development. *Reprod Med Biol*, *17*(1), 11-19. doi:10.1002/rmb2.12075
- Koeppen, B., & Stanton, B. (2009). *Berne & Levy Physiology* (6 ed.).
- Kozziel, R., Pircher, H., Kratochwil, M., Lener, B., Hermann, M., Dencher, N. A., & Jansen-Durr, P. (2013). Mitochondrial respiratory chain complex I is inactivated by NADPH oxidase Nox4. *Biochem J*, *452*(2), 231-239. doi:10.1042/BJ20121778
- Kuroda, J., Nakagawa, K., Yamasaki, T., Nakamura, K., Takeya, R., Kuribayashi, F., Imajoh-Ohmi, S., Igarashi, K., Shibata, Y., Sueishi, K., & Sumimoto, H. (2005). The superoxide-producing NAD(P)H oxidase Nox4 in the nucleus of human vascular endothelial cells. *Genes Cells*, *10*(12), 1139-1151. doi:10.1111/j.1365-2443.2005.00907.x
- Laan, M., Grigorova, M., & Huhtaniemi, I. T. (2012). Pharmacogenetics of follicle-stimulating hormone action. *Curr Opin Endocrinol Diabetes Obes*, *19*(3), 220-227. doi:10.1097/MED.0b013e3283534b11
- Laemmli, U. K. (1970). Cleavage of structural proteins during the assembly of the head of bacteriophage T4. *Nature*, *227*(5259), 680-685.
- Lambeth, J. D., & Neish, A. S. (2014). Nox enzymes and new thinking on reactive oxygen: a double-edged sword revisited. *Annu Rev Pathol*, *9*, 119-145. doi:10.1146/annurev-pathol-012513-104651
- Landomiel, F., Gallay, N., Jegot, G., Tranchant, T., Durand, G., Bourquard, T., Crepieux, P., Poupon, A., & Reiter, E. (2014). Biased signalling in follicle stimulating hormone action. *Mol Cell Endocrinol*, *382*(1), 452-459. doi:10.1016/j.mce.2013.09.035
- Lee, H. J., Jee, B. C., Kim, S. K., Kim, H., Lee, J. R., Suh, C. S., & Kim, S. H. (2016). Expressions of aquaporin family in human luteinized granulosa cells and their correlations with IVF outcomes. *Hum Reprod*, *31*(4), 822-831. doi:10.1093/humrep/dew006
- Luderer, U. (2014). Ovarian toxicity from reactive oxygen species. *Vitam Horm*, *94*, 99-127. doi:10.1016/b978-0-12-800095-3.00004-3
- Macklon, N. S., Stouffer, R. L., Giudice, L. C., & Fauser, B. C. (2006). The science behind 25 years of ovarian stimulation for in vitro fertilization. *Endocr Rev*, *27*(2), 170-207. doi:10.1210/er.2005-0015
- Maraldi, T., Resca, E., Nicoli, A., Beretti, F., Zavatti, M., Capodanno, F., Morini, D., Palomba, S., La Sala, G. B., & De Pol, A. (2016). NADPH oxidase-4 and MATER expressions in granulosa cells: Relationships with ovarian aging. *Life Sci*, *162*, 108-114. doi:10.1016/j.lfs.2016.08.007
- Margoliash, E., Novogrodsky, A., & Schejter, A. (1960). Irreversible reaction of 3-amino-1:2:4-triazole and related inhibitors with the protein of catalase. *Biochem J*, *74*, 339-348.

- Mayerhofer, A., Fohr, K. J., Sterzik, K., & Gratzl, M. (1992). Carbachol increases intracellular free calcium concentrations in human granulosa-lutein cells. *J Endocrinol*, *135*(1), 153-159.
- Mayerhofer, A., Kunz, L., Krieger, A., Proskocil, B., Spindel, E., Amsterdam, A., Dissen, G. A., Ojeda, S. R., & Wessler, I. (2006). FSH regulates acetylcholine production by ovarian granulosa cells. *Reprod Biol Endocrinol*, *4*, 37. doi:10.1186/1477-7827-4-37
- Mayerhofer, A., Sterzik, K., Link, H., Wiemann, M., & Gratzl, M. (1993). Effect of oxytocin on free intracellular Ca²⁺ levels and progesterone release by human granulosa-lutein cells. *J Clin Endocrinol Metab*, *77*(5), 1209-1214. doi:10.1210/jcem.77.5.8077313
- McConnell, N. A., Yunus, R. S., Gross, S. A., Bost, K. L., Clemens, M. G., & Hughes, F. M., Jr. (2002). Water permeability of an ovarian antral follicle is predominantly transcellular and mediated by aquaporins. *Endocrinology*, *143*(8), 2905-2912. doi:10.1210/endo.143.8.8953
- Meitzler, J. L., Antony, S., Wu, Y., Juhasz, A., Liu, H., Jiang, G., Lu, J., Roy, K., & Doroshow, J. H. (2014). NADPH oxidases: a perspective on reactive oxygen species production in tumor biology. *Antioxid Redox Signal*, *20*(17), 2873-2889. doi:10.1089/ars.2013.5603
- Mesquita, F. S., Dyer, S. N., Heinrich, D. A., Bulun, S. E., Marsh, E. E., & Nowak, R. A. (2010). Reactive oxygen species mediate mitogenic growth factor signaling pathways in human leiomyoma smooth muscle cells. *Biol Reprod*, *82*(2), 341-351. doi:10.1095/biolreprod.108.075887
- Miller, E. W., Dickinson, B. C., & Chang, C. J. (2010). Aquaporin-3 mediates hydrogen peroxide uptake to regulate downstream intracellular signaling. *Proc Natl Acad Sci U S A*, *107*(36), 15681-15686. doi:10.1073/pnas.1005776107
- Miller, W. L. (1988). Molecular biology of steroid hormone synthesis. *Endocr Rev*, *9*(3), 295-318. doi:10.1210/edrv-9-3-295
- Miller, W. L. (2017). Steroidogenesis: Unanswered Questions. *Trends Endocrinol Metab*, *28*(11), 771-793. doi:10.1016/j.tem.2017.09.002
- Miller, W. L., & Auchus, R. J. (2011). The molecular biology, biochemistry, and physiology of human steroidogenesis and its disorders. *Endocr Rev*, *32*(1), 81-151. doi:10.1210/er.2010-0013
- Nassif, J., Abbasi, S. A., Nassar, A., Abu-Musa, A., & Eid, A. A. (2016). The role of NADPH-derived reactive oxygen species production in the pathogenesis of endometriosis: a novel mechanistic approach. *J Biol Regul Homeost Agents*, *30*(1), 31-40.
- Niemietz, C. M., & Tyerman, S. D. (2002). New potent inhibitors of aquaporins: silver and gold compounds inhibit aquaporins of plant and human origin. *FEBS Lett*, *531*(3), 443-447.
- Nishi, Y., Yanase, T., Mu, Y., Oba, K., Ichino, I., Saito, M., Nomura, M., Mukasa, C., Okabe, T., Goto, K., Takayanagi, R., Kashimura, Y., Haji, M., & Nawata, H. (2001). Establishment and characterization of a steroidogenic human granulosa-like tumor cell line, KGN, that expresses functional follicle-stimulating hormone receptor. *Endocrinology*, *142*(1), 437-445. doi:10.1210/endo.142.1.7862
- Nlandu Khodo, S., Dizin, E., Sossauer, G., Szanto, I., Martin, P. Y., Feraille, E., Krause, K. H., & de Seigneux, S. (2012). NADPH-oxidase 4 protects against kidney fibrosis during chronic renal injury. *J Am Soc Nephrol*, *23*(12), 1967-1976. doi:10.1681/ASN.2012040373
- Orisaka, M., Tajima, K., Tsang, B. K., & Kotsuji, F. (2009). Oocyte-granulosa-theca cell interactions during preantral follicular development. *J Ovarian Res*, *2*(1), 9. doi:10.1186/1757-2215-2-9
- Patterson, H. C., Gerbeth, C., Thiru, P., Vogtle, N. F., Knoll, M., Shahsafaei, A., Samocho, K. E., Huang, C. X., Harden, M. M., Song, R., Chen, C., Kao, J., Shi, J., Salmon, W., Shaul, Y. D., Stokes, M. P., Silva, J. C., Bell, G. W., MacArthur, D. G., Ruland, J., Meisinger, C., & Lodish, H. F. (2015). A respiratory chain controlled signal transduction cascade in the mitochondrial intermembrane space mediates hydrogen peroxide

- signaling. *Proc Natl Acad Sci U S A*, 112(42), E5679-5688. doi:10.1073/pnas.1517932112
- Perez Mayorga, M., Gromoll, J., Behre, H. M., Gassner, C., Nieschlag, E., & Simoni, M. (2000). Ovarian response to follicle-stimulating hormone (FSH) stimulation depends on the FSH receptor genotype. *J Clin Endocrinol Metab*, 85(9), 3365-3369. doi:10.1210/jcem.85.9.6789
- Pfaffl, M. W. (2001). A new mathematical model for relative quantification in real-time RT-PCR. *Nucleic Acids Res*, 29(9), e45.
- Pierce, J. G., & Parsons, T. F. (1981). Glycoprotein hormones: structure and function. *Annu Rev Biochem*, 50, 465-495. doi:10.1146/annurev.bi.50.070181.002341
- Pizzino, G., Irrera, N., Cucinotta, M., Pallio, G., Mannino, F., Arcoraci, V., Squadrito, F., Altavilla, D., & Bitto, A. (2017). Oxidative Stress: Harms and Benefits for Human Health. *Oxid Med Cell Longev*, 2017, 8416763. doi:10.1155/2017/8416763
- Practice Committee of American Society for Reproductive Medicine, A. (2008). Gonadotropin preparations: past, present, and future perspectives. *Fertil Steril*, 90(5 Suppl), S13-20. doi:10.1016/j.fertnstert.2008.08.031
- Prasad, S., Tiwari, M., Pandey, A. N., Shrivastav, T. G., & Chaube, S. K. (2016). Impact of stress on oocyte quality and reproductive outcome. *J Biomed Sci*, 23, 36. doi:10.1186/s12929-016-0253-4
- Radu, A., Pichon, C., Camparo, P., Antoine, M., Allory, Y., Couvelard, A., Fromont, G., Hai, M. T., & Ghinea, N. (2010). Expression of follicle-stimulating hormone receptor in tumor blood vessels. *N Engl J Med*, 363(17), 1621-1630. doi:10.1056/NEJMoa1001283
- Reczek, C. R., & Chandel, N. S. (2015). ROS-dependent signal transduction. *Curr Opin Cell Biol*, 33, 8-13. doi:10.1016/j.ceb.2014.09.010
- Reed, B. G., & Carr, B. R. (2000). The Normal Menstrual Cycle and the Control of Ovulation. In L. J. De Groot, G. Chrousos, K. Dungan, K. R. Feingold, A. Grossman, J. M. Hershman, C. Koch, M. Korbonits, R. McLachlan, M. New, J. Purnell, R. Rebar, F. Singer, & A. Vinik (Eds.), *Endotext*. South Dartmouth (MA): MDText.com, Inc.
- Revelli, A., Piane, L. D., Casano, S., Molinari, E., Massobrio, M., & Rinaudo, P. (2009). Follicular fluid content and oocyte quality: from single biochemical markers to metabolomics. *Reproductive Biology and Endocrinology*, 7(1), 40. doi:10.1186/1477-7827-7-40
- Richards, J. S., & Pangas, S. A. (2010). The ovary: basic biology and clinical implications. *J Clin Invest*, 120(4), 963-972. doi:10.1172/JCI41350
- Rizzo, A., Roscino, M. T., Binetti, F., & Sciorsci, R. L. (2012). Roles of reactive oxygen species in female reproduction. *Reprod Domest Anim*, 47(2), 344-352. doi:10.1111/j.1439-0531.2011.01891.x
- Rosario, R., Araki, H., Print, C. G., & Shelling, A. N. (2012). The transcriptional targets of mutant FOXL2 in granulosa cell tumours. *PLoS One*, 7(9), e46270. doi:10.1371/journal.pone.0046270
- Ross, M. H., & Wojciech, P. (2015). *Histology: A Text and Atlas* (7th ed.): Wolters Kluwer.
- Ruiz-Ojeda, F. J., Gomez-Llorente, C., Aguilera, C. M., Gil, A., & Ruperez, A. I. (2016). Impact of 3-Amino-1,2,4-Triazole (3-AT)-Derived Increase in Hydrogen Peroxide Levels on Inflammation and Metabolism in Human Differentiated Adipocytes. *PLoS One*, 11(3), e0152550. doi:10.1371/journal.pone.0152550
- Saller, S., Kunz, L., Berg, D., Berg, U., Lara, H., Urra, J., Hecht, S., Pavlik, R., Thaler, C. J., & Mayerhofer, A. (2014). Dopamine in human follicular fluid is associated with cellular uptake and metabolism-dependent generation of reactive oxygen species in granulosa cells: implications for physiology and pathology. *Hum Reprod*, 29(3), 555-567. doi:10.1093/humrep/det422
- Saller, S., Merz-Lange, J., Raffael, S., Hecht, S., Pavlik, R., Thaler, C., Berg, D., Berg, U., Kunz, L., & Mayerhofer, A. (2012). Norepinephrine, active norepinephrine transporter, and norepinephrine-metabolism are involved in the generation of reactive oxygen

- species in human ovarian granulosa cells. *Endocrinology*, 153(3), 1472-1483. doi:10.1210/en.2011-1769
- Sanchez, F., & Smitz, J. (2012). Molecular control of oogenesis. *Biochim Biophys Acta*, 1822(12), 1896-1912. doi:10.1016/j.bbadis.2012.05.013
- Sato, E. F., Kobuchi, H., Edashige, K., Takahashi, M., Yoshioka, T., Utsumi, K., & Inoue, M. (1992). Dynamic aspects of ovarian superoxide dismutase isozymes during the ovulatory process in the rat. *FEBS Lett*, 303(2-3), 121-125.
- Schroder, K., Zhang, M., Benkhoff, S., Mieth, A., Pliquett, R., Kosowski, J., Kruse, C., Luedike, P., Michaelis, U. R., Weissmann, N., Dimmeler, S., Shah, A. M., & Brandes, R. P. (2012). Nox4 is a protective reactive oxygen species generating vascular NADPH oxidase. *Circ Res*, 110(9), 1217-1225. doi:10.1161/circresaha.112.267054
- Shiose, A., Kuroda, J., Tsuruya, K., Hirai, M., Hirakata, H., Naito, S., Hattori, M., Sakaki, Y., & Sumimoto, H. (2001). A novel superoxide-producing NAD(P)H oxidase in kidney. *J Biol Chem*, 276(2), 1417-1423. doi:10.1074/jbc.M007597200
- Shirasuna, K., & Iwata, H. (2017). Effect of aging on the female reproductive function. *Contracept Reprod Med*, 2, 23. doi:10.1186/s40834-017-0050-9
- Shkolnik, K., Tadmor, A., Ben-Dor, S., Nevo, N., Galiani, D., & Dekel, N. (2011). Reactive oxygen species are indispensable in ovulation. *Proc Natl Acad Sci U S A*, 108(4), 1462-1467. doi:10.1073/pnas.1017213108
- Sies, H. (2017). Hydrogen peroxide as a central redox signaling molecule in physiological oxidative stress: Oxidative eustress. *Redox Biol*, 11, 613-619. doi:10.1016/j.redox.2016.12.035
- Sies, H., Berndt, C., & Jones, D. P. (2017). Oxidative Stress. *Annu Rev Biochem*, 86, 715-748. doi:10.1146/annurev-biochem-061516-045037
- Simoni, M., Gromoll, J., & Nieschlag, E. (1997). The follicle-stimulating hormone receptor: biochemistry, molecular biology, physiology, and pathophysiology. *Endocr Rev*, 18(6), 739-773. doi:10.1210/edrv.18.6.0320
- Sirokmany, G., Donko, A., & Geiszt, M. (2016). Nox/Duox Family of NADPH Oxidases: Lessons from Knockout Mouse Models. *Trends Pharmacol Sci*, 37(4), 318-327. doi:10.1016/j.tips.2016.01.006
- Sirokmány, G., Donkó, Á., & Geiszt, M. (2016). Nox/Duox Family of NADPH Oxidases: Lessons from Knockout Mouse Models. *Trends in Pharmacological Sciences*, 37(4), 318-327. doi:http://dx.doi.org/10.1016/j.tips.2016.01.006
- Spitz, D. R., Azzam, E. I., Li, J. J., & Gius, D. (2004). Metabolic oxidation/reduction reactions and cellular responses to ionizing radiation: a unifying concept in stress response biology. *Cancer Metastasis Rev*, 23(3-4), 311-322. doi:10.1023/B:CANC.0000031769.14728.bc
- Stephoe, P. C., & Edwards, R. G. (1978). Birth after the reimplantation of a human embryo. *Lancet*, 2(8085), 366.
- Teixeira, G., Szyndralewicz, C., Molango, S., Carnesecchi, S., Heitz, F., Wiesel, P., & Wood, J. M. (2016). Therapeutic potential of NADPH oxidase 1/4 inhibitors. *Br J Pharmacol*. doi:10.1111/bph.13532
- Themmen, A. P. N., & Huhtaniemi, I. T. (2000). Mutations of gonadotropins and gonadotropin receptors: elucidating the physiology and pathophysiology of pituitary-gonadal function. *Endocr Rev*, 21(5), 551-583. doi:10.1210/edrv.21.5.0409
- Tremblay, P. G., & Sirard, M. A. (2017). Transcriptomic analysis of gene cascades involved in protein kinase A and C signaling in the KGN line of human ovarian granulosa tumor cellsdagger. *Biol Reprod*, 96(4), 855-865. doi:10.1093/biolre/iox024
- Turner, E. C., Hughes, J., Wilson, H., Clay, M., Mylonas, K. J., Kipari, T., Duncan, W. C., & Fraser, H. M. (2011). Conditional ablation of macrophages disrupts ovarian vasculature. *Reproduction*, 141(6), 821-831. doi:10.1530/rep-10-0327
- Van Voorhis, B. J. (2007). Clinical practice. In vitro fertilization. *N Engl J Med*, 356(4), 379-386. doi:10.1056/NEJMcp065743

- Verkman, A. S., & Mitra, A. K. (2000). Structure and function of aquaporin water channels. *Am J Physiol Renal Physiol*, 278(1), F13-28. doi:10.1152/ajprenal.2000.278.1.F13
- Vilema-Enriquez, G., Arroyo, A., Grijalva, M., Amador-Zafra, R. I., & Camacho, J. (2016). Molecular and Cellular Effects of Hydrogen Peroxide on Human Lung Cancer Cells: Potential Therapeutic Implications. *Oxid Med Cell Longev*, 2016, 1908164. doi:10.1155/2016/1908164
- Vloeberghs, V., Peeraer, K., Pexsters, A., & D'Hooghe, T. (2009). Ovarian hyperstimulation syndrome and complications of ART. *Best Pract Res Clin Obstet Gynaecol*, 23(5), 691-709. doi:10.1016/j.bpobgyn.2009.02.006
- Walker, C. L., Pomatto, L. C. D., Tripathi, D. N., & Davies, K. J. A. (2018). Redox Regulation of Homeostasis and Proteostasis in Peroxisomes. *Physiol Rev*, 98(1), 89-115. doi:10.1152/physrev.00033.2016
- Watanabe, S., Moniaga, C. S., Nielsen, S., & Hara-Chikuma, M. (2016). Aquaporin-9 facilitates membrane transport of hydrogen peroxide in mammalian cells. *Biochem Biophys Res Commun*, 471(1), 191-197. doi:10.1016/j.bbrc.2016.01.153
- Wong, J. L., Creton, R., & Wessel, G. M. (2004). The oxidative burst at fertilization is dependent upon activation of the dual oxidase Udx1. *Dev Cell*, 7(6), 801-814. doi:10.1016/j.devcel.2004.10.014
- Yamashita, Y., Hishinuma, M., & Shimada, M. (2009). Activation of PKA, p38 MAPK and ERK1/2 by gonadotropins in cumulus cells is critical for induction of EGF-like factor and TACE/ADAM17 gene expression during in vitro maturation of porcine COCs. *J Ovarian Res*, 2, 20. doi:10.1186/1757-2215-2-20
- Yamashita, Y., & Shimada, M. (2012). The release of EGF domain from EGF-like factors by a specific cleavage enzyme activates the EGFR-MAPK3/1 pathway in both granulosa cells and cumulus cells during the ovulation process. *J Reprod Dev*, 58(5), 510-514.
- Yang, Y., Zhang, J., Zhu, Y., Zhang, Z., Sun, H., & Feng, Y. (2014). Follicle-stimulating hormone induced epithelial-mesenchymal transition of epithelial ovarian cancer cells through follicle-stimulating hormone receptor PI3K/Akt-Snail signaling pathway. *Int J Gynecol Cancer*, 24(9), 1564-1574. doi:10.1097/IGC.0000000000000279
- Ye, H., Li, X., Zheng, T., Liang, X., Li, J., Huang, J., Pan, Z., & Zheng, Y. (2016). The effect of the immune system on ovarian function and features of ovarian germline stem cells. *Springerplus*, 5(1), 990. doi:10.1186/s40064-016-2390-3
- Zhang, Z., Wang, Q., Ma, J., Yi, X., Zhu, Y., Xi, X., Feng, Y., & Jin, Z. (2013). Reactive oxygen species regulate FSH-induced expression of vascular endothelial growth factor via Nrf2 and HIF1alpha signaling in human epithelial ovarian cancer. *Oncol Rep*, 29(4), 1429-1434. doi:10.3892/or.2013.2278

6. Acknowledgements

This thesis has received tremendous support by many people, to whom I would like to express gratitude and appreciation.

I am deeply grateful to Prof. Dr. Artur Mayerhofer for giving me the opportunity to join his laboratory and offer me such an interesting study of investigation. During my entire PhD time, I had the pleasure of enjoying his support, his optimism, his limitless ideas, and important discussion.

Special thanks go to PD Dr. Lars Kunz for supervising and assessing this dissertation. Numerous times he has offered extremely helpful advice and constructive feedback, for which I am grateful.

Both together are a brilliant team and deserve many thanks for their highly competent remarks and suggestions as well as for reviewing and commenting my doctoral thesis. Their great motivation made it easy for me to work hard and learn a tremendous amount. Their constant and immediate support during my research was vital for driving my understanding and interest in this topic.

The next persons I would like to thank, and without their support my research would have been impossible, is Prof. Dr. Dieter Berg, Dr. Ulrike Berg and all employees of the IVF-laboratory A.R.T. Bogenhausen, Munich.

I especially thank Dr. Toshihiko Yanase, Professor, Fukuoka University, Japan for supplying KGN cells.

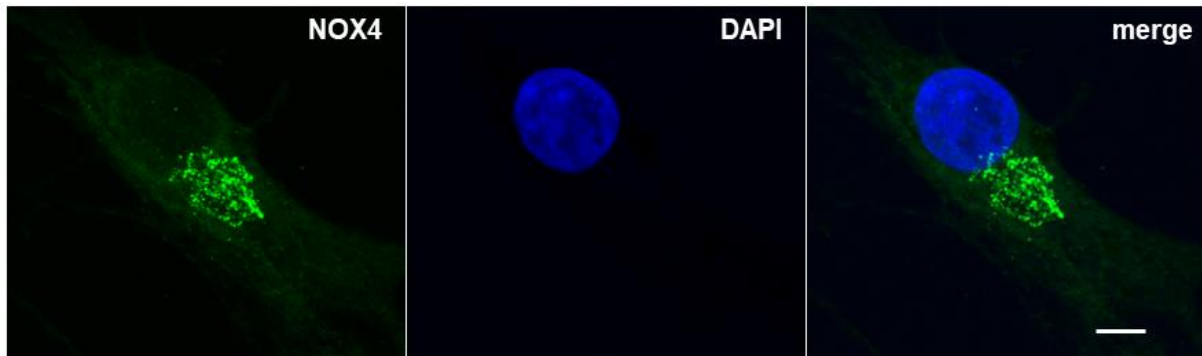
Furthermore, a great thank you goes to my colleagues of the department for Cell Biology, Anatomy III, at the BioMedical Center Munich for their invaluable support, pleasant working atmosphere and for giving me a comfortable and inspiring time. I greatly appreciate the committed support of Dr. Jan Blohberger for answering my many questions regarding the project, Karin Metzrath for her administrative support, Daniel Aigner, Astrid Tiefenbacher, Carola Herrmann, and Kim Dietrich for their great technical support and patience as well as Katja Eubler, Nina Schmid, Lena Walenta, Dr. Sabine Meinel, Dr. Stefanie Windschüttl, Dr. Verónica Rey Berutti, and Dr. Harald Welter for helpful discussions, and last but not least to the great Kampfovar-team Konstantin Bagnjuk, Carsten Theo Hack, and Verena Kast for their amazing teamwork, helpful discussions, and important results.

Above all, the continuous support from my parents Reinhold and Sabine and siblings Veronika, Lisa and Felix, and especially their way of believing in me and encouraging me to pursue my interests and to realize my plans and dreams made my years of studying an enjoyable journey. My wonderful friends, especially Simon Bohner, Ramona Murr, Anna Pratsinis, and Helena Ederle deserve great thanks for their moral and philosophical support throughout my studies.

Finally, I would like to thank, with all my heart, Matthias Müller for his unconditional support, patience, and the right sense of humour. There is no way I could have done this without him.

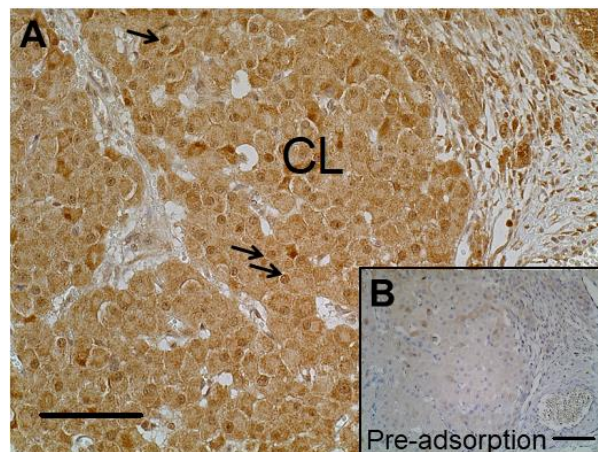
7. Supplement

In addition, a further specific antibody was used and positive staining for NOX4 was detected in GCs on culture day 2 (Supplementary Figure 1). Note, the intracellular compartments were stained only, the nucleus lacked staining. Negative controls of all immunocytochemical experiments performed without primary antibody did not show any staining (data not shown).



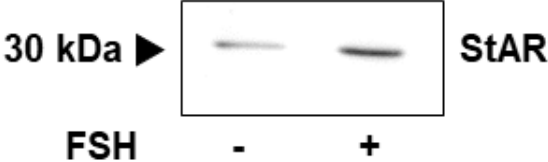
Supplementary Figure 1 - Localization of NOX4 in cultured human GCs. Staining in intracellular compartments of GCs (d2; antibody No. 3). Scale bar = 5 μ m.

The CL showed staining of the nucleus (Supplementary Figure 2, arrow). The pre-adsorption of the anti-NOX4 antibody No. 2 with a specific blocking peptide (Table 11) and omission of primary antibody prevented staining (inset, Supplementary Figure 2).



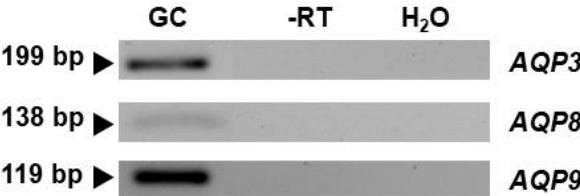
Supplementary Figure 2 - NOX4 localization in the CL. (A) Cells of CL of a human ovarian section are positive for NOX4 staining using immunohistochemistry and anti-NOX4 antibody No. 2. (A) Staining is seen in the cytoplasm and the nucleus (arrows) of luteinised cells. (B) The pre-adsorption control is devoid of staining. Scale bars = 50 μ m.

GCs on culture day 1 treated with FSH (1 IU/ml) for 2 h showed an increased protein expression of StAR.



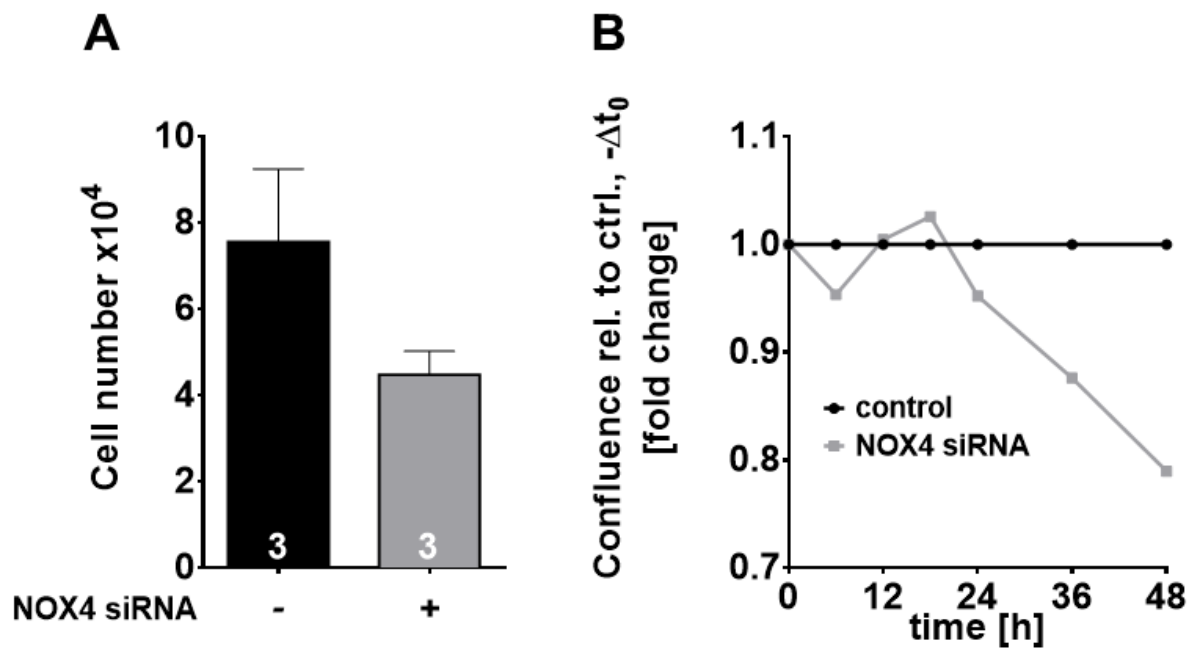
Supplementary Figure 3 - FSH increased StAR protein expression in cultured human GCs. The WB shows an increase in StAR protein expression after FSH treatment (2 h). The arrow shows the expected size (30 kDa).

The expression of AQP3, 8, and 9 in GCs could be shown by RT-PCR (experiment performed by Theo Hack).



Supplementary Figure 4 - H₂O₂-transporting peroxiporins in cultured human GCs. RT-PCR identified AQP 3, 8, and 9. Controls performed with RNA (-RT) and without cDNA (H₂O) were negative.

SiRNA-mediated knockdown of the NOX4 gene in the proliferating KGN cell line was achieved using the *Invitrogen™ Silencer™* Pre-designed siRNA by ThermoFisher Scientific (F: caa cuc aua ugg gac aag att; R: ucu ugu ccc aua uga guu gtt) and as negative control *Invitrogen™ Silencer™* Select Negative Control No. 1 siRNA. SiRNA transfections were carried out with Lipofectamine 2000 at a final concentration of 25 nM siRNA. Culture medium was exchanged 5 h post-transfection and the knockdown was analysed 48 h post-transfection by cell counting (n = 3) and confluence measurement (n = 1).



Supplementary Figure 5 - Preliminary experiments with siRNA transfection in KGN. RNA silencing led to decreased cell number and cell confluence of KGN cells. (A) Transfection of KGN cells with NOX4 siRNA for 48 h showed a reduction in cell number (n = 3) and confluence (B; n = 1). Statistics: (A) paired *t* tests (two-tailed).

8. Appendix

8.1 Publications

Blohberger, J., Buck T., Berg D., Berg U., Kunz L. and Mayerhofer A. (2016). "L-DOPA in the human ovarian follicular fluid acts as an antioxidant factor on granulosa cells." *J Ovarian Res* **9**(1): 62.

Buck, T., Hack C. T., Berg D., Berg U., Kunz L. and Mayerhofer A. (2018). „The NADPH oxidase 4 is a major source of hydrogen peroxide in human granulosa-lutein and KGN cells.” Submitted.

8.2 Poster

ROS-generating NOX enzymes in human ovary: The role of NOX4.

Buck T., Dietrich K., Blohberger J., Herrmann C., Berg D., Berg U., Mayerhofer A.

6. Kongress des Dachverbandes Reproduktionsbiologie und –medizin, Hamburg, 2015

ROS-generating NOX enzymes in human ovary: The role of NOX4.

Buck T., Blohberger J., Herrmann C., Dietrich K., Tiefenbacher A., Berg D., Berg U., Mayerhofer A.

59. Symposium der Deutschen Gesellschaft für Endokrinologie, Munich, 2016

ROS-generating NOX enzymes and H₂O₂ in human ovary and granulosa cells.

Buck T., Blohberger J., Herrmann C., Berg D., Berg U., Mayerhofer A.

50. Jahrestagung “Physiologie & Pathologie der Fortpflanzung”, Munich, 2017

NOX4 – a major source of H₂O₂ in the human ovary.

Buck T., Herrmann C., Berg D., Berg U., Mayerhofer A.

50th Annual Meeting of the Society for the Study of Reproduction, Washington D.C., USA, 2017